ALBERT-LUDWIGS
UNIVERSITÄT FREIBURG

iHf
HYDROLOGIE FREIBURG

Manuela Nied

Modelling Vulnerability of Stream Flow Allocations in International River Basins with Open Source Gridded Climate Input

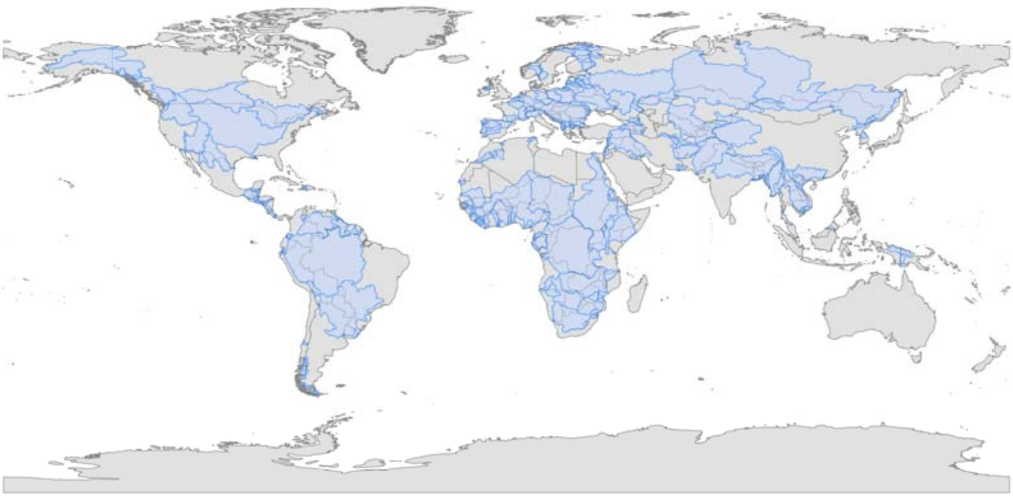

Diplomarbeit unter der Leitung von Prof. Dr. M. Weiler

Freiburg im Breisgau, November 2009

Institut für Hydrologie
Albert-Ludwigs Universität Freiburg im Breisgau

Manuela Nied

Modelling Vulnerability of Stream Flow Allocations in International River Basins with Open Source Gridded Climate Input

Supervisor: Prof. Dr. M. Weiler
Co-supervisor: Dr. K. Stahl

Diplomarbeit unter der Leitung von Prof. Dr. M. Weiler
Freiburg im Breisgau, November 2009

I Content

II List of Figures

III List of Figures in Appendix

IV List of Tables

V List of Tables in Appendix

VI List of Symbols

α	Recession rate	[-]
β	Peak response	[-]
υ	Volume proportion	[-]
Δ	Operating time step /Sampling interval	[h] / [d] / [month]
ACF	Auto correlation function	[-]
AET	Threshold	[-]
AM	Arithmetic mean	[mm] / [° C]
at	Actual evapotranspiration	[mm]
c	Mass balance parameter	[mm^{-1}]
cal	Calibration period	[d] / [month]
CCF	Cross correlation function	[-]
COV	Covariance	[-]
D	Maximum depth of soil	[mm]
dec	Declination of the sun	[°]
diff	Difference	[mm] / [° C]
exp	Euler's number	[-]
f	Temperature dependence of drying rate	[$°C^{-1}$]
F	Non-exceedance frequency	[%]
H	Average number of daylight hours	[h/d]
i	Index	[-]
j	Index	[-]
julday	Number of the day of the year	[-]
k	Time step	[d] / [month]
l	Soil moisture index threshold	[mm]
lat	Latitude	[rad] / [°]
long	Longitude	[rad] / [°]
MAE	Mean absolute error	[mm] / [° C]
MQ	Arithmetic mean of discharge	[m^3/s] / [mm]

NS	Nash-Sutcliffe efficiency	[-]
n	Number of elements	[-]
oflow	Overland flow	[mm]
P	Precipitation	[mm]
p	Non-linear response	[-]
PC	Pardé Coefficient	[-]
perc	Percolation	[mm]
pt	Potential evapotranspiration	[mm]
Q	Stream flow (IHACRES)	[mm] / [m³/s]
Q_o	Observed stream flow	[m³/s] / [mm]
Q_m	Simulated stream flow	[m³/s] / [mm]
q	Stream flow (Simple Bucket)	[mm/month]
r	Linear Pearson correlation coefficient	[-]
s	Antecedent precipitation index / catchment wetness index	[mm]
sha	Sunset hour angle	[°]
SP_{max}	Maximum percolation from soil to groundwater	[mm]
svp	Saturated water pressure	[mbar]
swc	Soil water content	[mm]
T	Air temperature	[°C]
t	Drying rate	[-]
t	Time point	
TC	Time constant	[d] / [month]
T_r	Reference air temperature	[°C]
t_w	Drying rate at reference temperature	[-]
u	Effective rainfall	[mm]
val	Validation period	[d] / [month]
VAR	Variance	[-]
X	Variable of time series	
Y	Variable of time series	

VII List of Abbreviations

BfG	Bundesanstalt für Gewässerkunde
CMD	Catchment moisture deficit accounting module
CRCCH	Cooperative Research Centre for Catchment Hydrology
CRU	Climate Research Unit
CSIRO	Commonwealth Scientific and Industrial Research Organisation
ECMWF	European Centre for Medium-Range Weather Forecasts
ERA-40	Reanalysis data of the ECMWF
FAO	Food and Agriculture Organization
fdc	Flow duration curve
GCM	General Circulation Model
GRDC	Global Runoff Data Centre
IAHS	International Association of Hydrological Science
iCAM	Integrated Catchment Assessment and Management Centre
IHACRES	Identification of unit Hydrographs And Component flows from Rainfall, Evapotranspiration and Stream flow data
ITCZ	Intertropical convergence zone
MCM	Million cubic meter
PUB	Predictions in Ungauged Basins
RCM	Regional Climate Model
TFDD	Transboundary Freshwater Dispute Database

VIII Summary

Developing skilful predictions of future river flow in International River Basins is important for economic, political and societal applications of the riparian states. In particular are such predictions crucial to aid water management expressed in a transboundary water allocation agreement. Due to climate and land use change and already experienced hydrological extreme situations, both droughts and floods, the prediction of seasonal river flows has been a topic of increasing interest. As data scarce regions will be most affected, the study analysed the skill of open source gridded climate datasets to model stream flow with the objective to evaluate the vulnerability of stream flow allocations. The transboundary river basins Kunene, Upper Niger and Upper Jordan served as case studies for this research. First, the study compared the spatial and temporal anomaly and correlation of precipitation between (1) the ERA-40 reanalysis data and (2) the CRU TS 2.1 interpolated data in the selected basins for the years 1958 - 2001. Second, the climate data served as input data to a simple bucket model operating on a monthly time step and the IHACRES rainfall-runoff model operating on a daily time step.

Results show that the climate data vary considerably in precipitation amount and regime as well as their correlation is neither constant in space nor in time. Rainfall-runoff modelling on a monthly time step illustrates the dissimilarities of the climate data sets resulting in mean differences of simulated flow up to 43 %. The simulation of the discharge regime resulted in a mean monthly underestimation of low flows up to 60 % and an overestimation of mean monthly low flows up to 350 %. Mean monthly peak flows are underestimated by maximal 40 %. Modelling on a daily time step was unsuccessful. This error range was compared with the existing terms of transboundary water allocation commitments in the selected transboundary river basins. The conclusion of this study is that while the mechanisms of water allocation agreements differ widely, predictions of the vulnerability of stream flow allocations will require accurate models which depend primarily on reliable climate input data. Gridded climate input data and the applied hydrological method provide unsatisfying results in regard to the evaluation of the vulnerability of stream flow allocation agreements in International River Basins.

Keywords: international river basin, water allocation agreement, vulnerability, gridded climate data, IHACRES, simple bucket model

IX Zusammenfassung

Die fachkundige Vorhersage von zukünftigen Abflussmengen in internationalen Flusseinzugsgebieten ist speziell für wirtschaftliche, politische und gesellschaftliche Anwendungen der Flussanrainerstaaten von Bedeutung. Auf Grund von zwischenstaatlich vertraglich geregelten Wasserliefermengen sind solche Vorhersagen insbesondere für die Wasserwirtschaft von entscheidender Relevanz. Durch den Klima- und Landnutzungswandel sowie durch bereits erfahrene Extremereignisse wie Dürren und Hochwässer, gewinnt die Vorhersage der saisonalen Abflussmengen an immer größerer Bedeutung. Da insbesondere diejenigen Gebiete in denen in der Vergangenheit wenig hydrologische Daten erhoben wurden am stärksten von den Auswirkungen des Klima- und Landnutzungswandels betroffen sein werden, untersuchte die vorliegende Studie die Eignung von frei verfügbaren Raster-Klimadaten in der Abflussmodellierung, mit dem Ziel die Vulnerabilität von zwischenstaatlichen Verträgen in Bezug auf garantierte Abflussmengen zu beurteilen. Dabei dienten die internationalen Flusseinzugsgebiete Kunene, Oberer Niger und Oberer Jordan als Fallstudien.

Zunächst verglich die vorliegende Studie räumliche und zeitliche Unterschiede und Korrelationen von zwei Raster-Niederschlags-Datensätzen. Dabei handelte es sich (1) um die ERA-40 Reanalyse-Daten und (2) um die interpolierten CRU TS 2.1 Daten. Der Vergleich erfolgte in den ausgesuchten Flusseinzugsgebieten für die Jahre 1958 - 2001. Des Weiteren dienten die Klimadaten als Eingangsdaten zu einem monatlichen Speicherüberlaufmodell und dem auf täglichen Eingangsdaten basierenden IHACRES Niederschlags-Abfluss-Modell.

Die Ergebnisse zeigen, dass die Rasterdaten sowohl in Niederschlagsmenge und Niederschlagsregime als auch in ihrer räumlichen und zeitlichen Korrelation erheblich variieren. Dies spiegelte sich ebenfalls in der monatlichen Niederschlags-Abfluss-Modellierung wider, welche mittlere Differenzen des simulierten Abflusses von bis zu 43 % aufweist. Die Simulation des mittleren monatlichen Abflussregimes führte von einer 60 % Unterschätzung der Niedrigwasserabflüsse bis hin zu einer Überschätzung von 350 %. Mittlere monatliche Spitzenabflüsse wurden bis zu 40 % unterschätzt. Die Modellierung auf Grundlage von Tageswerten blieb ohne Erfolg. Die erhaltene Schwankungsbreite der mittleren monatlichen Abflusswerte wurde mit den vertraglich geregelten Wassermengen in den internationalen Flusseinzugsgebieten verglichen.

Schlussfolgernd kann festgehalten werden, dass zwar die vertraglichen Möglichkeiten der Zusicherung von Wassermengen sehr variabel sind, Aussagen über die Vertragssicherheit in Bezug auf Abflussmengen jedoch präzise Modellierungen voraussetzen. Diese Modellierungen sind wiederum hauptsächlich von der Qualität der zur Verfügung stehenden Eingangsdaten abhängig. Raster-Klimadaten und die angewandte hydrologische Methode liefern unzufrieden stellende Ergebnisse in Bezug auf die Beurteilung der Vulnerabilität von vertraglich zugesicherten Wassermengen in internationalen Flusseinzugsgebieten.

Schlagwörter: Internationale Flusseinzugsgebiete, vertraglich geregelte Wassermengen, Vulnerabilität, Klima-Raster-Daten, IHACRES, Speicherüberlaufmodell

1. Introduction

1.1 General Introduction

As earth's fundamental natural resource, freshwater has various functions and is needed in all aspects of life. Freshwater serves as drinking water for humans and animals, is needed for sanitation issues and is vital to ecology, agriculture, economy and transport.

Compared to other natural resources, water is not stationary and does not respect administrative borders. Thus drainage basin's boundaries are not necessarily identical to political boundaries resulting in the existence of International River Basins. Within the basin, (surface) water can be distributed unequally which might lead to conflict among the riparian states about transboundary waters especially surface waters (*Wolf et al.*, 2003a). To prevent conflict and to manage the existing natural resource adequately, the partition of river flow can be regulated by bilateral or multilateral water allocation agreements (*Matthews & St. Germain*, 2007).

Faced to climate and land use change, population growth, rising water demand, urbanization and pollution, the existing water resources are under pressure (*Kundzewicz et al.*, 2007; *Bates et al.*, 2008). The competition over water quality and quantity of the shared water resources will increase in future and might result in conflict between different sectors on the one hand and riparian states on the other hand (*Giordano & Wolf*, 2003; *Lange et al.*, 2007). Therefore, the sustainable integrated basinwide management of transboundary water resources especially under the consideration of climate variability and unstationarity due to climate change (*Minville et al.*, 2008) is crucial to avoid and to resolve conflict among water users (*Kundzewicz et al.*, 2007; *Goulden et al.*, 2009; *Harou et al.*, 2009).
Due to different economic strength, social vulnerability and institutional capacity, the riparian states of International River Basins differ in their capacity to adapt to changing water availability and demand as well as to extreme climate events (*Goulden et al.*, 2009). In particular, semi arid to arid areas are affected by climate change expressed in a decrease of water resources (*Kundzewicz et al.*, 2007) and by a small adaptation capacity (*Goulden et al.*, 2009). Additionally, inadequate information and data scarcity about existing and future water availability and water demands hinder effective water sharing in those regions (*Draper*, 2007).

1.2 International River Basins and Water Allocation Agreements

In 1967, the International Law Association defined in Article 2 of the 'The Helsinki Rules on the Uses of the Waters of International Rivers' the term 'International Drainage Basin': "An international drainage basin is a geographical area extending over two or more States determined by the watershed limits of the system of waters, including surface and underground waters, flowing into a common terminus" (*International Law Association*, 1967). Frequently applied synonyms of International Drainage Basin are International River Basin, Transboundary River Basin or Transboundary Drainage Basin.

Wolf et al. (1999) identified 261 rivers flowing into the ocean or a terminal lake with at least one perennial tributary belonging to two or more states. Those watersheds cover an area of 45.3 % of the land's surface (excluding Antarctica) (*Wolf et al.*, 1999). 40 % of the world's population depends on transboundary waters (*Draper & Kundell*, 2007).

From an international point of view the riparian countries of an International River Basin are equal sovereigns which results in the exclusive use of natural resources within the own national territory. In contrast, legal principles require equal share of transboundary water resources and the sustainable management of the river basin. Thus, treaties according to water quantity and quality, administrative structures as well as geopolitical institutions like river basin organizations have to be created (*Matthews & St. Germain*, 2007). These processes are called hydropolitics. The risk of political dispute over the shared waters is defined as hydropolitical vulnerability (*Wolf*, 2007). Water quantity is considered as a mayor point in conflicts (*Matthews & St. Germain*, 2007). Almost 90 % of conflictive water events are related to water quantity and infrastructure (*Wolf*, 2007).

To prevent water conflict, in the years 1950 - 2000, 157 treaties have been negotiated initiating institutional agreements to cooperate (*Wolf et al.*, 2003a).
Related to water quantity Draper & Kundell (2007) identified five water sharing strategies:

1) Priorities of use according to specific water demands (e.g. agricultural, municipal)
2) Limitations placed on water storage by the upstream riparian
3) Delivery of a specific quantity of water by the upstream party at a particular location
4) Division among the parties according to a certain percentage of the flow at a particular location
5) Allocation of water according to a predetermined objective function (*Draper & Kundell*, 2007) (e.g. equal benefit in hydropower generation (*Wolf*, 2007)).

With regard to treaty formulation the hydrological conditions in quantity and variability have to be represented (*Draper & Kundell*, 2007). However, the majority of water allocation agreements does not include regulations for extreme hydrological conditions as droughts and floods (*Stahl*, 2005). Furthermore, they ignore the hydrological variability of river flow (*Giordano & Wolf*, 2003) whose consideration would be able to increase the efficiency of water allocation agreements (*Ansink & Ruijs*, 2008). The majority of recently signed treaties considers only floods and not droughts (*Drieschova et al.*, 2008) and Ansink & Weikard (2009) stated that contested water rights impede water trade due to overlapping claims to water as a scarce resource. In general, riparian countries based their initial position in water allocations on hydrography or chronology of use (*Wolf*, 2007) as well as irrigation needs or historic use (*Ansink & Weikard*, 2009). Especially upstream riparian countries favored the Harmon Doctrine, arguing "that water rights originate where the water falls" (*Wolf*, 2007). In arid regions treaties were signed according to agricultural and human needs (*Wolf*, 2007).

1.3 International River Basins and Water Allocation Agreements – Review

In literature, a wide range of research on International River Basins relating to conflict and cooperation exists and different approaches can be identified. Social and political science discussed international and regional water law (e.g. *Zaag van der*, 2009), international transboundary water management (e.g. *Giordano & Wolf*, 2003) and analyzed water allocation agreements (e.g. *Drieschova et al.*, 2008) as well as their adaptation to climate change (e.g. *Draper & Kundell*, 2007; *Ansink & Ruijs*, 2008). They analyzed a particular transboundary river basin (e.g. *Sneddon & Fox*, 2006; *Lange et al.*, 2007) as well as conflict and cooperation in International River Basins in general (e.g. *Wolf et al.*, 2003a; *Wolf et al.*, 2003b). The applied methods ranged from descriptive (e.g. *Sneddon & Fox*, 2006), to empirical (e.g. *Stahl*, 2005), to theoretical approaches like game models (e.g. *Ansink & Ruijs*, 2008). Whereas, economics and hydrology applied hydroeconomic modelling approaches (e.g. *Juízo & Lidén*, 2008).

Various studies analyzed treaty stability, conflict and cooperation in one selected International River Basin delineating the past and current situation by focusing on conflict. In recent years, studies used a more general approach. The Transboundary Freshwater Dispute Database (TFDD) (http://www.transboundarywaters.orst.edu) merged event data of conflict and cooperation, social data like population density and physical information like national and watershed borders, as well as climate on the river basin scale. This offers the possibility to link water relations to political, socioeconomic and physical information in general as well as chronologically (*Yoffe et al.*, 2004).
Applying the TFDD, Wolf et al. (2003b) used an empirical approach to identify International River Basins with the greatest risk of conflict in the next five to ten years (named as 'basins at risk'). The analysis was based on observed conflict and cooperation events between riparian states worldwide in the years 1950 - 2000. A BAR scale provided clear definitions and graduations of different levels of conflict and cooperation. They drew the following conclusions: (i) basin wide networks and river basin organizations attenuate conflict, (ii) internationalization and unilateral basin development like. dams are the only stand alone parameters which might result in conflict, (iii) widely assumed conflict parameters like climate, democracy and economic development have to interact to result in conflict, (iv) the development of new technologies as well as new river basin management concepts might invalidate their empirical approach for future predictions (*Wolf et al.*, 2003b). Opposed to Wolf et al. (2003b), Wolf et al. (2003a) applied relative frequency distributions of conflict / cooperation levels based on basin country polygons (country's share of an International River Basin) instead of basin-wide averages of conflict and cooperation. They concluded that the frequency distribution of events depends on the climate region. In arid and semi arid regions the relative frequency of most conflictive events was significantly higher compared to random samples, low for neutral to slightly cooperative events and high for most cooperative events resulting in neutral when averaging all events. Stahl (2005) used a classification tree model to classify International River Basins according to conflict and cooperation. The root node was an index of aridity and Stahl (2005) identified a greater number of conflictive events on the arid part of the classification tree confirming the importance of annual precipitation as well as its seasonality in the evaluation of conflict and cooperation in International River Basins as stated by Wolf et al (2003a). There-

fore, the examination of the vulnerability of stream flow allocations especially in semi arid to arid regions is of great importance.
Though, those regions are faced to data scarcity. Stahl (2005) emphasized the importance of river discharge in conflict analysis as hydro climatology datasets may not represent river flow in quantity and in temporal distribution as well as water quality and anthropogenic influences (e.g. dams, irrigation systems) and pointed out the problem of data availability. Consequently, the inclusion of river discharge data in the evaluation of the vulnerability of water allocation agreements is essential. One possibility is the consideration of global grid water resource data e.g. modelled under the consideration of human water consumption (*Döll et al.*, 2003) as well as under the consideration of crop growth, reservoir operation and environmental flow requirements (*Hanasaki et al.*, 2007).

Beside the evaluation of river discharge, the water allocation agreement itself is essential considering the vulnerability of water allocations in International River Basins. Drieschova et al. (2008) identified the current employed strategies in water allocation agreements to cope with flow variability. These were percentage flow allocations, infrastructure to regulate flow, cooperative institutions, data exchange and advance warning systems. They stated that the mayor challenge in treaty formulation is to balance treaty flexibility and enforceability.
Especially, the consideration of future treaty vulnerability gained in importance. Up to now, this was done generally. Drapper & Kundell (2007) specified the adaptability of different water agreements types to climate change classified by geographical region. They concluded that future challenges are the unknown quantity and timing of discharge because current water allocations are based on past flow records which become invalid under the aspect of land use and climate change. A further method to analyze the influence of climate change on water agreement's stability is the application of game theoretic models with the help of sharing rules as did Ansink & Ruijs (2008). They concluded: (i) a decrease in mean river flow lowers the stability of an agreement, (ii) an increase in variance of mean river flow can either have a positive or a negative effect on treaty stability, (iii) the stability of a water allocation agreement is highest for fixed upstream allocation followed by proportional allocation and lowest for fixed downstream allocation (*Ansink & Ruijs*, 2008).

To test and to simulate the compliance of water allocation agreements hydroeconomic models, combing hydrological conditions and economic, social and environmental aspects, are applied. Therefore, rainfall runoff models, historical or stochastic stream flow time series are linked to system analysis tools (nodal networks) which model anthropogenic systems (dams, water distribution networks etc.) and water distribution rules are applied. The water allocation can be related to individual users, infrastructure, environment, various sectors as well as nations. The aim of hydroeconomic models is to minimize costs or rather maximize benefits in terms of integrated water resource management (*Harou et al.*, 2009). With respect to transboundary water management and transboundary water allocation agreements, hydroeconomic models refer to the fifth water sharing strategy of Draper & Kundell (2007).
A great variety of system analysis tools exists and has been applied to transboundary river basin conflicts to evaluate the benefits of different water policies (*Harou et al.*, 2009).

Medellín-Azuara et al. (2007) analyzed water supply options for environmental restoration of the Colorado River Basin testing the option of additional Colorado River flow from the United States applying the CALVIN model. Fisher et al. (2002) used the Water Allocation System (WAS) model to assist in the formation of water policies of Israel, Jordan and Palestine. Juízo & Lidén (2008) applied three system analyses tools (WAFLEX, WEAP21, WRYM) to the Umbeluzi River Basin shared between Swaziland and Mozambique to simulate different basin development scenarios (construction of dams, increasing water demand) for the year 2025 after natural stream flow was simulated with the Pitman Rainfall-Runoff Model. Lange et al. (2007) tested a framework for water accounting for the Orange River Basin shared between Botswana, Namibia, Lesotho and South Africa.

Harou et al. mentioned (2009) that up till now, these approaches are still theoretical and not yet put into practice. Problems arise due to high data requirement and high uncertainties (*Harou et al.*, 2009). This incapacitates hydroeconomic models for a fast and easy transferable evaluation of the vulnerability of stream flow allocations.

1.4 Objectives

Considering the evaluation of the vulnerability of stream flow allocations regarding the presented literature the following conclusion can be drawn:

Skilful predictions of river flow in International River Basins are important for economic, political and societal applications of the riparian states and in particular for water management expressed in a transboundary water allocation agreement. As data scarce regions will be most affected by climate and land use change, the study analyzed the skill of open source gridded climate datasets to model stream flow with the objective to evaluate the past, present and future vulnerability of stream flow allocations.

This was achieved in three steps with their respective questions in the International River Basins Kunene, Upper Niger and Upper Jordan.

1) Analysis of the spatial and temporal anomaly and correlation of different gridded precipitation datasets.
2) Modelling of stream flow on a daily time step and on a monthly time step applying gridded climate data - raising the following key questions:
   - Is it possible to model stream flow with open source gridded climate input data on a monthly and on a daily time step?
   - If there are differences between the climate datasets what are their impacts on the modelling results?
   - Does an optimal input data – model combination exist?
3) Comparison of the gained modelling results with existing terms of transboundary water allocation commitments - raising the following key questions:
   - Is it possible to judge the past, present and future vulnerability of stream flow allocations with open source gridded climate input data from a hydrological point of view?
   - Does the choice of the climate input dataset and the choice of the model impact the evaluation of the vulnerability of water allocation agreements?

- What kind of water allocation thresholds referring to amount, variability and time step can be represented by the selected hydrological method?

2. Study Areas

For the identification of a river basin suitable for a case study, I established three main case study selection criteria: (i) Open source input data to be able to transfer the methodological framework to as many river basins as possible. (ii) Existence of a water allocation agreement and (iii) a minimum of discharge control structures to facilitate the modelling of stream flow.
Based on the listed case study selection criteria the Kunene River Basin was chosen as a first case study. The Jordan River Basin and the Niger River Basin followed. The choice of the latter was not primarily based on the selection criteria.

2.1 The Kunene River Basin

2.1.1 Geography

The Kunene (Cunene) River Basin (Figure 1) covers an area of about 110,000 km² (*TFDD*, 2007) stretches out over 1,050 km and has an average elevation above mean sea level of 1,900 m (*Heyns*, 2003). Angola shares 86.68 % of the Kunene River Basin, Namibia 13.32 % (*TFDD*, 2007). The source of the Kunene River is located in south-western Angola in the Sierra Encoco Mountains near Huambo (*Heyns*, 2003). Flowing southward the river turns westerly at the Ruacana Falls. Henceforward, the Kunene River marks the national border between Angola and Namibia at a length of about 340 km before reaching the Atlantic Ocean at Foz do Cunene.

2.1.2 Climate

In the Angolan headwaters of the Kunene River Basin mean annual precipitation is about 1,200 mm decreasing from North to South (Matala 600 mm; Ruacana 200 mm). According to the Köppen-Geiger climate classification climate is referred to as Cwb (temperate – dry winter – warm summer). The Namibian part of the Kunene River Basin belongs to BSh (arid – steppe – hot) / BWh (arid – desert – hot) climate (*Peel et al.*, 2007) with mean annual precipitation ranging from 200 mm in the East to about 30 mm at the coastal plain in the West (*Oldenborgh van*, 2009).

2.1.3 Transboundary Freshwater Resources

The discharge at Ruacana averages 5.5 km³/a including a high seasonality (*BfG*, 2009). The lower reaches of the river are almost waterless at the end of the dry season. Through the construction of the Kunene River scheme (section 2.1.4), including a hydroelectric power station and several dams, the river flow should be regulated (*FAO*, 2005).
The FAO AQUASTAT Database (*FAO*, 2005) points out that 86.4 % (39.3 km³/a) of Namibians natural renewable freshwater resources are transboundary. 11.6 km³/a of transboundary

surface water is underwritten by treaties, yielding to a dependency ratio (ratio of actual external renewable water resources guaranteed trough treaties and total actual renewable water resources) of 65 % (Angola 0 %). These numbers indicate the importance of transboundary waters to Namibia. At the Kunene River 0.185 km³/a of 5 km³/a of natural available water is guaranteed trough treaties (details section 2.1.4). This water supply is essential to the 700,000 people living in Northern Namibia. The highest water demand is in October, which conforms with minimum flow in the Kunene (*FAO*, 2005).

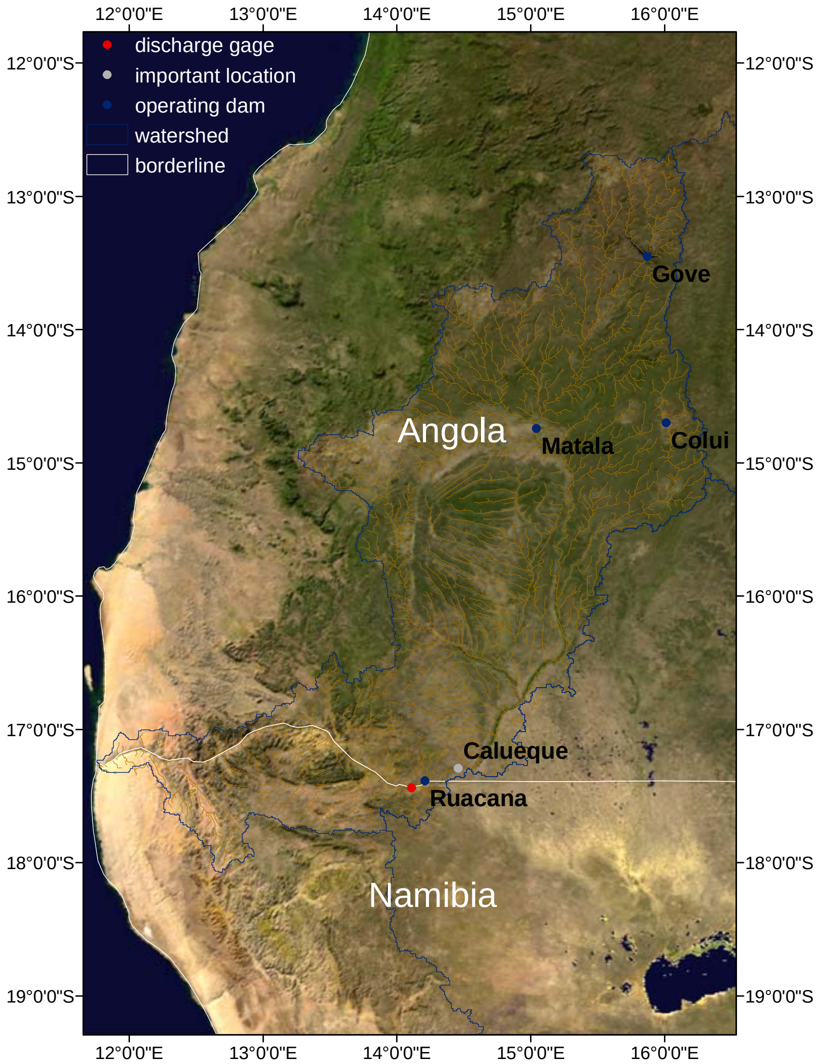

Figure 1: Map of the Kunene River Basin (dams refer to Heyns, 2003; FAO, 2006; Tarr, 2007 validated via Google Maps; Kluge et al., 2008), (satellite image: Map Maker Trust, 2007).

2.1.4 Water Allocations

The riparian countries in the Kunene River Basin concluded four mayor agreements related to water allocations in the years 1926, 1964, 1969 and 1990.

In the following section I will point out the mayor subjects related to water quantity determined in these agreements.

In July 1926, Portugal and South Africa regulate the use of the water of the Kunene River concerning irrigation and hydropower. Preconditioning a water schema, Namibia has the right to use half of the flow (*Heyns*, 2003). Followed by an agreement in 1931, expressing the supply of drinking water to the inhabitants of Ovamboland (Southern Angola / Northern Namibia) for drinking and cattle (*TFDD*, 2007).
In January 1969, Portugal and South Africa sign the "Agreement between the Government of the Republic of South Africa and the Government of Portugal in regard to the first phase of development of the water resources of the Cunene River Basin" in pursuance of "The Agreement between the Government of the Republic of South Africa and the Government of Portugal in regard to rivers of mutual interest and the Cunene River scheme" signed in October 1964 declaring equitable share of the international water resources for an optimum of benefit within the available quantity of water including other international river basins as Okavango, Incomati and Limpopo (*Heyns*, 2003).

2.1.4.1 The Cunene River Scheme

The agreement establishes the Permanent Joint Technical Commission (PJTC) "to study and report on matters relating to the present Agreement" (article 2.2). A mayor point is "the regulation of flow of the Cunene River" (article 1.2). In view of water quantity, the following subitems are arranged (*South Africa & Portugal*, 1969):

- Construction of the Gove dam (article 4.1) to improve the generation of hydroelectric power at Matala and to begin "irrigation and supply of water for human and animal requirements in the middle-Cunene". Based on the financial participation of South Africa and the planned generation of hydroelectric power at Ruacana, "Portugal agrees not to abstract more than 50 per cent of the resulting regulated flow of the river which […] shall be taken as 80 m³/s at Ruacana" (article 4.1.11). This value can be adjusted when hydrological analyses are available.
- Construction of the Calueque dam (article 4.2) "in accordance with the requirements of the power station to be built at Ruacana" including "a scheme at Calueque for pumping water from the Cunene River to supply water for human and animal requirements in South West Africa and initial irrigation in Ovamboland" (article 4.2.1). The abstracted water is "limited to one half of the natural flow of the river at the point of abstraction during that week, subject to a maximum pumping rate of 6 m³/s" (article 4.2.2). After further negotiations between Portugal and South Africa, the amount of abstracted water can be augmented "when the regulation of the river justifies this, and in keeping with the mutually agreed best joint utilization of the river" (article 4.2.3).
- Construction of a hydroelectric power station at Ruacana (article 4.3) for the supply of power mainly to South West Africa. "The South African authorities shall […] have the exclusive use in perpetuity of the flow of the river regulated by the dams of the first phase, from the upstream limit of the Ruacana diversion weir basin to below the Ruacana power fall" (article 4.3.4).

After the Namibian declaration of independence in 1990, Angola and Namibia affirm the agreement of 1969 (*Heyns*, 2003; *Meissner*, 2003) in the "Agreement in regard to the development and utilization of the water potential of the Kunene River" (*FAO et al.*, 2008) with the aim to terminate the Cunene River scheme of 1969 and to develop it further (*Meissner*, 2003).

2.1.4.2 Realization of the Cunene River Scheme and present situation

Due to the Angolan civil war, the Cunene River scheme of 1969 is not realized entirely as well as some constructions got damaged as a result of military force (*Heyns*, 2003). In 1975, South African troops moved into Angola to occupy the Gove dam and the Ruacana power station temporarily to defend the water resources (*Meissner*, 2003).

Related to regulation problems and damages at the Gove dam the seasonal river flow is not regulated (*FAO*, 2005) and Ruacana power station can not work under full capacity during the dry season (*Heyns*, 2003; *Tarr*, 2007). The dams at Matala and Coliu are operating. It is planned to build an additional dam at the border section to generate further electricity. Because of a high gradient this river section is important to hydropower generation (*Heyns*, 2003). At the outset, Namibia favoured the Epupa site (after Ruacana), Angola the Baynes site (further downstream) (*Meissner*, 2003; *Böge*, 2005). International and local critique on the relocation of the Himba (*Böge*, 2005), ecological damages (*Tarr*, 2007) and the limited economic resources of Angola deferred the project at Epupa site (*Meissner*, 2003). According to Tarr (2007), Namibia has abandoned Epupa site and favours Baynes site now.

The pipeline at Calueque has a length of 300 km and a capacity of 3.2 m^3/s and is planned to be extended to supply the agreed 6 m^3/s (185 M m^3/a) (*Heyns*, 2003). Current pumping rates undercut the agreed amount ranging between 47 M m^3/a and 63 M m^3/a (*Klintenberg et al.*, 2007).

2.1.4.3 Interbasin relationship

Meissner (2003) noted that the "Kunene River seems to be the antithesis of the traditional assumptions about conflict in international river basins in arid regions". He mentioned the cooperation among the riparian states in regard to the transbasin water transfer to the Cuvelai basin at Calueque under Namibian authority on Angolan territory.

In contrast, Klintenberg et al. (2007) and Kluge et al. (2008) pointed out that due to economic and demographic development water demand on Angolan and on Namibian side will increase. Additionally, Angola has a high irrigation potential in the middle Kunene. Thus, should Angola decide to use more water themselves, it might lead to conflict between the two governments on the one hand and water users in the Angolan part of the Kunene basin and the Namibian part of the Cuvelai basin on the other hand. The difficult political conditions and the claim of various water sectors amplify the risk of conflict (*Klintenberg et al.*, 2007; *Kluge et al.*, 2008).

Wolf et al. (2003b) identified the Kunene River Basin as a 'basin at risk' in the next five to ten years.

2.2 The Niger River Basin

2.2.1 Geography

The Niger River Basin (Figure 2) covers an area of about 2,113,200 km². The main channel stretches out over 4,200 km. The Niger River Basin is shared by eleven nations (Nigeria 26.59 %, Mali 25.58 %, Niger 23.56 %, Algeria 7.63 %, Guinea 4.54 %, Cameroon 4.17 %, Burkina Faso 3.93 %, Benin 2.14 %, Ivory Coast 1.08 %, Chad 0.78 % and Sierra Leone < 0.00 %) whereas the main stream is merely shared by Guinea, Mali, Niger and Nigeria (*TFDD*, 2007). The source of the Niger River is located in the Fouta Djallon Mountains in Guinea. It flows in a north easterly direction traversing the interior plateau towards the Niger delta in southern Mali. This interior delta can extend over 450 km in length and more than 200 km in width during the flood season. Afterwards, making a bend, the river flows in a south eastern direction to Niger. Subsequently, the river marks the border between Niger and Benin before it enters Nigeria and reaches the Atlantic Ocean at the Gulf of Guinea. The Niger River has several important tributaries. In Guinea the Niandan, the Milo and the Tinkisso River, in Mali the Fie and the Sangarani River, both rising in Guinea, flow into the Niger River. The most important tributary in Mali is the Bani River stretching out over 1,120 km rising in Ivory Coast and Burkina Faso. In Niger the Faroul, the Dargol, the Sirba, the Garoubi and the Tapoa River and in Benin the Mekrou River contribute to the waters of the main channel. Nigeria has several important tributaries of the Niger River (e.g. Sokoto, Malendo, Kaduna, Benue). The Benue River is the mayor tributary rising in Cameroon (*Godana*, 1985; *Shahin*, 2002).

2.2.2 Climate

Due to the large extent of the Niger River basin climate is various. In the southern parts along the Atlantic coast, climate is described as Aw (tropical – Savannah) according to the Köppen-Geiger climate classification. This is expressed in a monthly mean air temperature above 18 °C throughout the whole year and precipitation of the driest month less than [100 - mean annual precipitation [mm]/25] leading to a pronounced dry season (*Peel et al.*, 2007). This precipitation seasonality is caused by the south eastern anti-cyclone monsoon. In the upper reaches of the Niger River basin, mean annual precipitation is about 2,032 mm mainly limited to the rainy season from April to November (*Godana*, 1985). In the interior northern areas a transition from BSh (arid – steppe – hot) to BWh (arid – desert – hot) climate can be found (*Peel et al.*, 2007). Precipitation in the Niger delta is only 254 mm. Turning southwards precipitation rises over 2,000 mm again. Since the 1970, Western Africa is exposed to severe droughts due to declining precipitation and a shift in the rainfall regime (*Dezetter et al.*, 2008; *Owusu et al.*, 2008).

2.2.3 Transboundary Freshwater Resources

The climate variety is transmitted to the discharge regime of the Niger River. In the Upper Niger, peak flow is in June and low flow occurs in December. In the middle Niger, maximum discharge values are reached in January, minimum values in April to July. In the lower Niger, low flow is in April and May and maximum flow occurs in September due to the influence of the

Benua River having its peak flow in August / September and its low level in March (*Godana*, 1985). The evolution of the mean annual river discharge can be seen in a discharge profile along the river. At the Guinean Malay border mean annual discharge is around 31.5 km³/a (*BfG*, 2009) decreasing slightly in the interior parts due to seepage and high evapotranspiration losses in the delta region (*Godana*, 1985). Afterwards, discharge increases reaching 78.8 km³/a after the confluence of the Kaduna River, 157.7 km³/a after the confluence of the Benue River and 220.7 km³/a at the river mouth (*Shahin*, 2002; *BfG*, 2009).

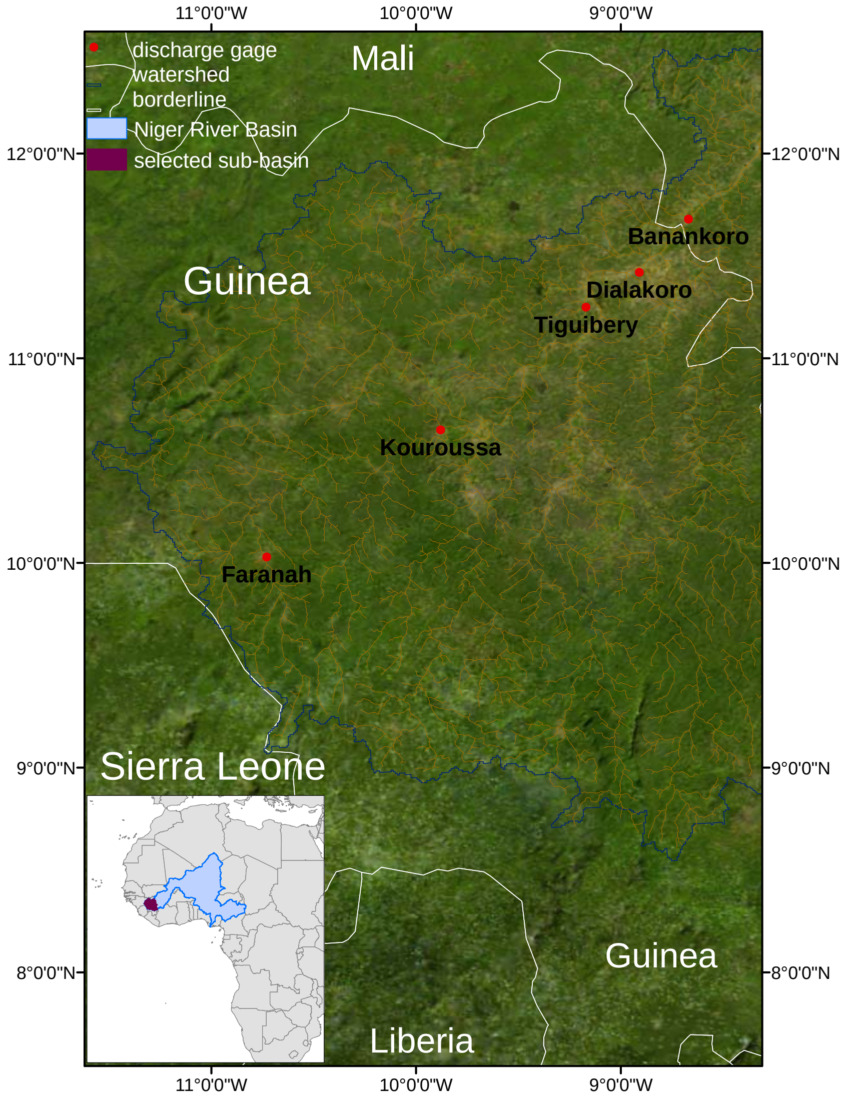

Figure 2: Map of the Upper Niger River Basin and the Niger River Basin (small map) (satellite image: Map Maker Trust, 2007).

2.2.4 Water Allocations

According to the TFDD (2007) one treaty with regard to water allocation in the Niger River Basin exists. This treaty, negotiated between Niger and Nigeria, covers several transboundary sub-basins of the Niger River Basin. “Each Contracting Party is entitled, within its territory, to an equitable share in the development, conservation and use of the water resources in the shared river basins" (article 2). This equitable share is gained by taking factors like rainfall patterns, the contribution of each riparian state to the rivers water balance, surface hydrology, hydrogeology, water use, future water use, social and economic development, dependence on the water resource and environment into account (*Nigeria & Niger*, 1990).

2.3 The Jordan River Basin

2.3.1 Geography

The Jordan River Basin (Figure 3) extends over 42,800 km² and is shared between Jordan (48.13 %), Israel (21.26 %), Syria (11.45 %), the West Bank (7.48 %), Egypt (6.31 %), the Golan Heights (3.5 %) and Lebanon (1.33 %) (*TFDD*, 2007).
The Jordan River evolves of the Dan, the Hasbani and the Banyas River whose springs are located in Israel, Lebanon and Syria respectively at the Southern and Western slopes of the karstified Mt. Hermon (*Rimmer & Salingar*, 2006). The 40 km long drainage system above the Sea of Galilee is called Upper Jordan River and is characterized by a high elevation gradient. The Lower Jordan River marks the border between Jordan, Israel and the West Bank respectively before draining into the Dead Sea. The principal tributary of the Lower Jordan River is the Yarmouk River. It has its source in Syria, flows westwards along the Syrian-Jordan border and marks the border between Jordan and Israel afterwards (*Elhance*, 1999).

2.3.2 Climate

Climate in the Jordan River Basin is referred to as Csa (temperate, dry and hot summer) (*Peel et al.*, 2007). In the Upper Jordan River, annual precipitation is higher than 1,300 mm at the snow affected Mt. Hermon and declines sharply southwards. Precipitation is restricted to the wet season ranging from October to April (*Rimmer & Salingar*, 2006).

2.3.3 Transboundary Freshwater Resources

The discharge at Obstacle Bridge averages 0.46 km³/a including a high seasonality (*BfG*, 2009). The FAO AQUASTAT Database (*FAO*, 2005) points out that 58 % (1.03 km³/a) of Israel's natural renewable freshwater resources are transboundary (Jordan 58 % (0.94 km³/a)). The dependency ratio is 57.9 % (Lebanon 0.785 %, Syria 72.4 %, Jordan 27.2 % and Occupied Palestinian Territory 2.99 %) (*FAO*, 2005). However, it has to be taken into account that these numbers are estimated for the entire country and not on the basin scale. The high dependency ratio of Syria is based on a more important transboundary water resource - the Euphrates.
Elhance (1999) stated that there is a great spatial mismatch of water resources and demand in the Middle East. Therefore, Israel completed the National Water Carrier in 1964 distributing water from the Sea of Galilee which serves as a natural water storage system, to the western areas (*Elhance*, 1999). The lake provides 35 % of Israel's drinking water (*Rimmer & Salingar*,

2006). Jordan constructed the East Ghor Channel as an irrigation system taking water from the Yarmouk River (*Elhance*, 1999).

Figure 3: Map of the Jordan River Basin (satellite image: Google, 2009).

2.3.4 Water Allocations

The "Johnston Negotiations" of 1955 between Israel, Jordan, Lebanon and Syria were one of the first attempts to allocate the water of the Jordan River. Although, they have never been ratified, they continue to serve as a guideline (*Elhance*, 1999; *FAO*, 2005). Based on the area of irrigable land, Syria should receive 132 MCM, Jordan 720 MCM, Israel 400 MCM and Lebanon 35 MCM. Additionally, the Negotiations arranged the construction of cannels, dams, storage systems and distribution networks (*Israel et al.*, 1955).

The Jordanian-Israeli Peace Treaty, signed in 1994, is the only treaty between riparian states of the Jordan River Basin related to water allocation both river discharge and groundwater. In the winter period, Israel receives 13 MCM (12 MCM in the summer period) of the Yarmouk River for personal use and 20 MCM for storage in the Sea of Galilee which have to be returned to Jordan in the summer period. In the case of the Jordan River, no precise allocation exists. “Israel is entitled to maintain its current uses of the Jordan River waters between its confluence with the Yarmouk, and its confluence with the Tiral Zvi / Wadi Yabis. Jordan is entitled to an annual quantity equivalent to that of Israel, provided however, that Jordan's use will not harm the quantity or quality of the above Israeli uses” (article I.2.c). In winter, Jordan obtains a minimum average of 20 MCM of flood water south of the confluence with the Yarmouk. Additionally, Jordan receives 50 % of about 20 MCM desalinated water of saline springs annually and the two states “shall cooperate in finding sources of the supply to Jordan of an additional quantity of 50 MCNV / year” (article I.3) as well as in the construction of additional storage systems. For survey, the two riparian states established a Joint Water Committee (*State of Israel & The Hashemite Kingdom of Jordan*, 1994).

In 1995, Israel and the Palestine Liberation Organisation signed “The Israeli - Palestinian Interim Agreement on the West Bank and the Gaza Strip” assigning territorial jurisdiction to the Palestinians including subsoil and territorial waters. The treaty regulates the available and future water quantity for the West Bank and the Gaza Strip by focusing on groundwater and establishes a Joint Water Committee (*State of Israel & Palestine Liberation Organization*, 1995).

3. The Models

Regarding the vulnerability evaluation of water allocation agreements the available water resource stream flow has to be assessed. Therefore, a simple water-balance model was required to simulate stream flow. Simple is defined herein with low data requirement and a small number of parameters. In addition, the model should be able to cope with semi arid to arid conditions. Compared to humid regions, semi arid to arid regions are in general characterized by a high rainfall variability in space and in time, by different runoff processes like Horton overland flow, and transmission losses, by vegetation dynamics strongly that are dependant on the amount of available water and by a lack of observed event data as well as a low data accuracy of stream flow due to variable cross sections and high bed loads. These conditions complicate rainfall-runoff modelling in semi arid regions and lead to different approaches than those applied in humid regions (*Pilgrim et al.*, 1988).

On the one hand, there are low data requiring conceptual rainfall-runoff models, where time series on air temperature and precipitation as input data and stream flow for calibration are necessary. Xu & Singh (1998) gave a brief summary of simple monthly water balance models e.g. the three parameter Tα-model (*Alley*, 1984). On the other hand, there are models especially developed for flow processes in semi arid to arid regions like Sacramento Soil Moisture Accounting Model, Pitman Model (applied by e.g. *Hughes*, 1995). Those models are process orientated and thus have a much more complicated structure and a greater number of calibration parameters. However, in respect to water allocations stream flow is the relevant model output. The modified version of the IHACRES (Identification of unit Hydrographs And Component flows from Rainfall, Evapotranspiration and Stream flow data) (*Jakeman et al.*, 1990; *Jakeman & Hornberger*, 1993) rainfall–runoff model by Ye (1997) fulfils both requirements: being simple and being able to simulate rainfall-runoff relationship in semi arid to arid regions. IHACRES is also well documented.

3.1 The IHACRES Rainfall - Runoff Model

IHACRES is a lumped metric-conceptual water balance model developed by Jakeman et al. (1990) and Jakeman & Hornberger (1993), extended to ephemeral streams by Ye et al. (1997), to snow affected catchments by Schreider et al. (1997) and by a more physically based catchment moisture deficit accounting module (CMD) by Croke & Jakeman (2004). Littelwood (2002) extended the IHACRES model to improve the adaptation on low flows.

IHACRES has been successfully applied to a large number of catchments varying in scale, time step and climate. Originally, IHACRES was developed to model stream flow in humid regions. The first application was realized in two small humid upland catchments in Wales (*Jakeman et*

al., 1990). The first application in semi arid to arid catchments was accomplished by Ye et al. (1997) who applied a modified version of IHACRES to three low-yielding ephemeral catchments in Western Australia.
IHACRES has been applied to regionalization studies (e.g. *Post & Jakeman*, 1996; *Kokkonen & Jakeman*, 2002) and used in the framework of the Predictions in Ungauged Basins (PUB) initiative of the International Association of Hydrological Science (*Croke & Jakeman*, 2008). Further applications have examined the impact of climate and land use change. Sefton & Boorman (1997) applied eight hypothetical climate change scenarios and two climate change scenarios using GCMs to three British catchments. Schreider et al. (2000) applied IHACRES to three ephemeral Australian catchments to evaluate the effect of climate change on urban flooding using GCMs and a stochastic weather generator. Evans & Schreider (2002) and Evans (2003) coupled CMD-IHACRES and GCMs / RCMs to specify the impact of climate change on stream flow. An estimation of land use change by analyzing model (CMD-IHACRES) residuals has been accomplished by Kokkonen & Jakeman (2002). Jakeman & Letcher (2003) coupled IHACRES with a crop, a sheet erosion and an economic model for integrated water resources assessment.

In this thesis I applied the IHACRES v2.1.2 open source software (http://www.toolkit.net.au/Tools/IHACRES) released June 2006 by iCAM (Integrated Catchment Assessment and Management Centre), CRCCH (Cooperative Research Centre for Catchment Hydrology) and CSIRO (Commonwealth Scientific and Industrial Research Organisation), implementing the modified version of Ye et al. (1997).

The lumped approach of the IHACRES model assumes that the spatial and temporal distribution of infiltration capacity, rainfall and rainfall intensity are homogenous within the whole catchment (*Jakeman et al.*, 1990). IHACRES consists of a non-linear and a linear module leading to the "hypothesis that, after allowing for antecedent conditions, the response to a catchment is predominantly linear over a wide range of temperate climatological regimes and down to small catchment scale" (*Jakeman & Hornberger*, 1993).

The non-linear module estimates effective rainfall u, that part of observed precipitation r becoming stream flow, at each time step k. In literature, different non-linear modules have been applied (*Jakeman & Hornberger*, 1993; *Ye et al.*, 1997; *Croke & Jakeman*, 2004; 2008). The IHACRES v2.1.2 software implements a reformulated algorithm of the non-linear module of Ye et al. (1997) to calculate effective rainfall by reducing observed precipitation r (*Croke & Jakeman*, 2008).
The antecedent precipitation index or catchment wetness index s_k is calculated by exponential weighting of the observed rainfall time series P_k:

$$s_k = P_k + (1 - t_k^{-1}) s_{k-1} \tag{1}$$

where the drying rate t_k describes the rate at which the catchment wetness declines in the absence of rainfall. This drying rate t_k is given by:

$$t_k = t_w \exp(0.062 f (T_r - T_k)) \tag{2}$$

where t_w represents the reference drying rate (*Croke & Jakeman*, 2008). The temperature modulation factor f determines how the reference drying rate t_w changes with temperature (*Jakeman & Hornberger*, 1993) thus represents the intraannual evapotranspiration change (*Post & Jakeman*, 1996). T_r is the reference temperature for which Post & Jakeman (1996) applied the annual mean temperature. T_k is the air temperature at time step k (*Croke & Jakeman*, 2008). The effective rainfall u_k is calculated as follows:

$$\begin{aligned} u_k &= [c(s_k - l)]^p P_k && \text{if } s_k > l \\ u_k &= 0 && \text{otherwise} \end{aligned} \tag{3}$$

(*Ye et al.*, 1997; *Croke & Jakeman*, 2008). Parameter c is adjusted to equal the volume of effective rainfall and stream flow (*Jakeman & Hornberger*, 1993). In the reformulated version, the mass balance parameter c is directly related to the gain of the transfer function to reduce the interaction between the parameters c and exponent parameter p. The non-linear loss module by Jakeman et al. (1990) is gained by setting the parameter value of l to zero and of p to one (*Croke & Jakeman*, 2008). The parameters of the non-linear module are calibrated via trial and error.

The linear module of IHACRES is based on the Unit Hydrograph Concept by Sherman which transforms calculated effective rainfall (non-linear module) into stream flow by a linear convolution integral. Depending on the catchment, different types of linear storage combinations (series / parallel) can be chosen.

In humid regions two parallel linear stores, representing a quick and a slow flow component, are commonly used (*Jakeman & Hornberger*, 1993). Higher order storage configurations lead to an increased parameter variance and not to an improvement in model performance (*Jakeman & Hornberger*, 1993; *Ye et al.*, 1997). Ye (1997) proposed the use of a single store for ephemeral rivers. For a single exponential store, daily stream flow Q_k is calculated as follows (*Croke & Jakeman*, 2008):

$$Q_k = -\alpha_i \, Q_{k-1} + \beta_i \, u_{k-\delta} \tag{4}$$

δ is the delay between rainfall and runoff estimated with the autocorrelation function. A second order transfer function represents the unit hydrograph response curve (details see *Croke & Jakeman*, 2008).

Each storage has a volumetric throughput υ_i relative to the other storages and a time constant TC_i representing the time for peak flow to recess to a value of exp(-1) of peak flow.

$$TC_i = -\frac{\Delta}{\ln(-\alpha_i)} \tag{5}$$

$$\upsilon_i = \beta_i / (1 + \alpha_i) \tag{6}$$

The parameters of the linear module are calculated by a refined instrumental algorithm (details see *Jakeman et al.*, 1990). Croke (2006) amplified the fitting procedure for ephemeral streams through the introduction of a power law form of the unit hydrograph.

3.1.1 Parameter Dependencies

Jakeman & Hornberger (1993) pointed out the problem of overparameterization as one of the major problems in rainfall-runoff modelling and stated that a model of low complexity as IHACRES is sufficient because the rainfall–runoff time series contains the adequate information.

The parameters of the two modules of IHACRES are independent from each other (*Jakeman & Hornberger*, 1993). The parameter values should not depend on the climate sequence used for calibration (*Post & Jakeman*, 1996; *Kokkonen & Jakeman*, 2002). Whereas, they are related to catchment attributes. Post & Jakeman (1996) found a relationship between the time constant of the quick flow recession and the drainage density and a slight relationship with the catchment area. The time constant of the slow flow recession was correlated with the catchment's slope and elongation. The evaporative loss was correlated with the amount of radiation received and the vegetative water use.

Storage parameters related to e.g. soil storage and parameters depending on vegetation can change in the long term due to climate and land use change as well as erosion. Leaving a parameter value constant to model a future scenario, it is assumed that the change of process, represented by the parameter, is small in contrast to the change in the climate input data (*Boorman & Sefton*, 1997).

3.2 Hamon's Method and Simple Bucket Model

To validate the results gained by the IHACRES rainfall-runoff model, a soil water balance model, based on the simple bucket concept (see e.g. *Xu & Singh*, 2004) and the Hamon's method (*Hamon*, 1961) to estimate potential evapotranspiration, was introduced.

Hamon's method (*Hamon*, 1961) is an empirical approach to calculate potential evapotranspiration pt in [mm/day] based on saturated water pressure svp and the average number of daylight hours per day H during the selected month. Following Haith & Shoemaker (1987) the potential evapotranspiration after Hamon is calculated as follows:

$$pt_k = \frac{2.1\, H_k^2\, svp_k}{T_k + 273.3} \tag{7}$$

The saturated water pressure svp and the average number of daylight hours per day H are estimated following Hornberger & Wiberg (2005).

The saturated vapour pressure svp depends on air temperature T:

$$svp_k = 0.6108 \exp(\frac{17.27\,T_k}{T_k + 237.3}) \tag{8}$$

For the estimation of the average hours of daylight H, the angle of the sunset hours sha has to be taken into account. This parameter depends on the latitude lat of the selected location in [rad] and the solar declination dec:

$$H_k = 24\,\frac{sha_k}{\pi} \tag{9}$$

$$sha_k = \arccos(-\tan(\frac{2\pi\,lat}{360})\,\tan(dec_k)) \tag{10}$$

The declination of the sun is related to the Julian day of the year:

$$dec_k = 0.4093 \sin((2\pi/365)\;julday_k - 1.405) \tag{11}$$

Oudin et al. (2005) analyzed 27 potential evapotranspiration models in 308 catchments covering a wide range of climate zones. They concluded that empirical potential evapotranspiration models based on extraterrestrial radiation and mean daily air temperature, as the Hamon's model, were most efficient in daily rainfall-runoff modelling when utilizing a lumped conceptual model as is the case in the simple bucket model. In general, the performance of a rainfall-runoff model was not significantly influenced by the potential evapotranspiration model. More complicated potential evapotranspiration models require further climate data which are frequently not available (*Oudin et al.*, 2005).

The simple bucket model calculates stream flow q as the sum of overflow oflow and percolation to the groundwater perc. The operation time step k is [mm/month].

$$q_k = oflow_k + perc_k \tag{12}$$

The percolation to the groundwater depends on the soil water content swc of the previous month, the maximum depth of soil D and the maximum percolation from soil to groundwater SP_{max}:

$$perc_k = \frac{swc_{k-1}}{D}\,SP_{\max} \tag{13}$$

The soil water content swc is based on the water balance equation:

$$swc_k = swc_{k-1} + P_k - perc_k - at_k \tag{14}$$

If the soil water content exceeds the maximum depth of soil, overflow oflow starts (equation 17) and percolation perc is maximal (equation 16).

$$swc_k > D \tag{15}$$

$$perc_k = SP_{\max} \tag{16}$$

$$oflow_k = swc_k - D \tag{17}$$

$$swc_k = D \tag{18}$$

The calculation of the actual evapotranspiration at depends on the threshold AET which is the proportion at which at equals pt related to D.
If

$$\frac{swc_{k-1}}{D} < AET \tag{19}$$

then pt is reduced by the moisture extraction function

$$at_k = pt_k \frac{swc_{k-1}}{AET\ D} \tag{20}$$

otherwise at equals pt

$$at_k = pt_k\ . \tag{21}$$

The parameters D and SP are estimated via uniform sampling. The parameter value of AET is adjusted by the comparison of the simulated and the observed flow duration curves.

4. Input Data

4.1 Reanalysis Data

Reanalysis data (ERA-40) are a global multi-decadal assimilated daily dataset of climate variables based on synoptic surface observations, radiosondes and satellite data. The dataset was developed by the European Centre for Medium-Range Weather Forecast (ECMWF) and ranges from September 1957 to August 2002. The Reanalysis data were generated by numerical weather predictions adapting the model state to observations in a statistically optimal manner via an objective function. The created daily field has a grid resolution of 2.5° x 2.5°. The data quality depends on the quality and coverage of the observations, the quality of the model and the analysis (*Uppala et al.*, 2005). The data are distributed by the Climate Explorer (*Oldenborgh van*, 2009).

Leander & Buishand (2007) as well as Lavers et al. (2007) applied ERA-40 climate data to simulate river discharge with the rainfall-runoff model HBV and the Probability Distributed Model respectively. Leander & Buishand (2007) adjusted the temperature and precipitation time series of ERA-40 by a linear and a nonlinear bias correction to reproduce the statistical properties of observed data and to run a regional atmospheric climate model first and the rainfall-runoff model for the Meuse catchment (21,000 km²) afterwards. Lavers et al. (2007) used ERA-40 data and downscaled ERA-40 data as direct model input for the Dyfi catchment (471.3 km²). Without downscaled climate data, river discharge was considerably underestimated which the authors related to the lack of representativeness of local effects e.g. orographic in the data. Dutra et al. (2008) used ERA-40 precipitation data to calculate a drought index based on the soil moisture content and the energy balance. To evaluate the reliability of the ERA-40 data, the authors compared them against observations of the Iberian Peninsula. They detected a systematic underestimation and a reduced mean annual cycle of the ERA-40 precipitation data.

4.2 CRU Data

CRU TS 2.1 climate data are provided by the Climate Research Unit (CRU). They incorporate further temporal and spatial information into CRU TS 1.0 climate data by New et al. (2000) and were additionally tested for inhomogeneities applying an automated detection algorithm. The climate data consist of 0.5° - latitude - longitude - gridded terrestrial monthly data of precipitation, mean and diurnal air temperature called primary variables and the secondary variables wet-day frequency, vapor pressure, cloud cover and ground frost frequency covering the years 1901 - 2002. The primary variables are based on an interpolated anomaly field of the variables ranging from 1901 - 2002 combined with a mean monthly value field from 1961 - 1990 which serves as the standard period (*Mitchell & Jones*, 2005). Interpolation was done by angular distance weighting taking the eight nearest stations with an exponential correlation decay function into account (*New et al.*, 2000). Where no station within the correlation decay distance (air temperature 1,200 km, precipitation 450 km) was available stations with zero anomalies were inserted (*Mitchell & Jones*, 2005). The interpolation algorithm disregards elevation which might lead to prediction errors especially in precipitation. However, the monthly anomalies are a function of general climate patterns where the dependence on elevation plays a minor role (*New et al.*, 2000).

New et al. (2000) recommended CRU climate data for hydrological modelling at the regional scale. Therefore, numerous examples can be found in literature.
Yang & Musiake (2003) downscaled a 2° climate data set with the help of CRU data to model Asians main river's discharge with a grid based distributed model. On the contrary, Schuol et al. (2008) downscaled CRU data (1901 - 1995) to a daily time step using a weather generator to estimate the freshwater availability at the sub-basin level. The authors modelled successful an area of 4 million km² including the Senegal, Niger, Volta and Benue basins applying the semi distributed Soil & Water Assessment Tool. Dezetter et al. (2008) utilized CRU climate data to test whether an optimal model - data combination to model runoff in 49 Western African catchments exists. They calibrated two semi distributed models applying three potential evapotranspiration datasets and four water holding capacity datasets without detecting an optimal model - data combination. Similar analysis were conducted by Arnell (1999) who applied CRU data, downscaled to a daily time step, to run a gridded macro scale hydrological model for Europe. Döll et al. (2003) estimated the long term average water resources on a 0.5° global grid scale applying the WaterGAP Global Hydrological Model and CRU data downscaled on a daily time step. George (2007) used CRU precipitation data to calculate lag times between precipitation and stream flow and to relate stream flow to the state of the atmospheric circulation afterwards.

To my knowledge, Simmons et al. (2004) are the only authors who compared CRU and ERA-40 data systematically on a global scale. They examined trends and low frequency variability of monthly anomalies of mean surface air temperature and concluded that the two datasets agree in general. The agreement enhanced after 1967 due to a higher number of synoptic surface data resulting in an improved ERA-40 performance. After the elimination of linear trends, the datasets showed a similar month to month variability (correlations Europe 99.6, North America 98.7, Australia 92.5) and a similar interannual variability. Linear trends (1958 - 2001) were lower in ERA-40 dataset and agreed spatially in 64 % (1979 - 2001) and in 55 % (1958 - 2001).

4.3 Discharge Data

Discharge data were provided by the Global Runoff Data Centre (GRDC) (*BfG*, 2009).
Ruacana gauging station (14.1109°/-17.43° (*Murwira & Mazvimavi*, 2007)), located next to the Angolan Namibian border, is the only gauging station listed in the GRDC database for the Kunene River Basin (*BfG*, 2009). The gage's catchment covers an area of 84,952 km² which is 80 % of the total basin area (*Murwira & Mazvimavi*, 2007). Discharge data are available over a period of 47 years (01/10/1961 - 31/01/2007) including a data gap from 25/09/1979 to 31/12/1983. Mean annual discharge is 175.5 m³/s (65 mm/a) (*BfG*, 2009). A mayor problem is the unknown influence of dams further upstream. According to Murwira & Mazvimavi (2007) the main functions of the Ruacana discharge gage are water resources planning, environmental management and transboundary water resources planning and management.
Due to the large extend of the Niger River Basin with various climate and discharge regimes a sub-basin was chosen. In the Upper Niger Basin several discharge stations exist. Tiguibery gage (-9.17°/11.25°) situated about 80 km before the Guinean Mali border was found to be most reliable. The gage represents an area of 70,000 km² and covers the time period of 06/1952 - 11/1979 (data gaps: 01/1964 - 05/1964, 02/1965 - 07/1967). Mean annual discharge is 1,100.5 m³/s (496 mm/a) (*BfG*, 2009).
Monthly values of the Jordan River are provided by the Obstacle Bridge gauging station (35.62°/33.03°) for the time period of 11/1969 - 10/2004. Its catchment area is 1,376 km², mean annual discharge 14.8 m³/s (339 mm/a) (*BfG*, 2009). Obstacle Bridge gage was chosen because it is located above the Lake of Galilee where water storage and abstractions take place which are not included in the modelling framework.

5. Methodology

5.1 Analysis of Input Data

5.1.1 Climate Data

To test the reliability and the comparability in space as well as in time of the two climate input datasets ERA-40 and CRU several analyses focusing on precipitation were carried out.
Those grid points who are situated in and who are surrounding the modelled (sub-)basins were selected for the analysis. The analysis was realized for the entire period of 1958 - 2001.
As the ERA-40 data are operating on a lower grid resolution, the CRU data were upscaled by taking the arithmetic mean per time step of the 25 grid points representing the same area as a single ERA-40 grid point. In this way, two time series could be compared directly. In several cases, especially close to the coastline, CRU data were not available for all 25 CRU grid points representing the individual ERA-40 grid point. Then, the arithmetic mean of the remaining grid points was calculated. ERA-40 data operating on a daily time step were aggregated to a monthly time step by taking the sum of daily precipitation amount and by taking the arithmetic mean of daily air temperature for each month, respectively. Annual sums of precipitation where calculated based on the calendar year.

$$P_{annual} = \sum_{January}^{December} P_i \tag{22}$$

To estimate the mean annual and the mean monthly water balance the arithmetic means of annual sums and monthly sums were calculated.

$$\overline{AM} = \frac{1}{n}\sum_{1}^{n} P_i \tag{23}$$

The discrepancy of the entire input time series was expressed by the mean absolute error which is the average of the absolute differences of the time series.

$$MAE = \frac{1}{n}\sum_{1}^{n} \left| P_{CRU\ i} - P_{ERA-40\ i} \right| \tag{24}$$

The difference of the two precipitation data sets in time was calculated by subtracting the annual sum of precipitation of the ERA-40 data from the annual sum of precipitation of the CRU data.

$$diff_{annual} = P_{CRU\ annual} - P_{ERA-40\ annual} \tag{25}$$

To estimate the correlation between the two precipitation time series the Pearson correlation coefficient r was calculated. r ranges from -1 to 1. $|1|$ implies that the relation between the two time series can be described perfectly by a linear equation. A value of 0 implies that there is no linear relation between them. The Pearson r is not robust to outliers (*Rodgers & Nicewander*, 1988).

$$r = \frac{\sum (CRU_i - \overline{CRU})(ERA_i - \overline{ERA})}{\left(\sum (CRU_i - \overline{CRU})^2 \sum (ERA_i - \overline{ERA})^2\right)^{\frac{1}{2}}} \tag{26}$$

The calculation of r and MAE was done for the time series as a whole to represent the spatial variability as well as for each specific month to represent the seasonal development of the correlation and discrepancy of the two climate data sets. The evolution of MAE and r in time was evaluated with the help of the moving mean absolute error and the moving Pearson correlation coefficient. This analysis was carried out for monthly values and a window size of 58 months for the moving MAE and for annual values and a window size of 8 years for the moving r.

As the selected river basins were assumed to be data sparse regions, the arithmetic mean of the number of observation systems within the correlation decay distance was calculated for those CRU grid points representing a single ERA-40 grid point. Hence, it was possible to receive a general overview of the availability of climate observations in space and time.

5.1.2 Stream Flow Data

Flow duration curves (fdc) expressing the percentage of time that stream flow exceeds or falls below (non-exceedance) a specified discharge value were calculated to summarize the temporal flow variability. To estimate the non-exceedance probability F, the discharge values are ranked from lowest to highest (rank i = 1 to n). The non-exceedance frequency F is calculated as follows and plotted against stream flow $q_{(i)}$ (*Dingman*, 2002).

$$F(q_{(i)}) = \frac{i}{n+1} 100 \tag{27}$$

5.2 *Modelling of Stream Flow*

The modelling of stream flow was carried out for the three (sub-)basins with both models, respectively.

5.2.1 Input Data

The modelled sub-basins of the Jordan River and the Niger River were represented by a single grid point (Niger -10.0°/10.0°, Jordan 35.0°/32.5°). The modelled sub-basin of the Kunene River Basin was represented by four grid points (15.0°/-12.5°, 15.0°/-15.0°, 15.0°/-17.5°, 12.5°/-15.0°). Each grid point was weighted according to its fraction of the watershed to receive one input time series. The percentages are 12 %, 65 %, 21 % and 2 %, respectively and were estimated with ArcMap.
Modelling on a monthly time step, in certain cases, a bias correction of the amount of precipitation was carried out to equal the volume of observed and modelled stream flow. For this bias correction the entire precipitation time series was multiplied by a constant factor (bias). The bias was chosen in dependence of the similarity of the observed and modelled flow duration curves.

5.2.2 Calibration

Sefton & Boorman (1997) stated that IHACRES is best calibrated over short time periods thus approximately three-year periods were chosen for calibration. The length of the calibration period of the Hamon's method and simple bucket model depended on the length of the individual stream flow time series. In general, the stream flow time series was divided in the middle into two segments. Each segment was used for calibration as well as for validation.

The parameters values of the two rainfall-runoff models were adjusted to the highest Nash-Sutcliffe efficiencies.

$$NS = 1 - \frac{\sum_i (Q_{o,i} - Q_{m,i})^2}{\sum_i (Q_{o,i} - \overline{Q_o})^2} \tag{28}$$

The numerator estimates the squared sum of the difference of observed discharge Q_o and modelled discharge Q_m. In the denominator, the squared sum of the difference between Q_o and the arithmetic mean of Q_o is calculated. The closer the NS value to 1 (the fraction to zero) the better is the model adjustment (*Nash & Sutcliffe*, 1970).

In dependence of the recorded stream flow hydrograph and the obtained Nash-Sutcliffe efficiency, the number and the order of exponential stores of the IHACRES model were chosen to optimize the modelling results.

5.2.3 Validation

The model validation was carried out using the objective functions mentioned in the calibration section. The validation period was considered as the period not used for calibration.

6. Results

6.1 Input Data

6.1.1 Reliability and Comparability of the Precipitation Datasets

The analysis of the reliability and the comparability of the two precipitation datasets in space as well as in time showed very heterogeneous results. This was most apparent in the monthly mean precipitation values of the CRU and ERA-40 time series representing the precipitation regime and confirmed in the analysis of the monthly mean absolute error.

The two datasets neither agreed in the progression of the rainy season nor in the mean monthly amount of precipitation in the rainy season. Even within one basin the resulting differences between the time series were not consistent.

In the Kunene River Basin (Figure 4), the CRU precipitation regime of the grid points 12.5°/-15.0° and 12.5°/-17.5° showed a maximum value in March, a hinted secondary maximum in November and a local minimum in January / February which was not obvious in the ERA-40 time series. ERA-40 grid point 12.5°/-20.0° had no clear rainy season compared to CRU. At longitudes 15.0° and 17.5° several CRU grid points (15.0°/-17.5°, 15.0°/-15.0°, 17.5°/-15.0° and 17.5°/-12.5°) showed a double peak in November / December and March whereas ERA-40 data showed a single peak around January. The amount of precipitation increased from West to East, exceptions were the ERA-40 grid points 12.5°/-20.0°and 17.5°/-12.5°, and from South to North except for ERA-40 grid point 10.0°/-20.0°. The relative difference of the amount of precipitation between the datasets was highest for the longitudes 12.5° and 15.0° and declined for longitude 17.5°. The maximum monthly mean absolute (relative) error was 120 mm (178 mm) in December / January for grid point 15.0°/-12.5°. In Figure 4 (bottom right), the precipitation time series used for modelling the Kunene River Basin is shown. The precipitation regime of the ERA-40 data was shifted one month compared to CRU with its peak value in January / February and an implied secondary peak in April. Contrary, the CRU time series had an implied secondary peak in November and a peak in February / March. The mean annual difference in model input precipitation was 128 mm.

In the Niger River Basin (Figure 5), the progression of the precipitation regime of the two time series agreed for latitude 12.5° and for latitude 10.0° in general with maximum precipitation values in July / August. As in the Kunene River Basin, double peaks were found in the CRU data whereas ERA-40 data showed a single peak (352.5°/7.5° and 355.0°/7.5°). Additionally, a double peak was observed in the ERA-40 data whereas CRU data showed a single peak (347.5°/7.5°). The amount of precipitation decreased from West to East, except for ERA-40 grid point 345.0°/10.0°, and from South to North, exceptions were ERA-40 grid points of latitude 7.5° and the ERA-40 grid points 347.5°/10.0°, 347.5°/12.5°. For latitude 10.0°, the relative difference of the amount of precipitation declined with increasing longitude. For latitude 12.5°, it was lowest for the longitudes 347.5° and 350.0°.

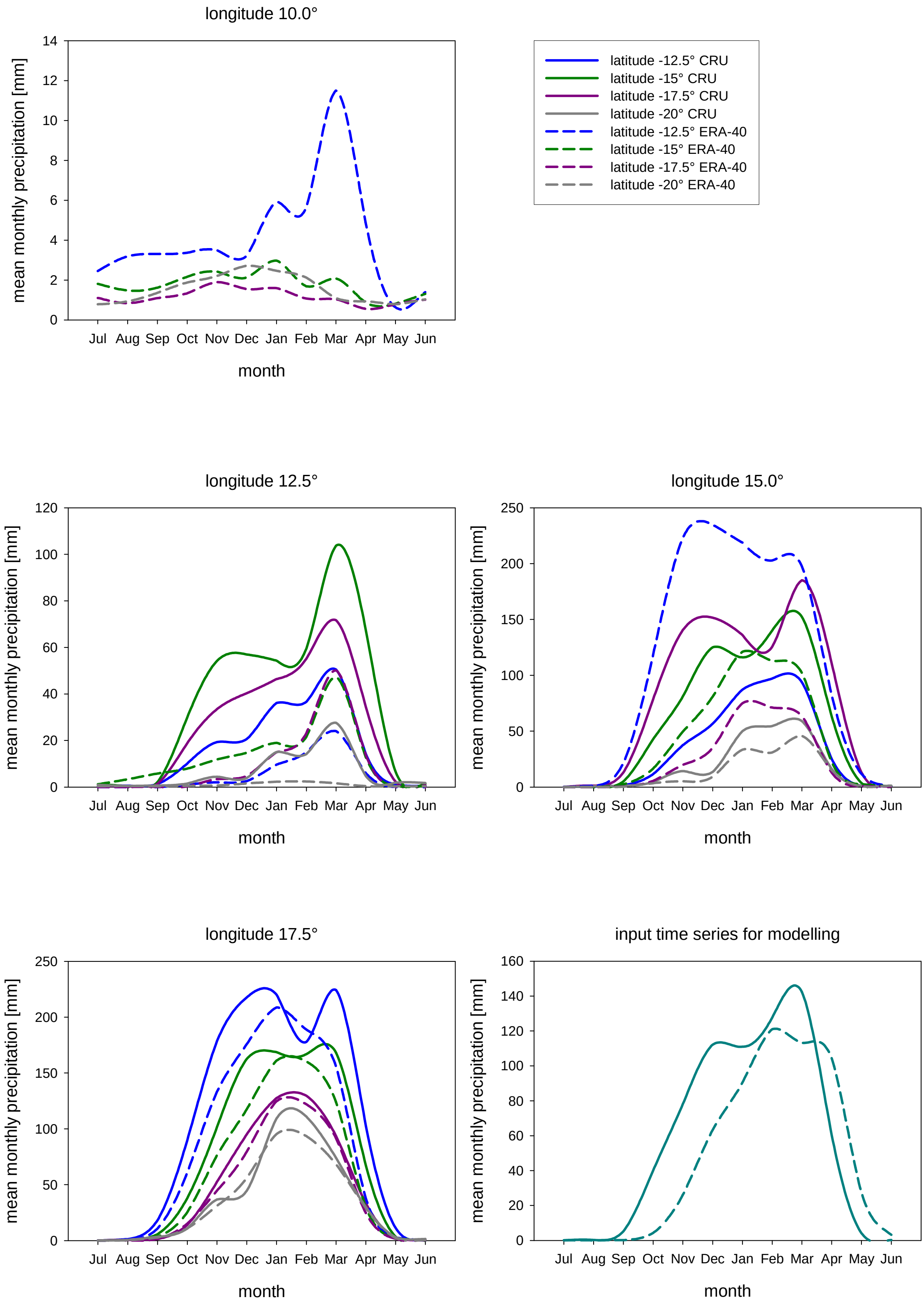

Figure 4: CRU and ERA-40 precipitation regimes in the Kunene River Basin. Precipitation time series for stream flow modelling (bottom right).

The maximum monthly mean absolute precipitation error was almost 300 mm at the beginning of the rainy season for grid point 345.0°/10.0° (Figure 7 top left).

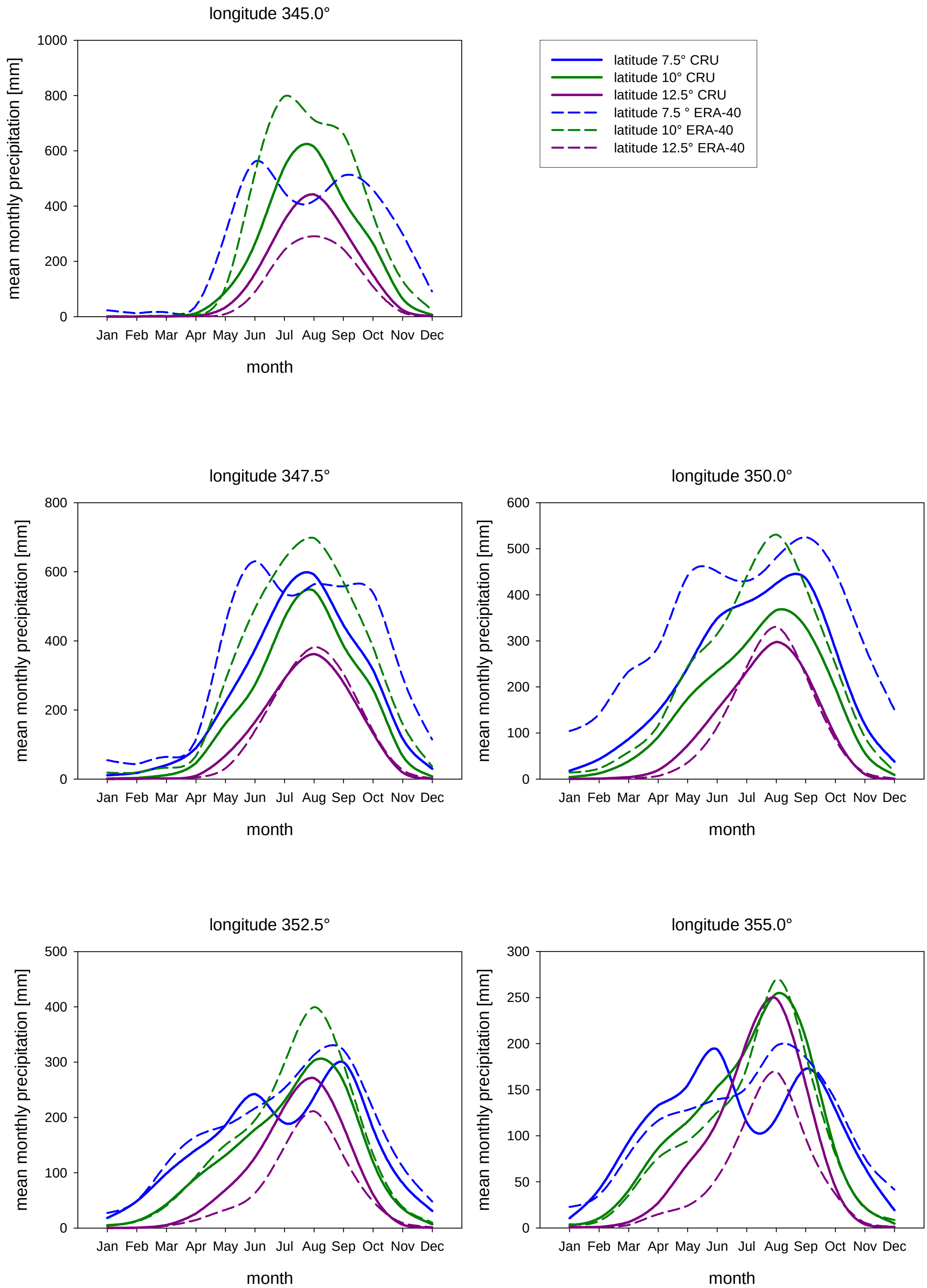

Figure 5: CRU and ERA-40 precipitation regimes in the Niger River Basin.

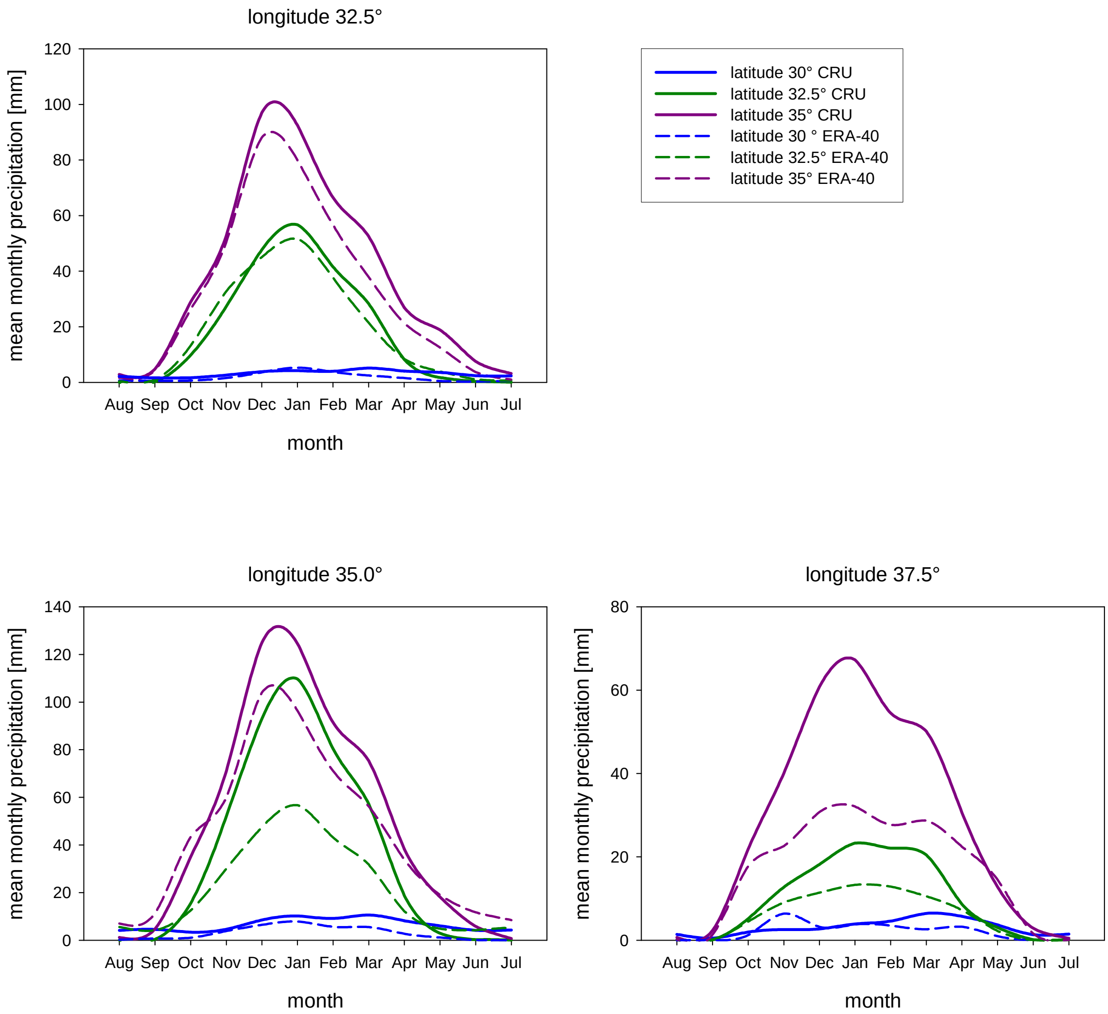

Figure 6: CRU and ERA-40 precipitation regimes in the Jordan River Basin.

In the Jordan River Basin (Figure 6), the progression of the rainy season and the time point of maximum precipitation agreed except for latitude 30.0°. Precipitation decreased from North to South and longitude 35.0° had maximum precipitation values compared to longitudes 32.5° and 37.5°. In general, the precipitation amount of the datasets agreed for longitude 32.5°. In contrast, the maximum precipitation values for longitude 35.0° and 37.5° were up to twice as high for CRU compared to ERA-40.

In contrary, the dry season was represented identical in the CRU and ERA-40 time series. The precipitation datasets agreed in general in the month of the start and the month the end of the dry period as well as in the precipitation amount. Expect for ERA-40 grid point 12.5°/-12.5° having a shorter rainy season compared to CRU, contrariwise was true for grid point 15.0°/ -12.5°. The dry period in the Kunene River Basin ranged from May till September, in the Niger River Basin from December till March / April and in the Jordan River Basin from June till September. Minimal mean monthly precipitation in the three basins was around 0 mm. ERA-40 grid point 350.0°/7.5° with minimum precipitation values above 100 mm was an exception.

Regarding the annual progression of the two precipitation datasets, the annual differences were neither constant in space nor in time (1958 – 2001). In the case of the Kunene River Basin, they did not show any obvious pattern. Contrary, in the Niger River Basin, the annual difference of the two datasets increased in the 1980s up to 2,500 mm for the grid points 347.5°/7.5° and 347.5°/10.0° (Figure 7 bottom left) as well as for the grid points 350.0°/7.5° and 350.0°/10.0°. In the Jordan River Basin, a drastic negative increase in the annual precipitation difference was found for latitude 35.0° in 1972 and a tendency to negative differences after 1990 for the grid points 32.5°/32.5° and 32.5°/35.0°. These differences in the amount of annual precipitation became additionally apparent considering the moving mean absolute error.

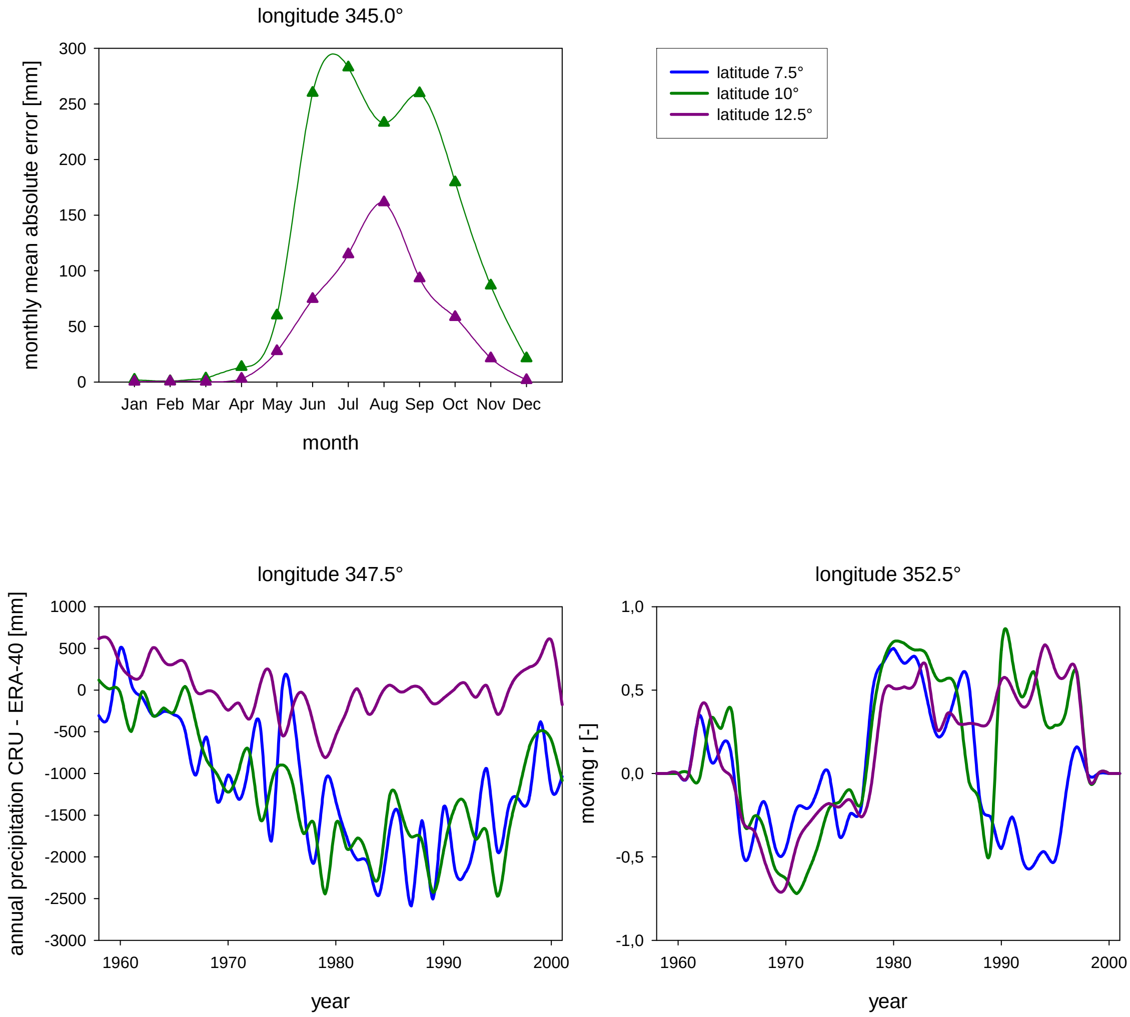

Figure 7: Monthly mean absolute error (top left), annual differences of CRU and ERA-40 precipitation time series (bottom left) and moving Pearson correlation coefficient (bottom right) for selected grid points in the Niger River Basin.

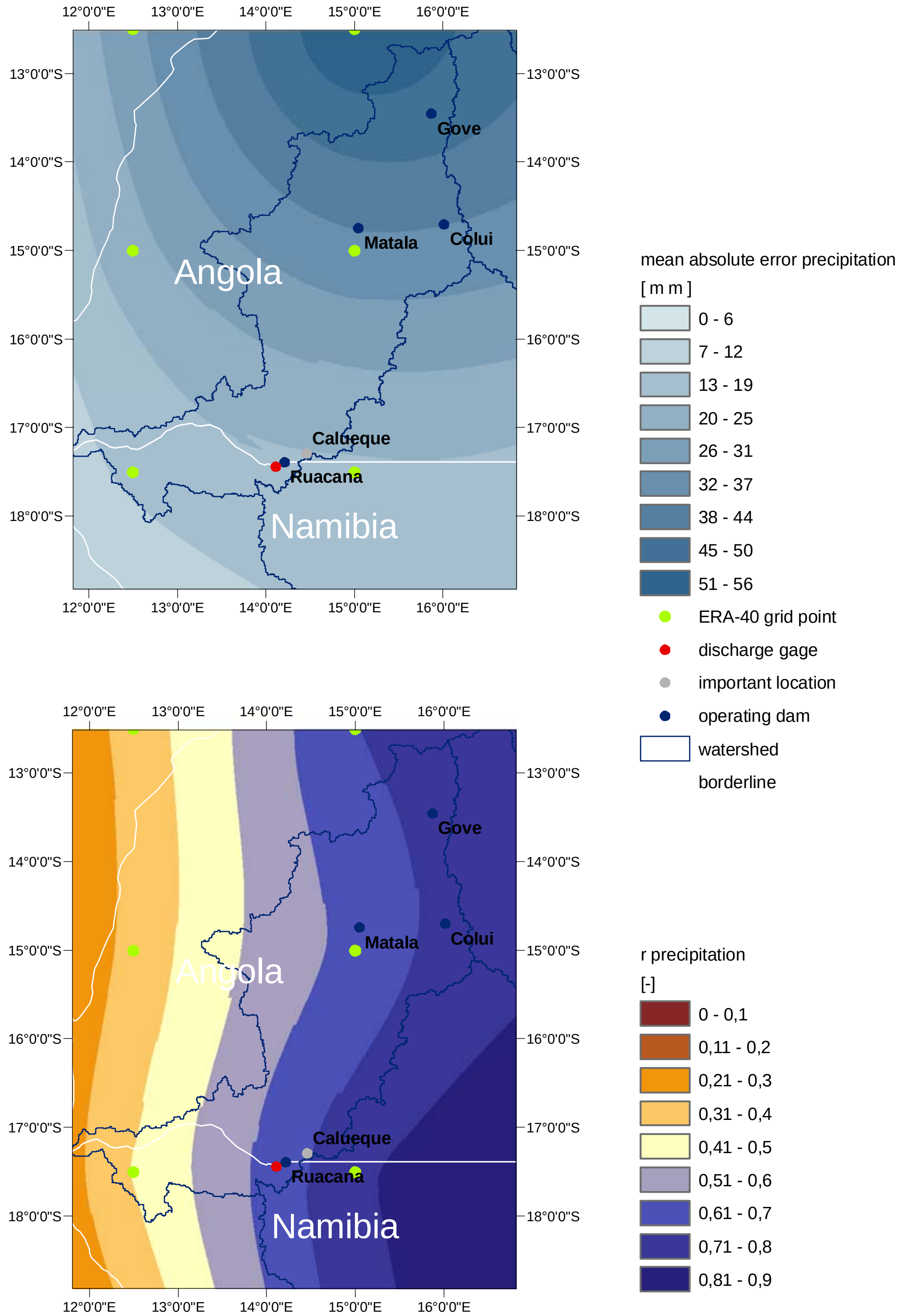

Figure 8: Mean absolute precipitation error (top) and Pearson correlation coefficient (bottom) in the Kunene River Basin.

The mean absolute error of precipitation in space is exemplified in Figure 8 (top) for the Kunene River Basin. It decreased from 56 mm to around 0 mm from North to Southwest. In the Niger River Basin, the pattern of the mean annual absolute error followed the spatial distribution of the mean annual CRU precipitation increasing in a northeast to southwest direction from 142 mm to around 0 mm. In the Jordan River Basin, the mean annual precipitation error decreased from North (20 mm) to South (~ 2 mm) following the pattern of the amount of mean annual precipitation too.

Beside the seasonal, annual and spatial distribution of precipitation amount of the CRU and ERA-40 time series, the Pearson correlation between the datasets was analysed. The monthly Pearson correlation coefficient r ranged between -0.2 and 0.8 in the three basins. In the case of the Kunene River Basin and the Niger River Basin, the seasonal progression did not show any seasonal or spatial pattern. In contrary, in the Jordan River Basin (Figure 9), the monthly Pearson correlation was consistent for the entire basin with minimum values in the dry period and was steeply increasing with increasing precipitation. However, there was no apparent latitudinal evolution of r following the precipitation gradient.

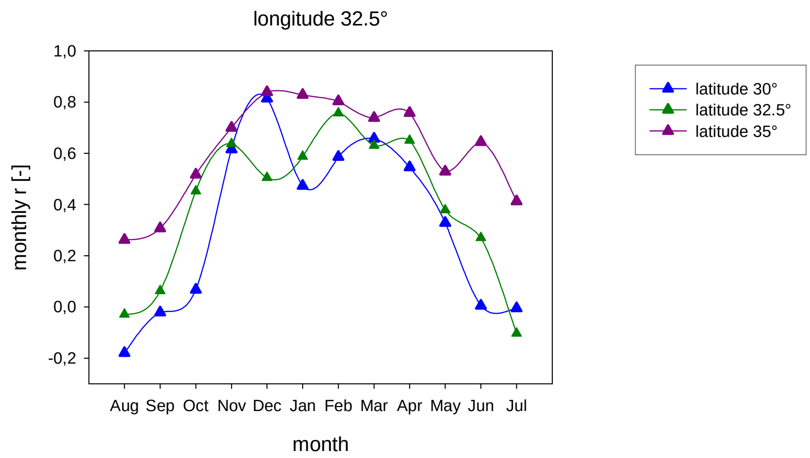

Figure 9: Monthly Pearson correlation coefficient in the Jordan River Basin.

The analysis of the moving Pearson correlation coefficient did not show any obvious patterns in the cases of the Kunene River Basin and the Jordan River Basin. In the Kunene River Basin, moving r fluctuated between positive and negative values. In the Jordan River Basin, moving r was mostly positive. In the Niger River Basin, the correlation changed from positive to negative values from 1965 until 1980 for the longitudes 352.5° (Figure 7 bottom right) and 355.0°. About 1990, the correlation became again negative for grid point 352.5°/7.5° and a short steep correlation decrease was observed for grid point 352.5°/10.0°.

The spatial distribution of the Pearson correlation coefficient for precipitation (1958 - 2001) of the Kunene River Basin is shown in Figure 8 (bottom). r rose from 0.21 along the coastline to 0.9 westwards. Hence, the spatial pattern of r was neither identical with the spatial pattern of the mean absolute error of precipitation nor with the spatial pattern of the mean annual amount of precipitation. The same was true for the Niger River Basin where the Pearson correlation coefficient increased from 0.77 in the coastal region to 0.89 in a northwest direction. In the Jordan River Basin, the spatial pattern of r followed the spatial pattern of the mean absolute error in precipitation and the mean annual amount of precipitation respectively decreasing from North (0.94) to South (0.48).

6.1.2 Availability of Climate Observations

An overview of the availability of climate observations is presented in Table 1 showing the minimum, mean and maximum numbers of stations within the correlation length of air temperature and precipitation for selected grid points of the CRU dataset. In addition to the grid points in the selected river basins, grid point 7.5°/47.5° situated in Central Europe which was assumed to be a data rich region, served as a reference grid point. Grid point 15.0°/-15.0° in the Kunene River Basin had the lowest number of observation stations in precipitation as well as in air temperature. The mean and the maximum number of precipitation stations in the Niger River Basin was approximately the same magnitude as the number of mean and maximum precipitation stations of the grid point representing Central Europe. In the case of no available stations within the correlation length, the precipitation / air temperature value of the particular month was substituted by the mean value of the reference period. The number of observation stations increased in the 1960s and 1970s continuously and remained almost constant until the 1990s with an observed very steep decline. The number of precipitation observing systems showed seasonality with minimum values in the dry season in the case of the grid points 15.0°/-15.0°, 35.0°/32.5° and -10.0°/10.0°.

Table 1: Number of stations within correlation length for air temperature and precipitation for selected grid points of CRU (1958-2001).

Longitude [°] /	number of stations air temperature			number of stations precipitation		
Latitude [°]	minimum	mean	maximum	minimum	mean	maximum
Niger -10 / 10	8	71	89	0	49	71
Kunene 15 / -15	0	12	20	0	3	7
Jordan 35 / 32.5	51	230	322	2	32	50
7.5 / 47.5	174	559	807	22	59	82

6.2 Modelling

6.2.1 IHACRES – Modelling on a daily time step

In regard to the recorded discharge at Ruacana gauging station a single exponential store was chosen to model stream flow of the Kunene River Basin. The best modelling result, according to the maximum Nash Sutcliff efficiency of over 100 calibrations runs varying in period, is presented in Table 2.

Table 2: Modelling results with the IHACRES rainfall-runoff model / ERA-40 daily data.

	NS		calibration period	total stream flow [mm]		simulated / observed
	cal.	val.		observed	simulated	[%]
Kunene Ruacana	0.89	-0.24	04/11/1970 - 08/08/1973	2251	2332	103.60
Niger Tiguibery	NaN	NaN	variable	NaN	NaN	NaN

As the Nash Sutcliffe efficiency NS decreased steeply in the validation period, the model performance in dependence of the amount of precipitation and discharge in the calibration period was calculated additionally. A correlation was not detectable. The cross correlation CCF between precipitation and stream flow of the hydrological year (October – September) was about zero.

$$CCF = \frac{COV(X_{i,t}, Y_{j,t-k})}{\sqrt{VAR(X_{i,t}, Y_{j,t})}} \tag{29}$$

Furthermore, the Pardé Coefficients PC (*Pardé*, 1947) were calculated.

$$PC_i = \frac{MQ_{month\ i}}{MQ_{year\ j}} \tag{30}$$

The Pardé values of October (month of lowest discharge) were correlated against the time constant TC of the IHACRES rainfall-runoff model to figure out whether years of high low flows (high October PC) are reflected in TC to deliver insight into the influence of storage systems in the basin. There was no correlation detectable as well. However, the autocorrelation ACF (1985 - 2006) of discharge was 0.45 for a lag time of one, pointing out some year to year storage.

$$ACF = \frac{COV(X_{i,t}, X_{i,t-k})}{VAR(X_{i,t})} \tag{31}$$

The other parameters of the IHACRES rainfall-runoff model did not show a progression in time either.

Likewise, it was unsuccessful to model river flow at Tiguibery gage in the Niger River Basin with the ERA-40 daily data, independent of the calibration period and the configuration of exponential storages. For the Upper Jordan, only monthly discharge data were available.

6.2.2 Simple Bucket Model - Modelling on a monthly time step

The bias correction of the CRU and ERA-40 precipitation time series resulted in an adaptation of the precipitation regimes of the two datasets. In the Niger River Basin, the mean monthly absolute error between the two precipitation input time series declined from 58.7 mm to 8.2 mm due to bias correction. In the Jordan River Basin, it declined from 17.8 mm to 5.4 mm.

Those model runs with the highest Nash Sutcliffe efficiencies are shown in Table 3. The model performance with CRU climate data was superior to ERA-40 data. Although, the Nash Sutcliffe efficiency was higher for the ERA-40 data in the calibration period at the Jordan River, it declined steeply in the validation period. A similar steep decline was observed for the ERA-40 data in the Upper Niger River Basin. The maximum decline of the Nash Sutcliffe efficiency in the validation period compared to the calibration period for the CRU data was 0.1 in the case of the Jordan River. In the Niger and in the Kunene River Basin, better results were achieved when the first half of the discharge time series was used for calibration.

First, the total amount of stream flow was considered (Table 3) which was defined as the sum of stream flow in the calibration and validation period. The discrepancy of the observed stream flow values in the same basin resulted from the different length of the two climate data time series. Modelled stream flow applying CRU climate data was always underestimated. The underestimation ranged between 2.11 % and 11.51 %. Modelling with ERA-40 climate data resulted in an underestimation of stream flow of 23.83 % up to an overestimation of stream flow of 40.78 %. The percentage discrepancy of the overall modelled stream flow of the two climate data sets is highest for the Niger River Basin and lowest for the Jordan River Basin.

Table 3: Modelling results with Hamon's method and the simple bucket model.

		NS		calibration period	total stream flow [mm]		simulated / observed [%]	difference [%]
		cal.	val.		observed	simulated		
Kunene	CRU	0.38	0.35	1962-1978	2336	2067	88.49	12.32
Ruacana	ERA-40	0.17	0.18	1962-1978	2326	1772	76.17	
Niger	CRU	0.82	0.75	1952-1965	12952	12679	97.89	42.89
Tiguiber.	ERA-40	0.48	-0.09	1952-1965	9860	13881	140.78	
Jordan	CRU	0.73	0.63	1986-2002	10718	10249	95.62	4.55
Obstacle	ERA-40	0.75	0.33	1986-2002	10668	9716	91.07	

Second, the seasonal progression of monthly mean modelled and observed stream flow focusing on the high and low flow periods was examined (Figure 10). It has to be pointed out that mean monthly values were considered and that the deviations in amount and time in a particular month of a year can differ drastically. The time points of the observed and modelled mean peak flow agreed for the Kunene River. In the Niger River Basin, the time point of observed and modelled stream flow agreed only in the case of the CRU climate data. The modelled peak flow of the ERA-40 climate data was one month earlier compared to the observed peak flow. At the Jordan River, the modelled maximum flows were half a month earlier compared to the observed.

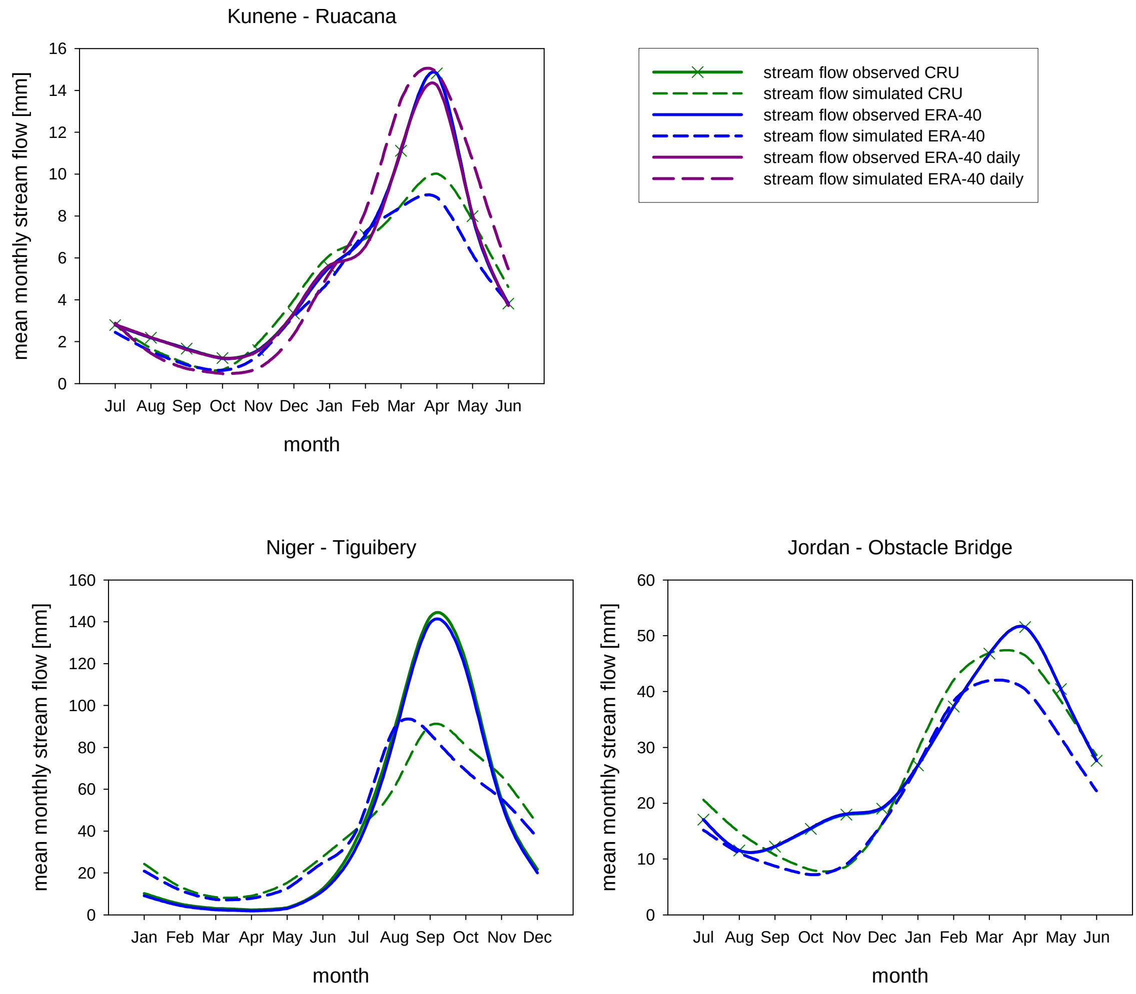

Figure 10: Observed and modelled stream flow regime at Ruacana (top left), Tiguibery (bottom left) and Obstacle Bridge (bottom right).

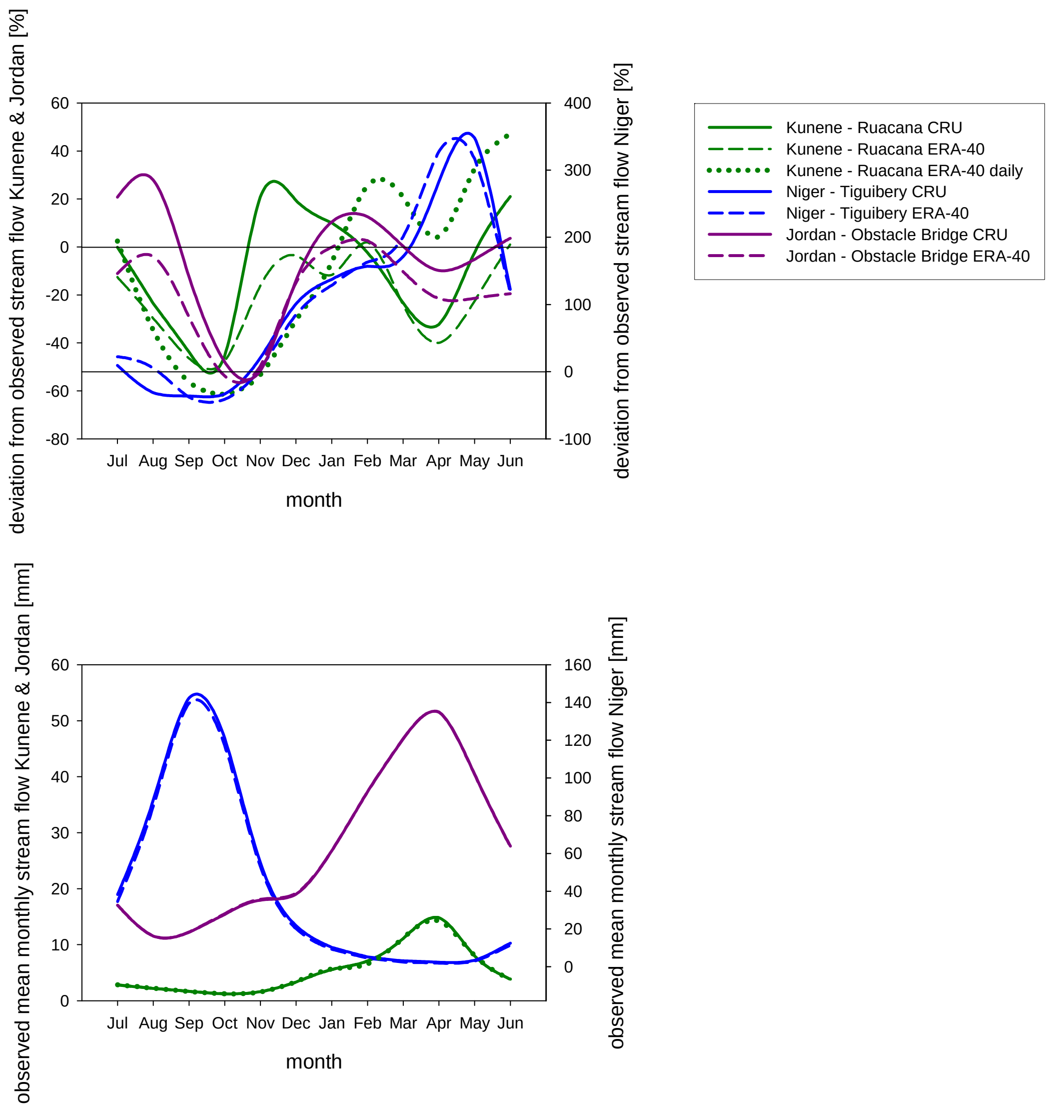

Figure 11: Observed flow regimes (bottom) and the percentage deviation of mean monthly stream flow of observed and modelled discharge (top).

Figure 11 shows the observed flow regimes (bottom) and the percentage deviation of mean monthly stream flow of observed and modelled discharge for the entire modelled time period (top). The flow regimes modelled with monthly CRU and monthly ERA-40 climate data respectively agreed better then the observed and modelled flow regimes did. At Ruacana gage in the Kunene River Basin, the peak flow in April was underestimated up to 40 % applying the simple bucket model and the ERA-40 data on a monthly time step. The same was true for the CRU data set. In contrary, applying the IHACRES rainfall-runoff model and ERA-40 climate data on a daily time step (31/10/1961 - 31/01/2001) the peak flow was well represented. The low flows of the Kunene River were underestimated almost equally on a monthly time step (~50 %) and underestimated by 60 % applying the IHACRES rainfall-runoff model. Peak stream flow at Tiguibery gage in the Niger River Basin was underestimated by 30 % for the CRU climate data. In the case of the ERA-40 data, the peak flow was overestimated by 5 %. The time points of modelled and observed peak stream flow did not agree as mentioned above. Low flows in April were overestimated up to 350 % by both climate datasets. At Obstacle Bridge at the Jordan River, peak flows are only minor underestimated applying the CRU climate data and underestimated by 20 % applying the ERA-40 data. Low flows in August were well represented by the ERA-40 data set and overestimated by the CRU climate data by 30 %. In October, the underestimation of 50 % is due to a simulated minimum discharge value but a measured local maximum value (Figure 10 bottom right). These differences became obvious in the flow duration curves as well.

7. Discussion

7.1 Input Data Reliability

7.1.1 Precipitation Reliability

The results showed that the climate precipitation datasets vary considerably in precipitation amount and regime as well as their correlation is neither constant in space nor in time. Therefore, their interpretation is complex. The discrepancy between the datasets may be ascribed to various causes: poor data quality due to precipitation measurement errors, insufficient station coverage, interpolation errors in the case of CRU precipitation data (*New et al.*, 2000) and reanalysis errors in the case of the ERA-40 precipitation data (*Uppala et al.*, 2005).

First, the differences ascribed to the applied precipitation estimation methods, interpolation and reanalysis, are considered. The progression of the amount of precipitation from North to South or East to West was consistent for the CRU precipitation data compared to the ERA-40 data. The reason might be that CRU data do not consider the influence of elevation on the amount of precipitation whereas ERA-40 can rebuild those local phenomena. However, it has to be proven whether orographic effects still have influence at the considered grid scale of 2.5° x 2.5°. The dissimilar precipitation estimation methodologies and errors in the precipitation estimation method itself e.g. calibration errors in the case of ERA-40 may also cause inconsistent differences in the annual progression of the datasets and an inconsistent moving Pearson correlation. A further reason may be poor input data quality in one of the datasets.
The disparity in the precipitation regime in the Kunene River Basin and in the Niger River Basin which resulted in a single precipitation peak value in one climate dataset whereas the other showed a double peak were caused by differences in the reproduction of the movement of the intertropical convergence zone (ITCZ). In the Niger Basin, this difference in the simulation of the south-eastern anti-cyclone monsoon was obvious at the grid points close to the coastline (latitude 7.5°) and at the time point of the maximum relative error at the beginning of the rainy season. Due to the decreasing influence of this rainfall pattern, the progression of the precipitation regime of the two time series agreed for latitude 12.5° and for latitude 10.0° in general. In the Kunene River Basin, only the CRU data simulated a double peak thus a movement of the ITCZ across the basin.

The number of observation systems within the correlation decay distance is a second reason for the discrepancy between the precipitation datasets. The analysis of the number of observations systems for the CRU data confirmed that especially the Kunene River Basin is a data scarce region. With the decline of observation systems in the 1990s the Niger River Basin and the Jordan River Basin followed. It is assumed that the data availability for the ERA-40 reanalysis was

in the same range. When no stations within the correlation decay distance were available, CRU applied the mean value of the reference period which leads to a data alignment to the defined reference period (*New et al.*, 2000). It is not clear, how the reanalyse of the ERA-40, especially model calibration, was carried out in the case of scarce data availability. Additionally, New et al. (2000) pointed out that in very data sparse regions as Angola the anomaly diverged from zero due to an error in interpolation. Therefore, the particular grid point was adjusted to receive zero anomalies by subtracting the interpolation error. In the cases of a relative high mean number of precipitation observation systems (Niger River Basin, Jordan River Basin), the spatial pattern of the mean absolute precipitation error followed the spatial pattern of mean monthly precipitation.
Not only the coverage of observation stations itself can be responsible for the discrepancies of the precipitation datasets also the number of CRU grid points representing one ERA-40 grid point might play a role. The high relative differences in the Kunene River basin for longitude 12.5° may be related to only 6 to 19 CRU grid points out of 25 representing one ERA-40 grid point.

A further reason for the discrepancy of the precipitation regime are the semi arid to arid climate conditions expressed in a high spatial and temporal variability of precipitation resulting in poor data quality and quantity (*Pilgrim et al.*, 1988). This might be a main point accounting for the differences in the Jordan River Basin for latitude 30.0°. Furthermore, it has to be proven whether one of the two precipitation estimation methodologies is superior in semi arid to arid regions.

The Jordan River Basin showed three specific characteristics. The amount of precipitation was common for longitude 35.0°, the monthly Pearson correlation was consistent and the spatial pattern of the Pearson correlation coefficient followed the spatial pattern of the mean absolute error in precipitation as well as the mean annual amount of precipitation. It is assumed that these features resulted from the higher coverage of observation stations on the one hand and from the missing influence of the ITCZ on the other hand.

To figure out the individual reasons for the discrepancy of the precipitation datasets and to be able to explain further characteristics, like the spatial pattern of the Pearson correlation coefficient in the Niger River Basin and in the Kunene River Basin additional regions of various climate should be tested.

As the required station density to describe the monthly spatial variability adequately is greater for precipitation than for air temperature (*New et al.*, 2000), the present results of the analysis of precipitation anomalies and correlation differs from the results of the analysis of air temperature gained by Simmons et al. (2004).

7.1.2 Discharge Data Availability and Reliability

In contrary to the gridded climate datasets, point measurements of discharge were required for the modelling of stream flow. During the case study selection a mayor difficulty was the non-availability of discharge time series. Further problems were the insufficient length and the unknown influence of storage systems and land use changes inside the basins which became obvious in the case of Ruacana gage in the Kunene River Basin. This affirmed the conclusions of Draper & Kundell (2007) who stated that for drawing conclusions on the vulnerability of flow allocations an accurate and precise knowledge of the hydrological conditions and especially anthropogenic influences like land use change, dams and withdrawals is needed for data interpretation and usage.
A second point were discharge measurement errors which were assumed to be high due to the strong seasonality of river flow ranging from over banking during flood season to extreme low flows at the end of the dry season as well as due to gage maintenance deficits (*Pilgrim et al.*, 1988).

7.2 Modelling of Stream Flow

7.2.1 Modelling with Gridded Climate Input

In the selected International River Basins modelling on a daily time step with the IHACRES rainfall-runoff model was unsuccessful. Instead, modelling on a monthly time step with Hamon's method and the simple bucket approach was successful with reliable climate and discharge input data as long as the Nash-Sutcliffe efficiencies were considered. In the case of Tiguibery gage in the Niger River Basin, similar satisfying Nash-Sutcliffe efficiencies as Schuol et al. (2008) were received. However, for the prediction of the vulnerability of stream flow allocations at least seasonal values and extreme values have to be considered. Schaefli & Gupta (2007) pointed out that the Nash-Sutcliffe efficiency referencing to the mean flow value is a poor predictor of model efficiency for discharge regimes with a high seasonality. This was confirmed by deviations from monthly low flows of 60 % underestimation up to 350 % overestimation what is not satisfying in regard to water allocation agreements with potential precise threshold values as identified by Draper & Kundell (2007).
The input data quality is the main control on the quality of the modelling results (*Arnell*, 1999). The climate input data quality as well as the discharge data quality, especially the unknown influence of storage systems as in the Kunene River Basin, are assumed to be the main reasons for this poor modelling results. However, Schuol and Abbaspour (2007) pointed out that in data scarce regions model runs with generated climate data were superior to model runs using the few available observed data. Döll et al. (2003) stated that compared to humid basins, semi arid to arid basins as well as basins with large artificial storage systems were modelled less satisfactory.
Further reasons for the poor seasonal model performance can be the catchment scale compared to the model scale and the catchment inhomogeneity in regard to precipitation input. However, previous work by Jakeman et al. (1990) and Jakeman & Hornberger (1993) showed that with

reliable input data the IHACRES rainfall-runoff model was transferable to a wide range of catchments sizes and climates. Jakeman et al. (1993) proposed to model each continent's major basins with the IHACRES rainfall-runoff model and stated that “present limitations are data rather than knowledge-based” (*Jakeman et al.*, 1993).
An additional point is that the unique hydrological characteristics of semi arid / arid regions as transmission losses, temporal and seasonal storages and the temporal influence of vegetation cover (*Pilgrim et al.*, 1988) were not represented in the two model designs.
Considering the Nash-Sutcliffe efficiencies as an indicator for the climate input data quality, the CRU climate data are superior compared to ERA-40 climate data.

7.2.2 Impact of Climate Input Data on Modelling Result

Rainfall-runoff modelling on a monthly time step illustrated the dissimilarities of the climate datasets resulting in mean differences of simulated flow up to 43 % for the entire simulation period. In the Jordan River Basin as well as in the Niger River basin, the precipitation regimes of the CRU and ERA-40 datasets had the same seasonal progression resulting in the same progression of mean monthly deviations from observed and modelled stream flow. Compared to the Jordan River Basin, the deviation extent was almost equal in the Niger River Basin indicating that discharge measurement errors or anthropogenic storage systems might play an important role. The progression of the deviation differences between the time series was not related to the progression of the mean monthly absolute error in precipitation.
In the case of the Kunene River Basin, different precipitation regimes served as model input. Their influence was mainly visible in the mean values of river flow during the first half of the rainy season from October till February. ERA-40 model input underestimated discharge whereas CRU model input overestimated discharge which was ascribed to the higher amount of precipitation in the CRU precipitation regime. The shift of the rainfall regime of the ERA-40 climate data was only slightly hinted in the modelled river regime.
As only one basin was modelled on a daily time step applying ERA-40 data, it is not possible to draw any conclusions on the impact of the climate dataset on the model results because factors like the reliability of the discharge data have influence, too.
Characteristics of the climate input datasets as the monthly Pearson correlation which is consistent the Jordan River Basin compared to the other basins, were not found to have any influence on the modelling results.

7.2.3 Optimal Input Data – Model Combination

Regarding the Nash-Sutcliffe efficiencies modelling with Hamon’s method and the simple bucket model applying CRU climate data was superior compared to ERA-40 data. However, the mean monthly deviation between observed and modelled river flow showed only minor differences between the two climate datasets. As there are various factors influencing the model efficiency, like the unknown influence of storage systems, no conclusion about an optimal input data – model combination can be drawn up till now. More basins have to be modelled to give adequate information about an optimal input data - model combination. Nevertheless, the results showed that modelling on a monthly time step is not yet satisfying and modelling on a daily time scale is even more challenging.

7.3 Evaluation of the Vulnerability of Stream Flow Allocations

Can we judge the past, present and future vulnerability of stream flow allocations with gridded climate input data regarding the previous discussed results? As modelling on a monthly time scale was not able to adequately reproduce the extreme values which may lead to a breach of treaty, lumped modelling with global gridded climate input data is unsatisfying in regard to the estimation of the vulnerability of stream flow allocations. In view of the past and present vulnerability of flow allocations, observed flow records are superior to modelled flow records. However, modelling of stream flow would be relevant for the estimation of natural flow, for the filling of data gaps as well as for the estimation of future stream flow and thus for the evaluation of the future vulnerability of stream flow allocations.

Nevertheless, comparing mean monthly flow records with the existing treaties the following can be concluded related to the past vulnerability.
In the case of the Kunene River Basin, a fixed water allocation threshold of 80 m³/s equalling 2.44 mm/month exists (*South Africa & Portugal*, 1969). This threshold was in the mean undercut regarding the observed stream flow in the months of August (2.18 mm/month), September (1.66 mm/month), October (1.21 mm/month) and November (1.60 mm/month). When modelling with CRU climate input this value was undercut in August (1.67 mm/month), September (0.94 mm/month), October (0.66 mm/month) and November (1.94 mm/month) when modelling with ERA-40 in the months of August (1.53 mm/month), September (0.88 mm/month), October (0.63 mm/month) and November (1.33 mm/month), too. Modelling with ERA-40 on a daily time step resulted in an undercut in August (1.44 mm/month), September (0.71 mm/month), October (0.47 mm/month) and November (0.73 mm/month) as well and an additional undercut in December (2.34 mm/month). In general, the threshold was undercut by 43 % of time for the observed discharge time series and undercut by 36 % (45 %) for modelled discharge with CRU (ERA-40) and by 49 % applying ERA-40 on a daily time step.
In the Jordan River Basin, flow allocations refer to a flow volume in a defined period. At Obstacle Bridge, mean observed stream flow was 96.4 mm (132.65 MCM) in the summer period (15. May – 15. October) and 227.5 mm (313.04 MCM) in the winter period. Modelling with CRU (ERA-40) resulted in mean summer stream flow of 97.8 mm (76.6 mm) and mean winter stream flow of 213.2 mm (192.3 mm). Due to the imprecise allocation of the water's of the Jordan River and a reference point of flow abstraction south of the confluence with the Yarmouk River, the vulnerability of the water allocation agreement of the Jordan River Basin could not be estimated.
In the Niger River Basin, it was not possible to draw any conclusions on the vulnerability of stream flow allocations as no treaty for the modelled sub-basin exists.

7.4 Representativeness of Water Allocation Thresholds

With the applied methodology only conclusions in respect to the third and fourth sharing rule of Draper & Kundell (2007) could be drawn. The time resolution of the hydrological model as well as of the analysis had to be considered in the vulnerability estimation of the water allocation agreement. A further constraint was the existence of a flow record at the particular point of water abstraction mentioned in the treaty. In the previous section, the evaluation of the vulnerability of stream flow allocations considered only monthly mean values. In the case of the Kunene River Basin, this resulted in almost similar months of threshold undercut in dependence of the observed / simulated stream flow time series. However, taking only mean monthly stream flow values into account might be too inexactly for the formulation of water allocation thresholds.

According to numerous authors (*Giordano & Wolf*, 2003; *Draper & Kundell*, 2007; *Ansink & Ruijs*, 2008) stream flow quantity as well as stream flow variability have to be represented in a water allocation agreement. As shown previously, it was difficult to simulate monthly stream flow with gridded climate data adequately and thus to draw conclusions about the vulnerability of stream flow allocations.

Compared to fixed threshold values, percentage threshold values of water allocations are always fulfilled. Ansink & Ruijs (2008) concluded that the stability of a water allocation agreement is highest for fixed upstream allocation followed by proportional allocation and lowest for fixed downstream allocation. This progression is not transferable to the evaluation of the vulnerability of stream flow allocations as fixed amounts were unsatisfied modelled.

8. Conclusion

The climate precipitation datasets varied considerably in precipitation amount and regime. Their correlation was neither constant in space nor in time. The discrepancy between the datasets was ascribed to various causes. To estimate each particular influence, the analysis of additional regions of various climate and data availability is required. The assumed data scarcity of the selected International River Basins was confirmed to some extent.
The non-availability of discharge time series was one of the main challenges in the case study selection process. Problems arose due to their insufficient length and the unknown influence of storage systems and land use change which made data interpretation and usage difficult. A further constraint in regard to the evaluation of the vulnerability of water allocation agreements was the existence of a flow record at the particular point of water abstraction mentioned in the treaty and clear allocation formulations.
Rainfall-runoff modelling on a monthly time step illustrated the dissimilarities of the climate data sets resulting in mean differences of simulated flow up to 43 %. The simulation of the discharge regime resulted in a mean monthly low flow underestimation up to 60 % and an overestimation up to 350 %. Mean monthly peak flows were underestimated up to 40 %. However, the mean monthly deviation between observed and modelled river flow showed only minor differences in progression and amount between the two climate datasets.
Modelling on a daily time step was unsuccessful. Therefore no conclusion about an optimal input data – model combination can be drawn. Considering the Nash-Sutcliffe efficiency as an indicator for the climate input data quality, the CRU climate data were superior compared to ERA-40.

As modelling on a monthly time scale was not able to adequately reproduce the extreme values what may lead to a breach of treaty, lumped modelling with global gridded climate input data is unsatisfying in regard to the vulnerability estimation of stream flow allocations. However, comparing the mean monthly error range gained from modelling with different climate input, with the existing terms of transboundary water allocation commitments resulted in almost similar months of threshold undercut. Nevertheless, the consideration of only mean monthly stream flow values might be too inexactly for the formulation of water allocation thresholds.

The conclusion of this study is that while the mechanisms of water allocation agreements differ widely, predictions of the vulnerability of stream flow allocations will require accurate models which depend primarily on reliable input data. Gridded climate input data and the applied hydrological method provide unsatisfying results in regard to the vulnerability evaluation of stream flow allocation agreements in International River Basins. Due to the enhanced vulnerability of semi arid to arid regions amplified by climate change, the quantification of the vulnerability of water allocation agreements in those regions remains crucial.

Acknowledgements

I like to thank Prof. Dr. Markus Weiler for making this work possible as well as Dr. Kerstin Stahl for supervising this study and spending as much time in advice and discussion.

Thanks to my fellow students who encouraged me with helpful discussions and cakes. Special thanks go to Karin, Bastian, Fabian, Olivier, Kathi and Maria.

Thanks to my follow students for their friendship and the wonderful study time in Freiburg.

Further thanks to my flat mate Celia for her friendship and balancing hydrology.

Thanks to all the musicians I listened to during my thesis for making me dreaming away.

Thanks to my mum and my dad for their all round support during my study. Thanks to my Schwesterherz for distracting me. Thanks to my grandparents, especially to my grandma and her relationship to God.

References

Alley, W. M. (1984), On the Treatment of Evapotranspiration, Soil Moisture Accounting and Aquifer Recharge in Monthly Water Balance Models, *Water Resources Research*, *20* (8), 1137-1149.

Ansink, E. & Ruijs, A. (2008), Climate Change and the Stability of Water Allocation Agreements, *Environmental and Resource Economics 41*, 249-266.

Ansink, E. & Weikard, H.-P. (2009), Contested water rights, *European Journal of Political Economy*, *25*, 247-260.

Arnell, N. W. (1999), A simple water balance model for the simulation of streamflow over a large geographic domain, *Journal of Hydrology*, *217*, 314-335.

Bates, B. C., Kundzewicz, Z. W., Wu, S. et al. (Eds.) (2008), *Climate Change and Water. Technical Paper of the Intergovernmental Panel on Climate Change, IPCC Secretariat, Geneva*, 210 pp.

BfG (2009), The Global Runoff Data Centre, 56068 Koblenz, Germany, http://www.bafg.de/cln_005/nn_294146/GRDC/Home/homepage__node.html?__nnn=true, accessed 20.05.2009.

Böge, V. (2005), A Glass Half Full or Half Empty? Water, Conflict and Cooperation in Southern Africa, in *Hamburg African Studies 14 - Resource Politics in Sub-Saharan Africa*, edited by M. Basedau & A. Mehler, pp. 273-304, Institute of African Affairs.

Boorman, D. B. & Sefton, C. E. M. (1997), Recognizing the uncertainty in the quantification of the effects of climate change on hydrological response, *Climatic Change*, *35*, 415-434.

Croke, B. F. W. & Jakeman, A. J. (2004), A catchment moisture deficit module for the IHACRES rainfall-runoff model, *Environmental Modelling & Software*, *19*, 1-5.

Croke, B. F. W. (2006), A technique for deriving an average event unit hydrograph from streamflow - only data for ephemeral quick-flow-dominant catchments, *Advances in Water Resources*, *29*, 493-502.

Croke, B. F. W. & Jakeman, A. J. (2008), Use of the IHACRES rainfall-runoff model in arid and semi-arid regions, in *Hydrological Modelling in Arid and Semi-Arid Areas*, edited by H. Wheater et al., pp. 41-48, Cambridge University Press.

Dezetter, A., Girard, S., Paturel, J. E. et al. (2008), Simulation of runoff in West Africa: Is there a single data-model combination that produces the best simulation results?, *Journal of Hydrology*, *354*, 203-212.

Dingman, S. L. (2002), *Physical hydrology*, 2 ed., Prentice-Hall, Inc.

Döll, P., Kaspar, F. & Lehner, B. (2003), A global hydrological model for deriving water availability indicators: model tuning and validation, *Journal of Hydrology*, *270*, 105-134.

Draper, S. E. (2007), Introduction to Transboundary Water Sharing, *Journal of Water Resources Planning and Management*, *September / October 2007*, 377-381.

Draper, S. E. & Kundell, J. E. (2007), Impact of Climate Change on Transboundary Water Sharing, *Journal of Water Resources Planning and Management*, *September / October*, 405-415.

Drieschova, A., Giordano, M. & Fischhendler, I. (2008), Governance mechanisms to address flow variability in water treaties, *Global Environmental Change*, *18*, 285-295.

Dutra, E., Viterbo, P. & Miranda, P. M. A. (2008), ERA-40 reanalysis hydrological applications in the characterization of regional drought, *Geophysical Research Letters*, *35* (L19402).

Elhance, A. P. (1999), *Hydropolitics in the Third World: conflict and cooperation in international river basins*, 309 pp., Endowment of the United States Institute of Peace, Washington, DC.

Evans, J. P. & Schreider, S. (2002), Hydrological Impacts of Climate Change on Inflows to Perth, Australia, *Climatic Change*, *55*, 361-393.

Evans, J. P. (2003), Improving the characteristics of streamflow modeled by regional climate models, *Journal of Hydrology*, *284*, 211–227.

FAO (2005), AQUASTAT - main country database, http://www.fao.org/nr/water/aquastat/dbase/index.stm, accessed 10.05.2009.

FAO (2006), Geo-referenced database on African dams, http://www.fao.org/nr/water/aquastat/damsafrica/index.stm, accessed 10.05.2009.

FAO, UNEP & IUCN (2008), EcoLex, http://www.ecolex.org, accessed 11.05.2009.

Fisher, F. M., Arlosoroff, S., Eckstein, Z. et al. (2002), Optimal water management and conflict resolution: The Middle East Water Project, *Water Resources Research*, *38* (11), 1243.

George, S. S. (2007), Streamflow in the Winnipeg River basin, Canada: Trends, extremes and climate linkages, *Journal of Hydrology*, *332*, 396-411.

Giordano, M. A. & Wolf, A. T. (2003), Sharing waters: Post-Rio international water management, *Natural Resources Forum*, *27*, 163-171.

Godana, B. A. (1985), *Africa's Shared Water Resources: Legal and Institutional Aspects of the Nile, Niger and Senegal River Systems*, 370 pp., Frances Pinter Ltd.

Google (2009), Google earth, http://earth.google.de/, accessed 05.10.2009.

Goulden, M., Conway, D. & Persechino, A. (2009), Adaption to climate change in international river basins in Africa: a review, *Hydrological Sciences Journal*, *54* (5), 805-828.

Haith, D. A. & Shoemaker, L. L. (1987), Generalized watershed loading functions for streamflow nutrients, *Water Resources Bulletin - American Water Resources Association*, *23* (3), 471-478.

Hamon, W. R. (1961), Estimating potential evapotranspiration, *Journal of the Hydraulics Division - Proceedings of the American Society of Civil Engineers*, *May, 1961*, 107-120.

Hanasaki, N., Kanae, S., Oki, T. et al. (2007), An integrated model for the assessment of global water resources - Part 1: Input meteorological forcing and natural hydrological cycle modules, *Hydrology and Earth System Sciences*, *4*, 3535-3582.

Harou, J. J., Pulido-Velazquez, M., Rosenberg, D. E. et al. (2009), Hydro-economic models: Concepts, design, applications and future prospects, *Journal of Hydrology*, *375*, 627-643.

Heyns, P. (2003), Water-resources management in Southern Africa, in *International waters in Southern Africa*, edited by M. Nakayama, pp. 5-37, United Nations University Press.

Hornberger, G. & Wiberg, P. (2005), Numerical Models in the Hydrological Sciences, *Special Publications Series 57*, American Geophysical Union.

Hughes, D. (1995), Monthly rainfall-runoff models applied to arid and semiarid catchments for water resource estimation purposes, *Hydrological Sciences -Journal- des Sciences Hydrologiques*, *40* (6).

International Law Association (1967), The Helsinki Rules on the Uses of the Waters of International Rivers Adopted by the International Law Association at the fifty-second conference, held at Helsinki in August 1966. Report of the Committee on the Uses of the Waters of International Rivers, International Law Association, London.

Israel, Jordan, Syria et al. (1955), Johnston Negotiations, *12/31/1995*, http://ocid.nacse.org/tfdd/tfdddocs/92ENG.htm.

Jakeman, A. J., Littlewood, I. G. & Whitehead, P. G. (1990), Computation of the instantaneous hydrograph and identifiable component flow with application to two small upland catchments, *Journal of Hydrology*, *117*, 275-300.

Jakeman, A. J., Chen, T. H., Post, D. A. et al. (1993), Assessing uncertainties in hydrological response to climate at large scale, *IAHS Publication 214*, 37-47.

Jakeman, A. J. & Hornberger, G. B. (1993), How much complexity is warranted in a rainfall-runoff model?, *Water Resources Research*, *29* (8), 2637-2649.

Jakeman, A. J. & Letcher, R. A. (2003), Integrated assessment and modelling: features, principles and examples for catchment management, *Environmental Modelling & Software*, *18*, 491-501.

Juízo, D. & Lidén, R. (2008), Water sharing in transboundary water resources systems, *Hydrology and Earth System Sciences*, *5*, 475-509.

Klintenberg, P., Mazambani, C. & Nantanga, K. (2007), Integrated Water Resources Management in the Namibian Part of the Cuvelai Basin, Central Northern Namibia. CuveWaters Papers, No. 2, 27 pp, Institute for Social-Ecological Research (ISOE).

Kluge, T., Liehr, S., Lux, A. et al. (2008), IWRM concept for the Cuvelai Basin in northern Namibia, *Physics and Chemistry of the Earth, Parts A/B/C*, *33* (1-2), 48-55.

Kokkonen, T. S. & Jakeman, A. J. (2002), Structural Effects of Landscape and Land Use on Streamflow Response, in *Environmental Foresight and Models: A Manifesto*, edited by M. B. Beck, pp. 303-321, Elsevier Science, Amsterdam.

Kundzewicz, Z. W., Mata, L. J., Arnell, N. W. et al. (2007), Freshwater resources and their management. Climate Change 2007: Impacts, Adaptation and Vulnerability. Contribution of Working Group II to the Fourth Assessment Report of the Intergovernmental Panel on Climate Change, edited by M. L. Parry et al., pp. 173-210, Cambridge University Press, Cambridge, UK.

Lange, G.-M., Mungatana, E. & Hassan, R. (2007), Water accounting for the Orange River Basin: An economic perspective on managing a transboundary resource, *Ecological Economics*, *61*, 660-670.

Lavers, D., Prudhomme, C., Hannah, D. M. et al. (2007), Comparison of the potential skill of raw and downscaled GCM output for river flow forecasting: a UK case study, *CLIVAR Exchanges*, *12* (4), 33-34.

Leander, R. & Buishand, T. A. (2007), Resampling of regional climate model output for the simulation of extreme river flows, *Journal of Hydrology*, *332*, 487-496.

Littlewood, I. G. (2002), Improved unit hydrograph characterisation of the daily flow regime (including low flows) for the River Teifi, Wales: towards better rainfall-streamflow models for regionalisation, *Hydrology and Earth System Sciences*, *6* (5), 899-911.

Map Maker Trust (2007), Map Library, http://www.maplibrary.org/index.php, accessed 20.05.2009.

Matthews, O. P. & St. Germain, D. (2007), Boundaries and Transboundary Water Conflicts, *Journal of Water Resources Planning and Management*, *133* (5), 386-396.

Medellín-Azuara, J., Lund, J. R., ASCE, M. et al. (2007), Water Supply Analysis for Restoring the Colorado River Delta, Mexico, *Journal of Water Resources Planning and Management*, *133* (5), 462-471.

Meissner, R. (2003), Interaction and existing constraints in international river basins, in *International waters in Southern Africa*, edited by M. Nakayama, pp. 249-273, United Nations University Press.

Minville, M., Brissette, F. o. & Leconte, R. (2008), Uncertainty of the impact of climate change on the hydrology of a nordic watershed, *Journal of Hydrology*, *358*, 70-83.

Mitchell, T. D. & Jones, P. D. (2005), An improved method of constructing a database of monthly climate observations and associated high-resolution grids, *International Journal of Climatology*, *25*, 693-712.

Murwira, A. & Mazvimavi, D. (2007), SADC-HYCOS Phase II Project - Final Report - Strategic and Optimum Network Design for the SADC-HYCOS Phase II Project, 71 pp, SADC-HYCOS.

Nash, J. E. & Sutcliffe, I. V. (1970), River Flow Forecasting Through Conceptual Models. Part I - A Discussion Of Principles, *Journal of Hydrology*, *10*, 282-290.

New, M., Hulme, M. & Jones, P. (2000), Representing Twentieth-Century Space - Time Climate Variability. Part II: Development of 1901-96 Monthly Grids of Terrestrial Surface Climate, *Journal of Climate*, *13* (13), 2217-2238.

Nigeria & Niger (1990), Agreement between the Federal Republic of Nigeria and the Republic of Niger concerning the equitable sharing in the development, conservation and use of their common water resources done at Maiduguri, 10 July 1990, http://ocid.nacse.org/tfdd/tfdddocs/182ENG.htm.

Oldenborgh van, G. J. (2009), Climate Explorer, http://climexp.knmi.nl, accessed 20.05.2009.

Oudin, L., Hervieu, F., Michel, C. et al. (2005), Which potential evapotranspiration input for a lumped rainfall-runoff model?: Part 2 -Towards a simple and efficient potential evapotranspiration model for rainfall-runoff modelling, *Journal of Hydrology*, *303* (1-4), 290-306.

Owusu, K., Waylen, P. & Qiu, Y. (2008), Changing rainfall inputs in the Volta basin: implications for water sharing in Ghana, *GeoJournal*, *71*, 201-210.

Pardé, M. (1947), *Fleuves et Rivieres*, sec, Edn. Colin, Paris.

Peel, M. C., Finlayson, B. L. & McMahon, T. A. (2007), Updated world map of the Köppen-Geiger climate classification, *Hydrology and Earth System Sciences*, *11*, 1633-1644.

Pilgrim, D. H., Chapman, T. G. & Doran, D. G. (1988), Problems of rainfall-runoff modelling in arid and semiarid regions, *Hydrological Sciences Journal*, *33* (4), 379-400.

Post, D. & Jakeman, A. J. (1996), Relationship between Catchment Attributes and Hydrological Response Characteristics in Small Australian Mountain Ash Catchments, *Hydrological Processes*, *10*, 877-892.

Rimmer, A. & Salingar, Y. (2006), Modelling precipitation-streamflow processes in karst basin: The case of the Jordan River sources, Israel, *Journal of Hydrology*, *331*, 524-542.

Rodgers, J. L. & Nicewander, W. A. (1988), Thirteen Ways to Look at the Correlation Coefficient, *The American Statistician*, *42* (1), 59-66.

Schaefli, B. & Gupta, H. V. (2007), Do Nash values have value?, *Hydrological Processes*, *21*, 2075-2080.

Schreider, S. Y., Whetton, P. H., Jakeman, A. J. et al. (1997), Runoff modelling for snow-affected catchments in the Australian alpine region, eastern Victoria, *Journal of Hydrology*, *200* (1-4), 1-23.

Schreider, S. Y., Smith, D. I. & Jakeman, A. J. (2000), Climate Change Impacts on Urban Flooding, *Climatic Change*, *47*, 91-115.

Schuol, J. & Abbaspour, K. C. (2007), Using monthly weather statistics to generate daily data in a SWAT model application to West Africa, *Ecological Modelling*, *201* (3-4), 301-311.

Schuol, J., Abbaspour, K. C., Srinivasan, R. et al. (2008), Estimation of freshwater availability in the West African sub-continent using the SWAT hydrologic model, *Journal of Hydrology*, *352* (1-2), 30-49.

Sefton, C. E. M. & Boorman, D. B. (1997), A regional investigation of climate change impacts on UK streamflows, *Journal of Hydrology*, *195*, 26-44.

Shahin, M. (2002), *Hydrology and Water Resources of Africa*, 659 pp., Kluwer Academic Publishers.

Simmons, A. J., Jones, P. D., da Costa Bechtold, V. et al. (2004), Comparison of trends and low-frequency variability in CRU, ERA-40, and NCEP/NCAR analyses of surface air temperature, *Journal of Geophysical Research*, *109* (D24115).

Sneddon, C. & Fox, C. (2006), Rethinking transboundary waters: A critical hydropolitcs of the Mekong basin, *Political Geography*, *25*, 181-202.

South Africa & Portugal (1969), Agreement between the Government of the Republic of South Africa and the Government of Portugal in regard to the first phase of development of the water resources of the Cunene River Basin. Lisbon, 21 January 1969, *Portugal, Dario do Governo*, *No. 250, 28 October 1970*, 1589, http://ocid.nacse.org/tfdd/tfdddocs/1143ENG.htm.

Stahl, K. (2005), Influence of Hydroclimatology and Socioeconomic Conditions on Water-Related International Relations, *Water International*, *30* (3), 270-282.

State of Israel & The Hashemite Kingdom of Jordan (1994), Treaty of peace between The State of Israel and The Hashemite Kingdom of Jordan, *Arava / Aqaba crossing point*, *26 October 1994*, http://ocid.nacse.org/tfdd/tfdddocs/168ENG.htm.

State of Israel & Palestine Liberation Organization (1995), The Israeli - Palestinian Interim Agreement on the West Bank and the Gaza Strip, *Washington, D.C.*, *September 28, 1995*, http://ocid.nacse.org/tfdd/tfdddocs/171ENG.htm.

Tarr, P. (2007), Epupa Dam Case Study, *International Journal of Water Resources Development*, *23* (3), 473-484.

TFDD (2007), International Freshwater Treaties Database, www.transboundarywaters.orst.edu, accessed 10.05.2009.

Uppala, S. M., Kållberg, P. W., Simmons, A. J. et al. (2005), The ERA-40 re-analysis, *Quarterly Journal of the Royal Meteorological Society 131*, 2961-3012.

Wolf, A. T., Natharius, J. A., Danielson, J. J. et al. (1999), International River Basins of the World, *Water Resources Development*, *15* (4), 387-427.

Wolf, A. T., Stahl, K. & Macomber, M. F. (2003a), Conflict and cooperation within international river basins: The importance of institutional capacity, *Water Resources Update*, *125*.

Wolf, A. T., Yoffe, S. B. & Giordano, M. (2003b), International waters: identifying basins at risk, *Water Policy*, *5*, 29-60.

Wolf, A. T. (2007), Shared Waters: Conflict and Cooperation, *Annual Review of Environment and Resources*, *32*, 3.1-3.29.

Xu, C.-Y. & Singh, V. P. (1998), A review on monthly water balance models for water resources investigations, *Water Resources Management*, *12*, 31-50.

Xu, C.-Y. & Singh, C.-Y. (2004), Review on Regional Water Resources Assessment Models under Stationary and Changing Climate, *Water Resources Management*, *18*, 591-612.

Yang, D. & Musiake, K. (2003), A continental scale hydrological model using the distributed approach and its application to Asia, *Hydrological Processes*, *17*, 2855-2869.

Ye, W., Bates, B. C., Viney, N. R. et al. (1997), Performance of conceptual rainfall-runoff models in low-yielding ephemeral catchments, *Water Resources Research*, *33* (1), 153-166.

Yoffe, S., Fiske, G., Giordano, M. et al. (2004), Geography of international water conflict and cooperation: Data sets and applications, *Water Resources Research*, *40*.

Zaag van der, P. (2009), Southern Africa: Evolving Regional Water Law and Politics, in *The Evolution of the Law and Politics of Water*, edited by J. W. Dellapenna & J. Gupta, Springer Science + Business Media B.V.

Appendix

Analysis of Input Data

Table A 1: Summary of Climate Input Data Analysis.

	long. [° E]	lat. [° N]	annual mean precipitation CRU [mm]	annual mean precipitation ERA-40 [mm]	annual mean temperature CRU [°C]	annual mean temperature ERA-40 [°C]	r precipitation [-]	r temperature [-]	mean absolute error pre. [mm]	mean absolute error temp. [°C]	number of CRU time series
Niger	-15.0	7.5	NaN	3178.74	NaN	26.94	NaN	NaN	-NaN	-NaN	0
	-15.0	10.0	2284.16	3326.98	26.62	26.44	0.85	0.30	116.83	0.90	5
	-15.0	12.5	1478.53	1000.85	26.94	27.92	0.90	0.83	46.39	1.16	25
	-12.5	7.5	2802.89	3964.31	26.40	26.04	0.78	0.83	131.10	0.58	11
	-12.5	10.0	2227.15	3398.38	25.94	25.45	0.88	0.85	112.48	1.12	23
	-12.5	12.5	1329.77	1320.36	27.00	27.44	0.89	0.96	37.82	0.82	25
	-10.0	7.5	2569.42	3982.71	25.31	24.00	0.73	0.86	141.99	1.32	24
	-10.0	10.0	1811.79	2515.23	25.31	25.01	0.81	0.82	87.41	0.94	25
	-10.0	12.5	1116.41	1058.49	27.25	27.30	0.87	0.97	34.27	0.75	25
	-7.5	7.5	1754.72	2023.75	25.29	24.72	0.73	0.82	61.37	0.82	25
	-7.5	10.0	1420.40	1673.86	25.86	25.49	0.82	0.87	52.72	0.88	25
	-7.5	12.5	971.32	662.42	27.47	27.53	0.83	0.94	36.30	0.70	25
	-5.0	7.5	1247.80	1313.48	26.55	25.62	0.65	0.91	43.84	0.95	25
	-5.0	10.0	1175.69	1084.12	26.90	26.18	0.81	0.93	35.40	0.82	25
	-5.0	12.5	876.66	528.99	27.76	27.65	0.85	0.96	33.73	0.50	25
Kunene	10.0	-12.5	NaN	48.97	NaN	22.11	NaN	NaN	-NaN	-NaN	0
	10.0	-15.0	NaN	21.30	NaN	20.21	NaN	NaN	-NaN	-NaN	0
	10.0	-17.5	NaN	13.83	NaN	18.80	NaN	NaN	-NaN	-NaN	0
	10.0	-20.0	NaN	18.27	NaN	18.51	NaN	NaN	-NaN	-NaN	0
	12.5	-12.5	437.18	146.43	22.32	23.22	0.34	0.87	29.50	1.23	8
	12.5	-15.0	305.25	110.42	20.26	24.78	0.33	0.74	22.68	4.52	17
	12.5	-17.5	191.23	60.15	17.12	25.96	0.41	0.78	13.91	8.84	19
	12.5	-20.0	76.97	10.94	17.25	18.31	0.26	0.77	5.83	1.33	6

	15.0	-12.5	955.78	1312.48	20.06	20.75	0.69	0.49	56.21	1.40	25
	15.0	-15.0	729.68	510.52	20.54	21.31	0.63	0.89	35.67	1.19	25
	15.0	-17.5	413.32	284.22	20.25	22.47	0.78	0.95	17.64	2.23	25
	15.0	-20.0	216.15	145.39	19.16	23.13	0.73	0.95	11.82	3.97	25
	17.5	-12.5	1242.04	974.95	19.99	19.79	0.78	0.81	41.96	1.09	25
	17.5	-15.0	882.87	700.04	20.96	21.01	0.79	0.90	31.67	1.07	25
	17.5	-17.5	550.27	505.33	22.97	22.12	0.89	0.96	15.90	1.02	25
	17.5	-20.0	424.76	390.16	21.18	20.76	0.89	0.98	12.53	0.78	25
	modelling		681.89	553.53	20.42	21.55	0.57	0.70	36.08	1.80	92
Jordan	32.5	30.0	37.62	21.24	20.73	20.08	0.45	1.00	2.28	0.66	25
	32.5	32.5	221.83	216.91	20.93	20.87	0.80	0.97	9.59	1.31	6
	32.5	35.0	454.30	383.68	18.16	19.71	0.90	0.99	12.25	1.62	8
	35.0	30.0	77.81	35.22	19.37	18.94	0.52	1.00	4.34	0.54	25
	35.0	32.5	430.22	257.74	19.28	19.03	0.90	1.00	19.02	0.54	18
	35.0	35.0	591.04	521.99	18.73	19.78	0.92	0.99	15.87	1.47	10
	37.5	30.0	36.37	24.97	19.94	19.04	0.33	1.00	2.92	1.00	25
	37.5	32.5	114.17	71.24	17.93	18.09	0.84	1.00	4.70	0.89	25
	37.5	35.0	344.44	199.65	16.48	17.24	0.78	1.00	14.67	1.22	25

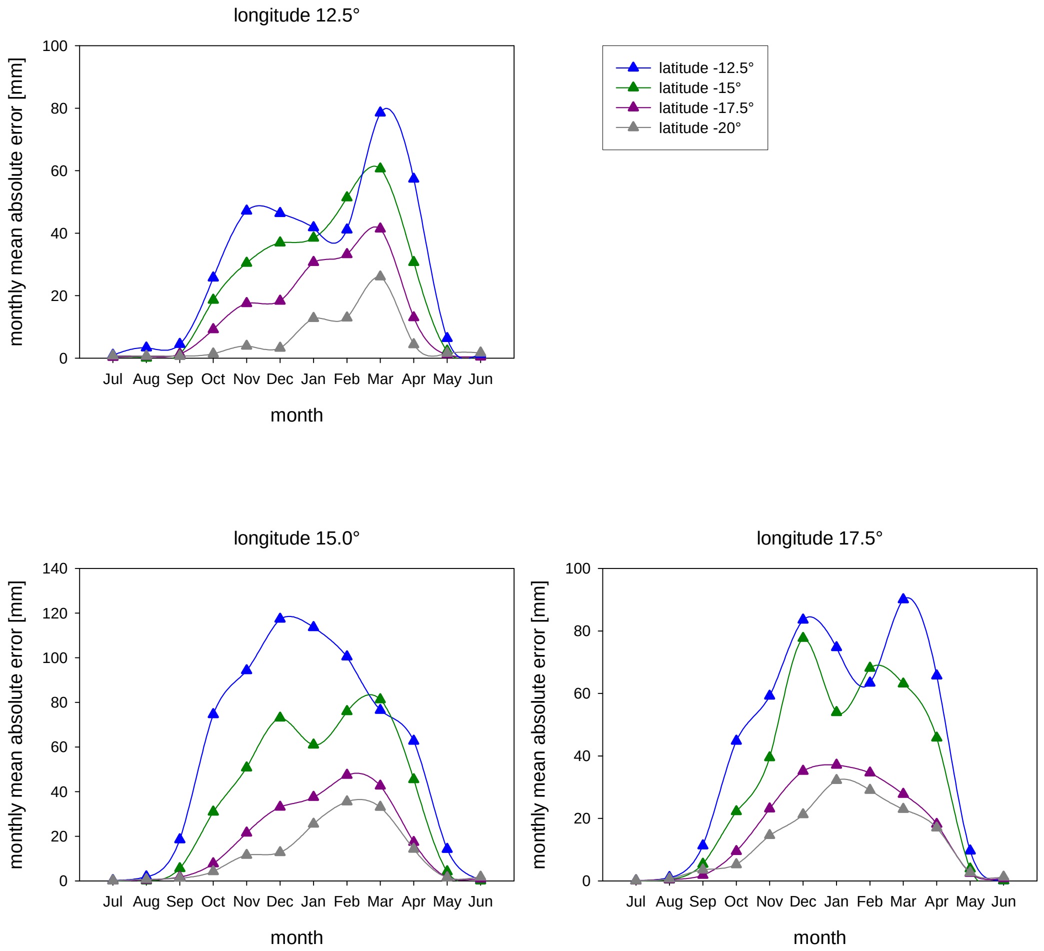

Figure A 1: Monthly mean absolute error Kunene River Basin.

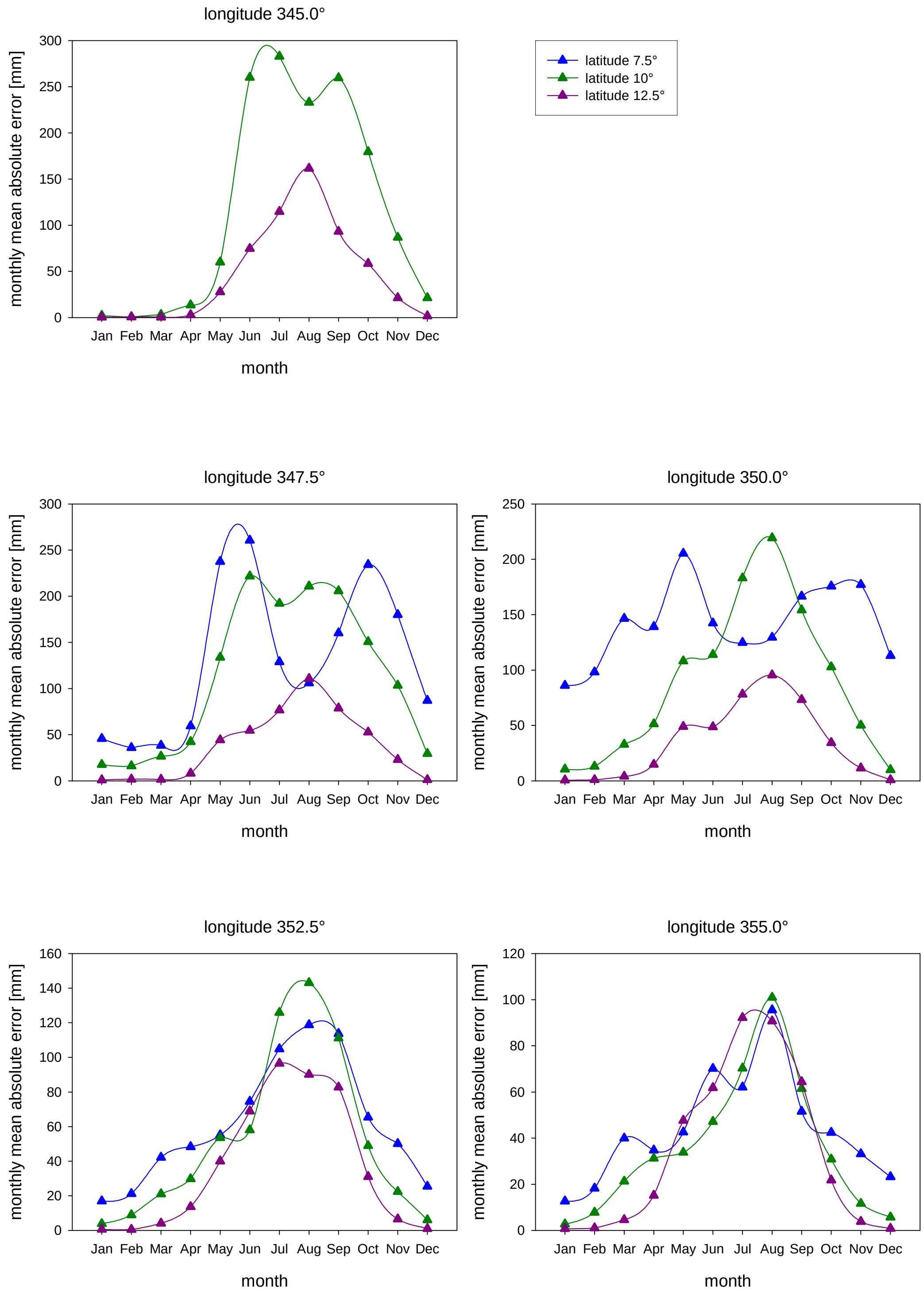

Figure A 2: Monthly mean absolute error Upper Niger River Basin.

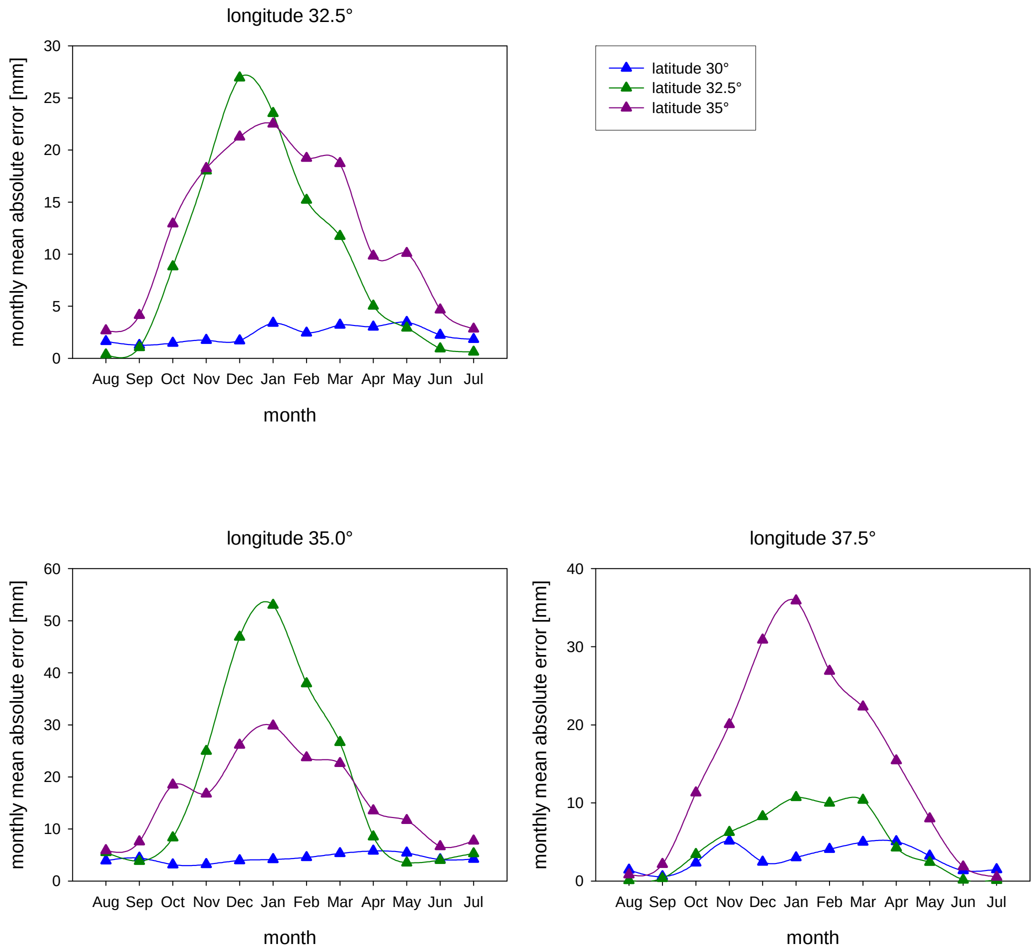

Figure A 3: Monthly mean absolute error Jordan River Basin.

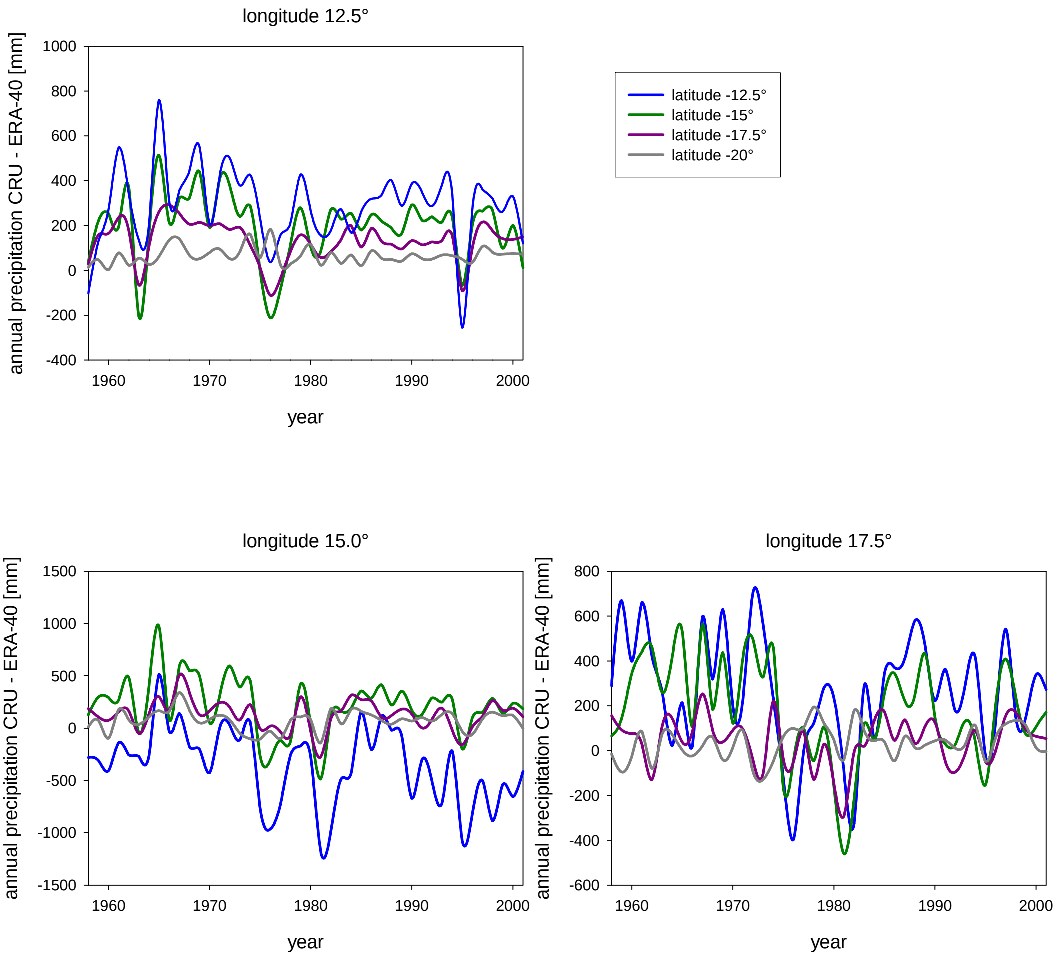

Figure A 4: Annual precipitation CRU - annual precipitation ERA-40 Kunene River Basin.

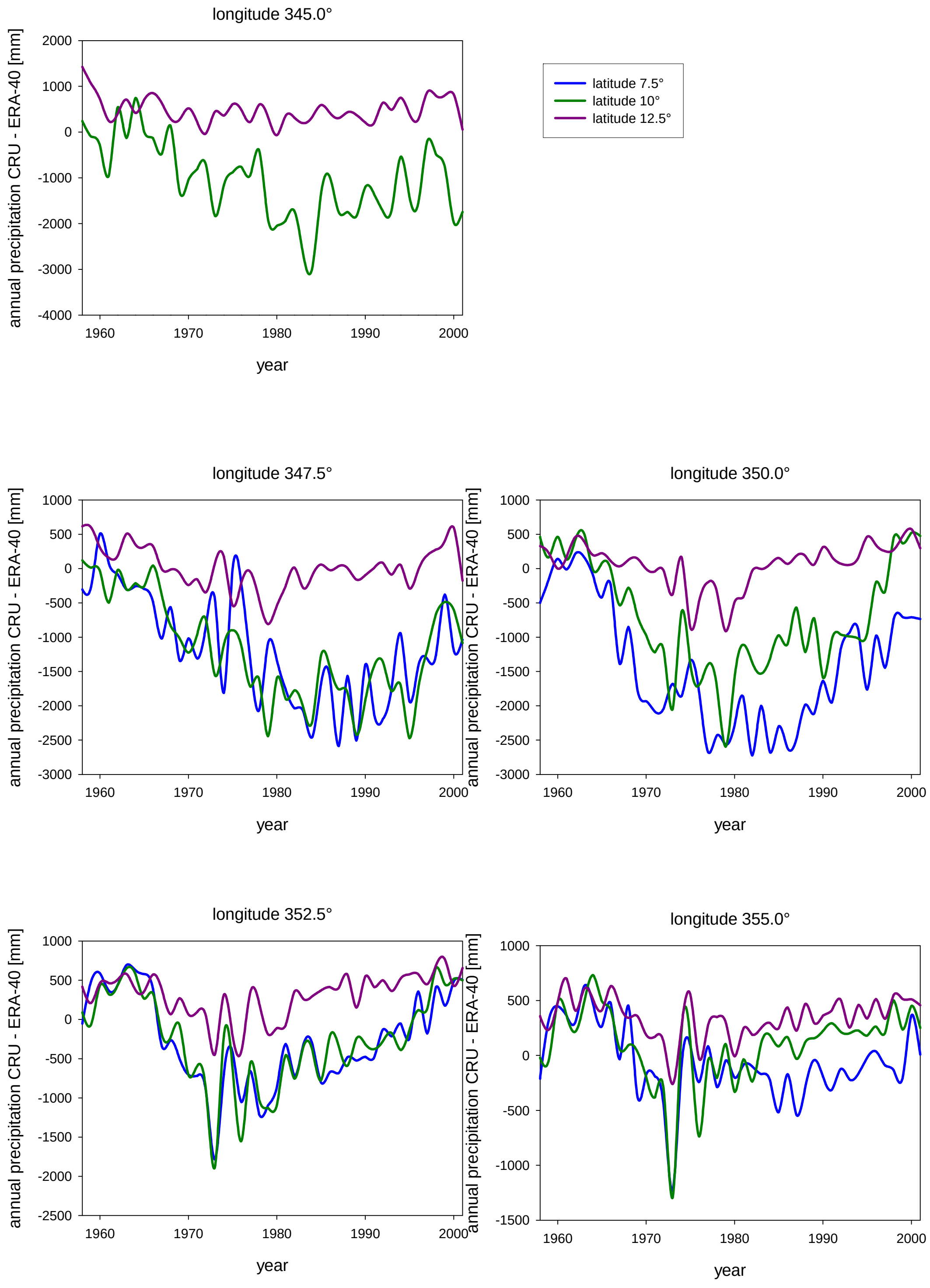

Figure A 5: Annual precipitation CRU - annual precipitation ERA-40 Upper Niger River Basin.

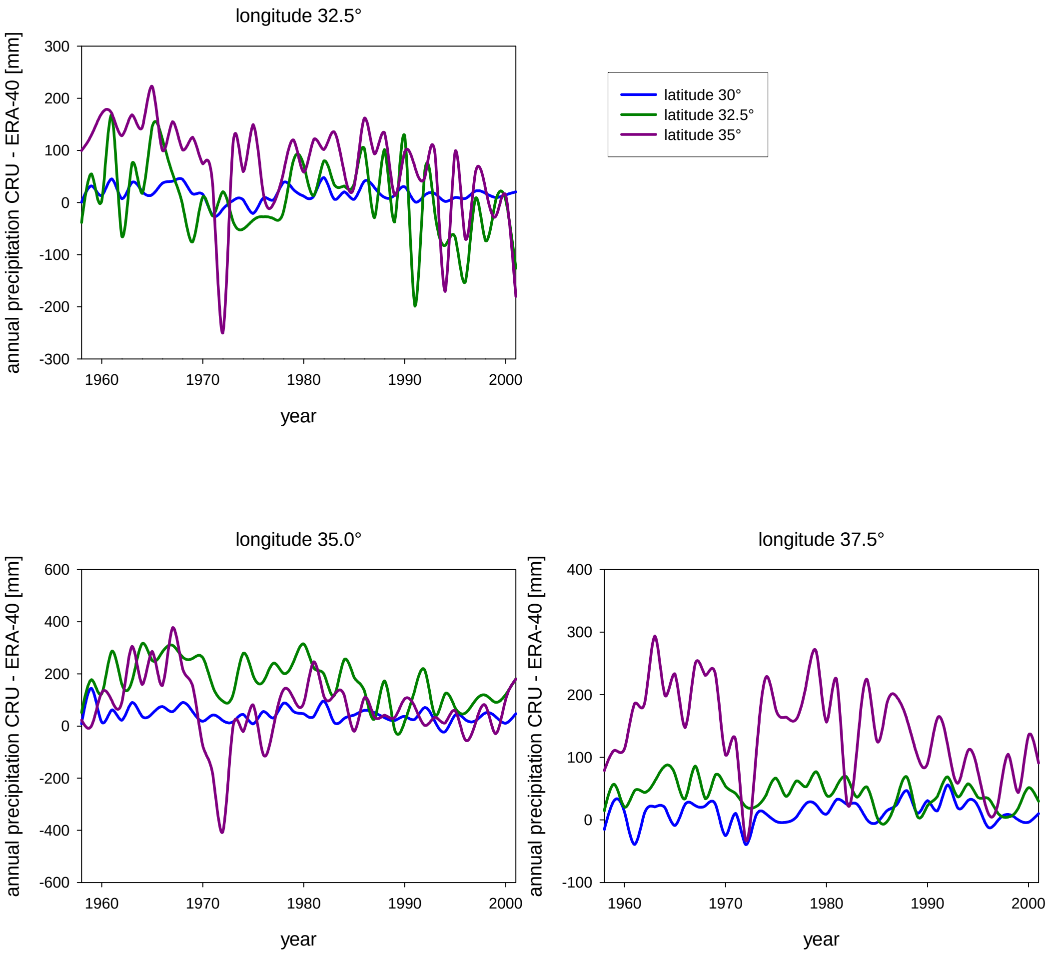

Figure A 6: Annual precipitation CRU - annual precipitation ERA-40 Jordan River Basin.

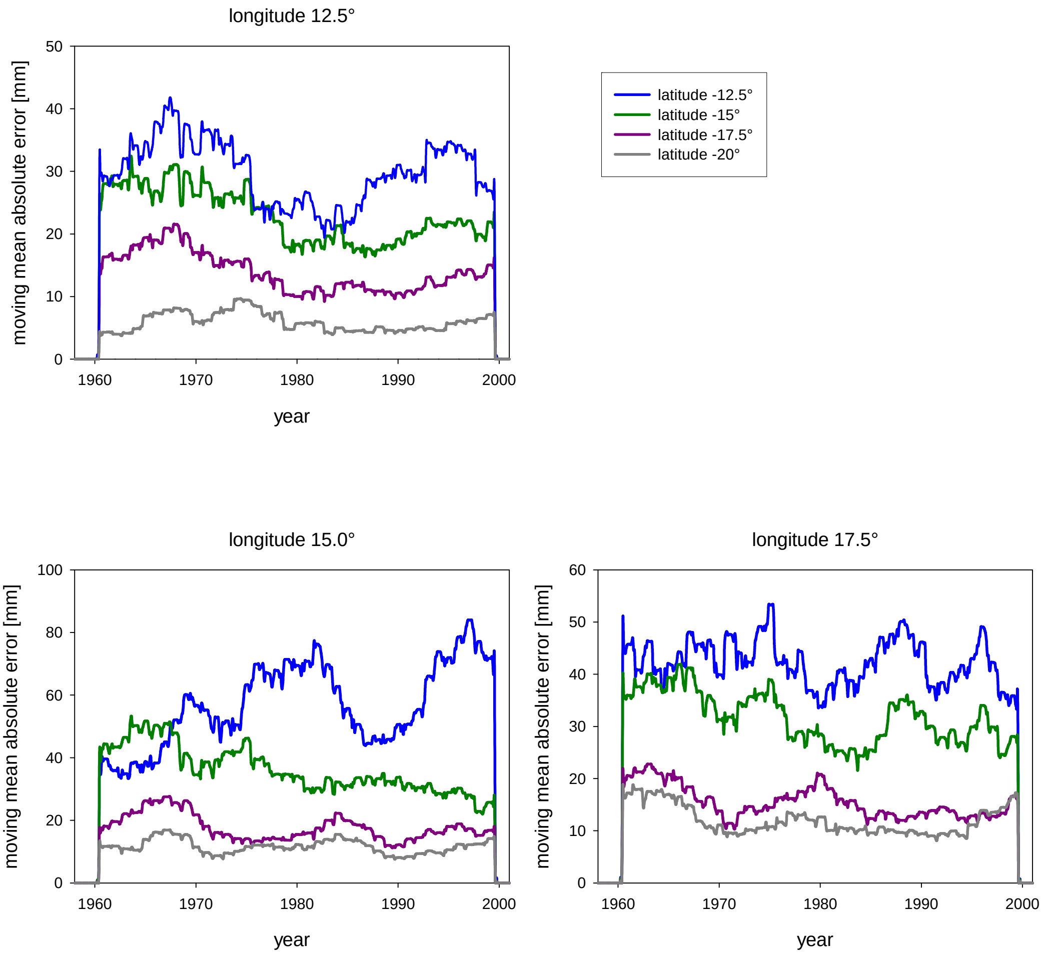

Figure A 7: Moving mean absolute error Kunene River Basin.

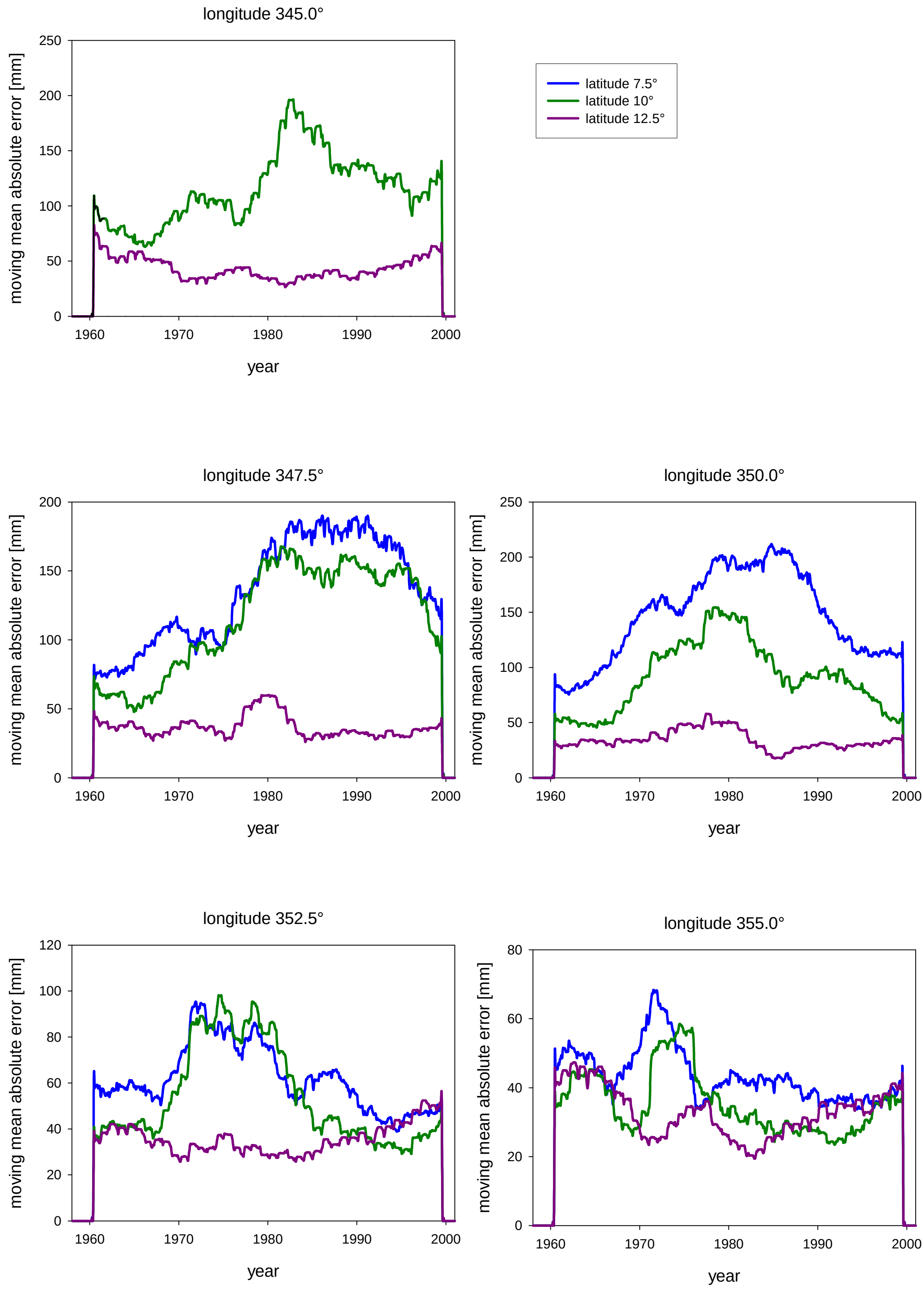

Figure A 8: Moving mean absolute error Upper Niger River Basin.

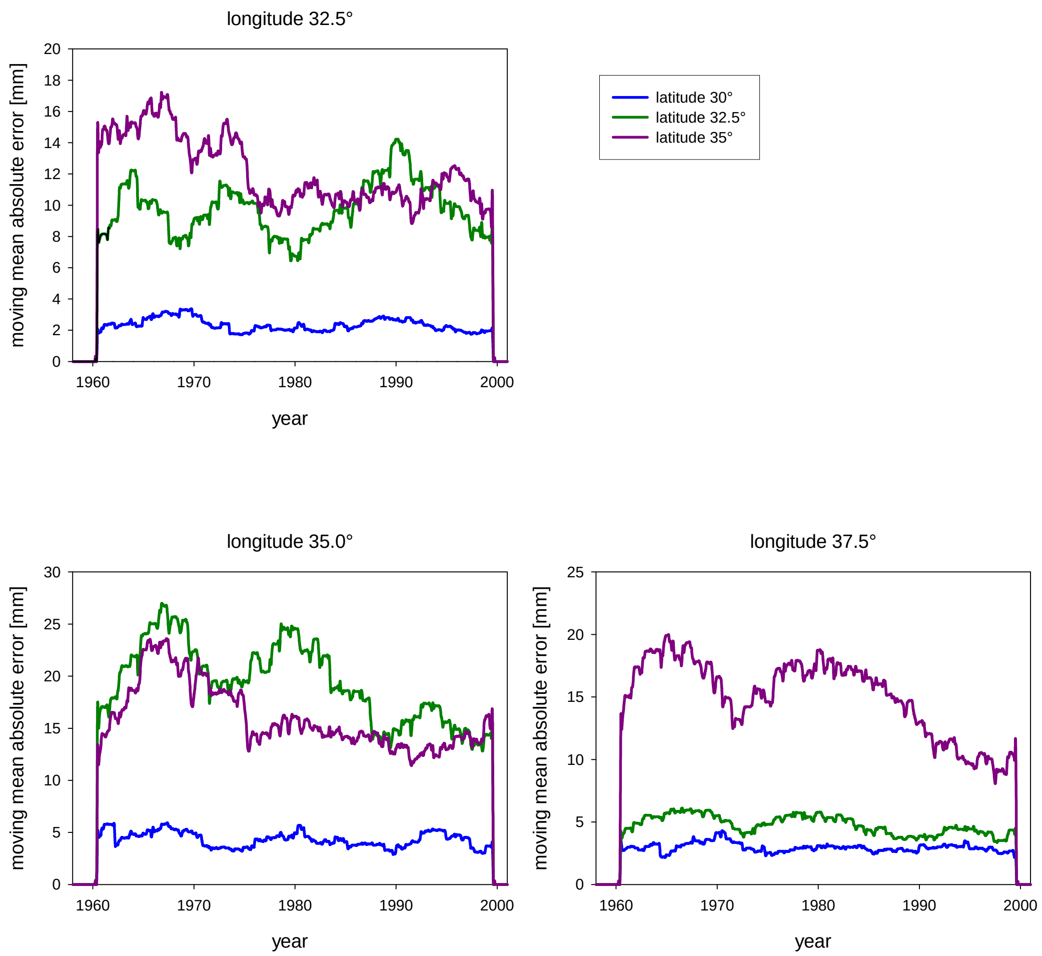

Figure A 9: Moving mean absolute error Jordan River Basin.

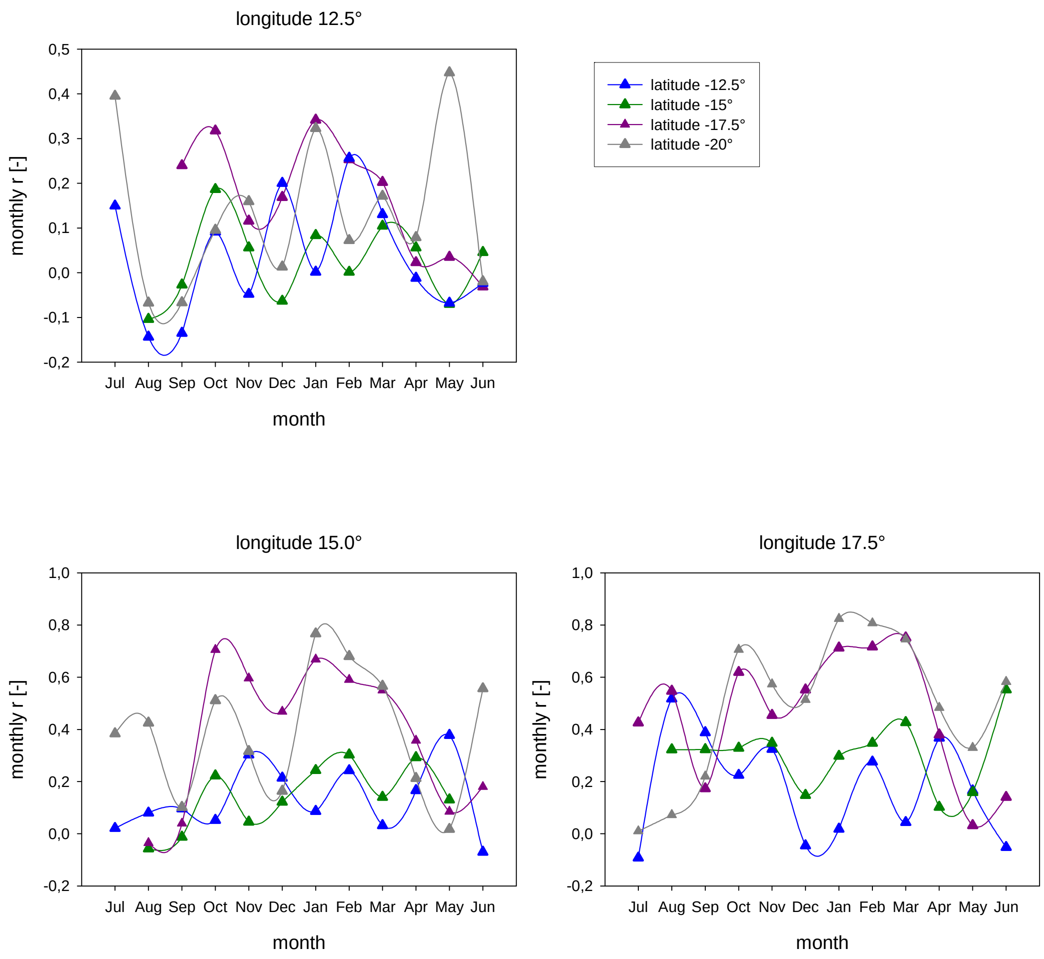

Figure A 10: Monthly Pearson correlation coefficient r Kunene River Basin.

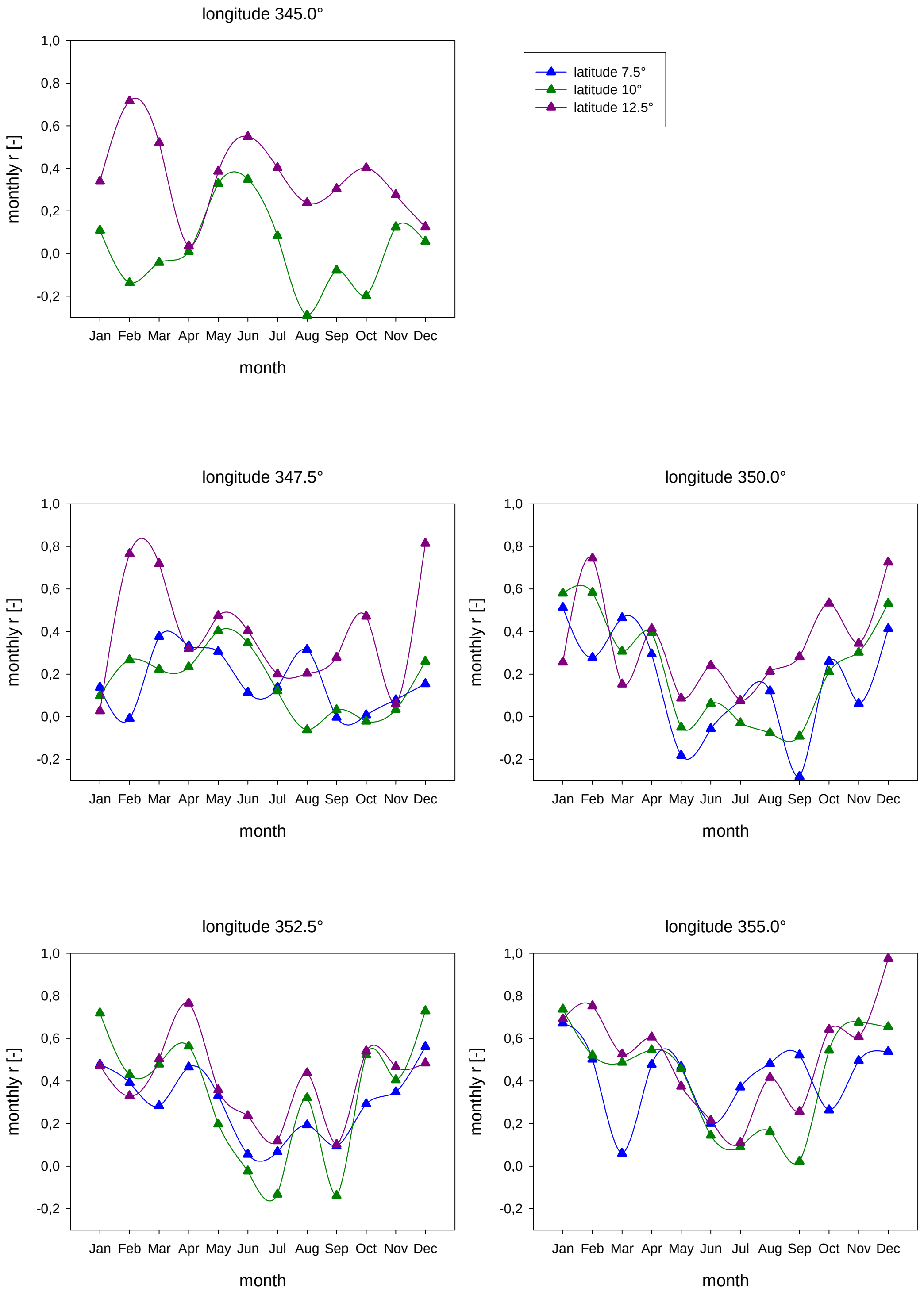

Figure A 11: Monthly Pearson correlation coefficient r Upper Niger River Basin.

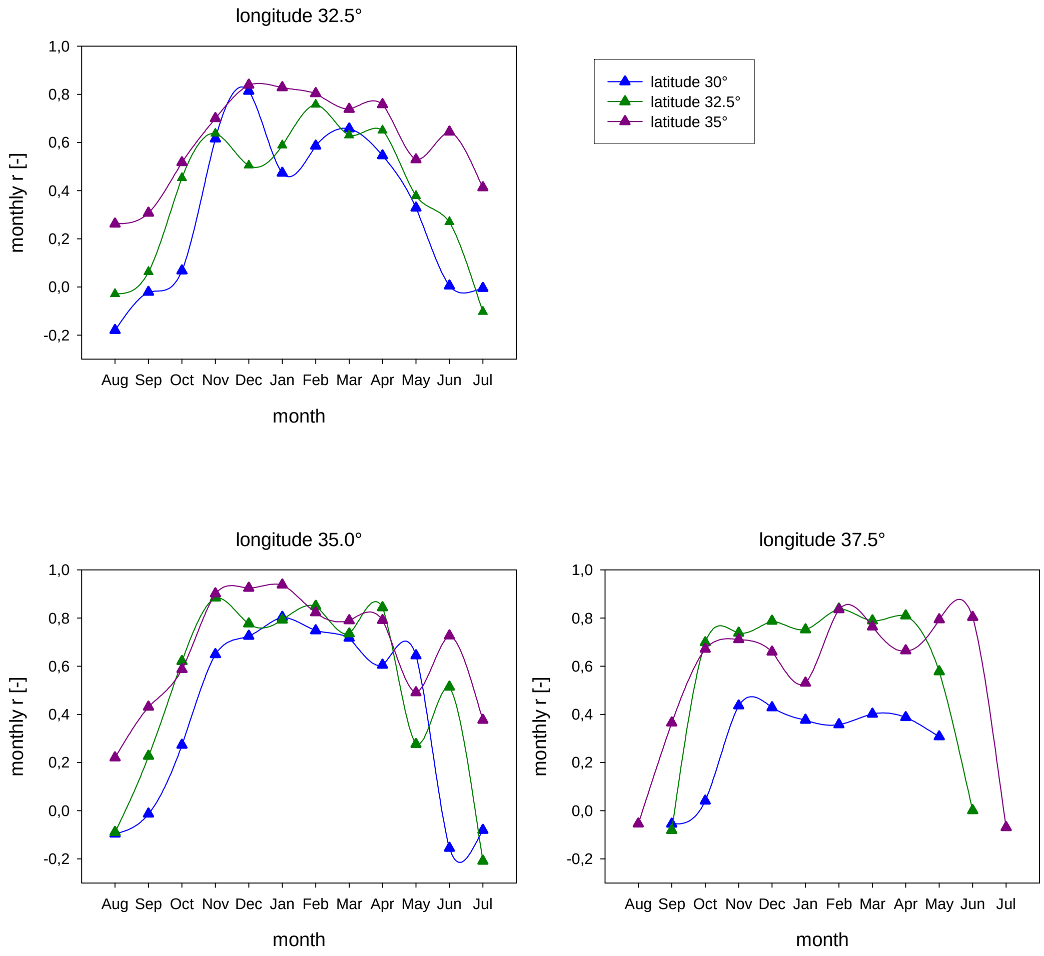

Figure A 12: Monthly Pearson correlation coefficient r Jordan River Basin.

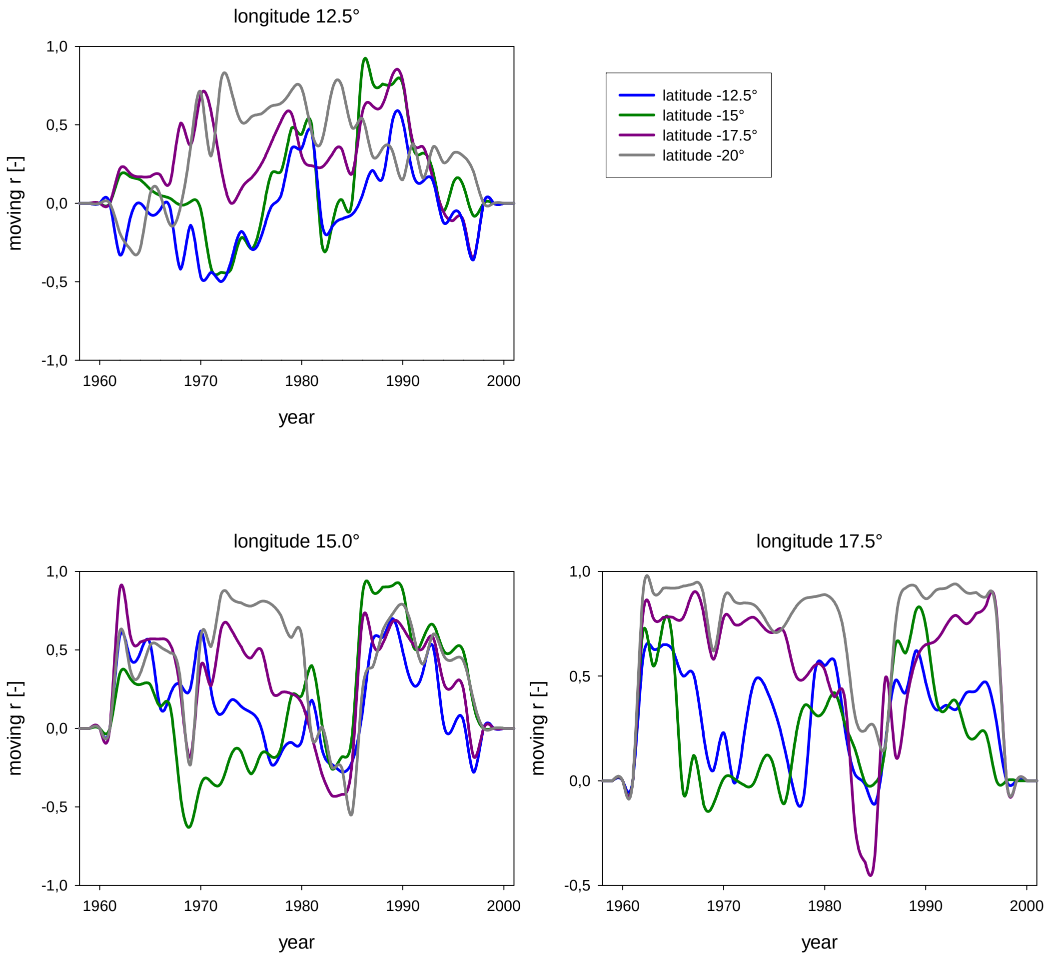

Figure A 13: Moving Pearson correlation coefficient r Kunene River Basin.

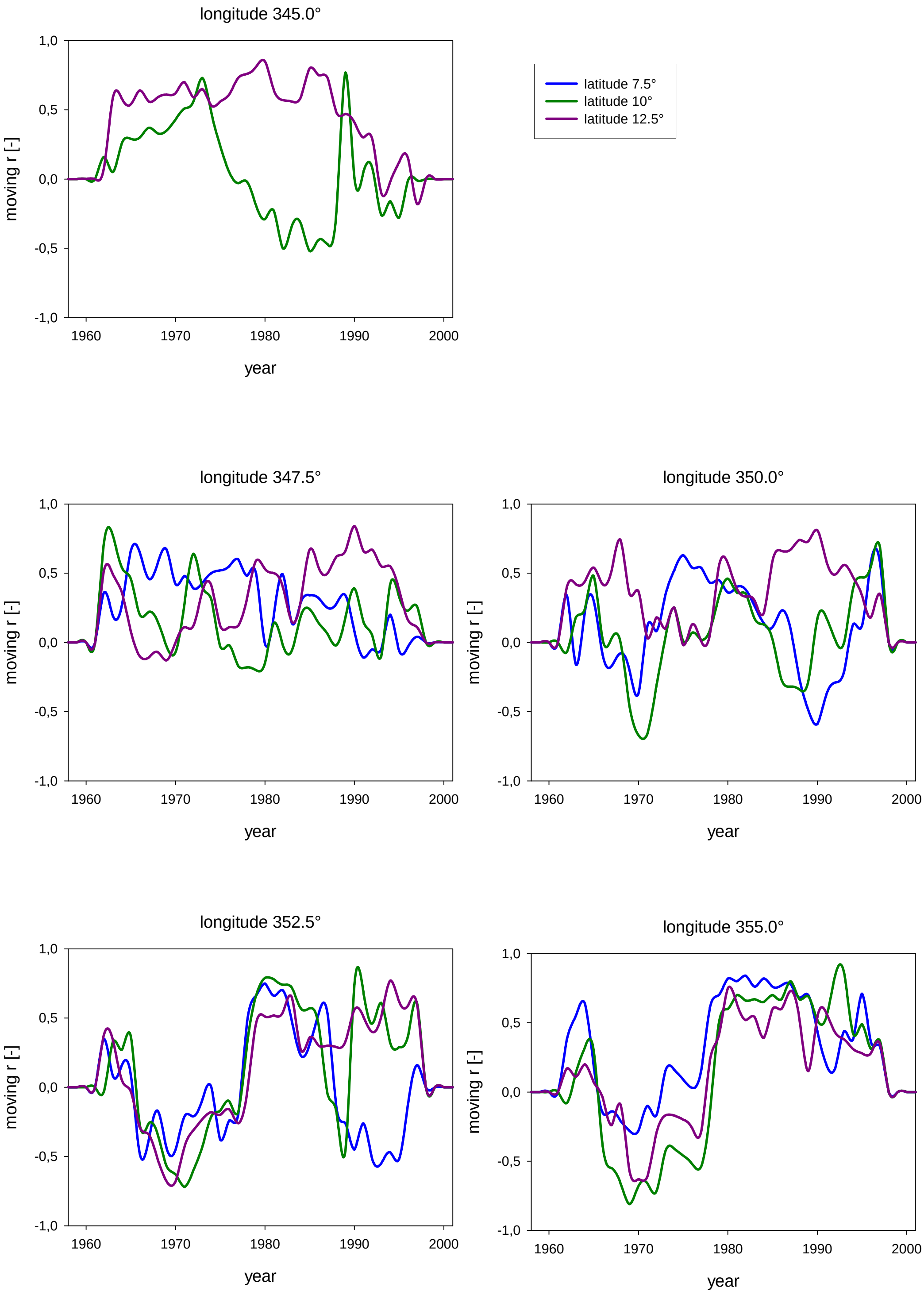

Figure A 14: Moving Pearson correlation coefficient r Upper Niger River Basin.

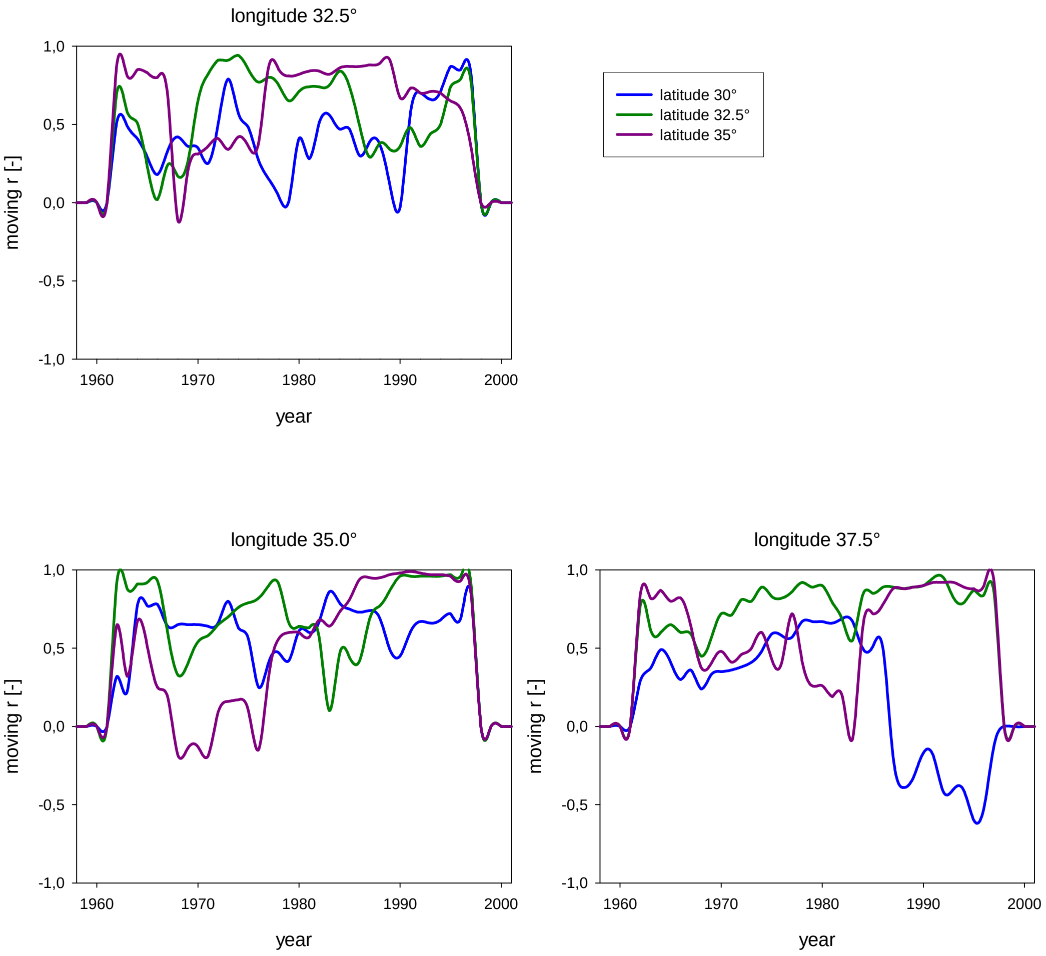

Figure A 15: Moving Pearson correlation coefficient r Jordan River Basin.

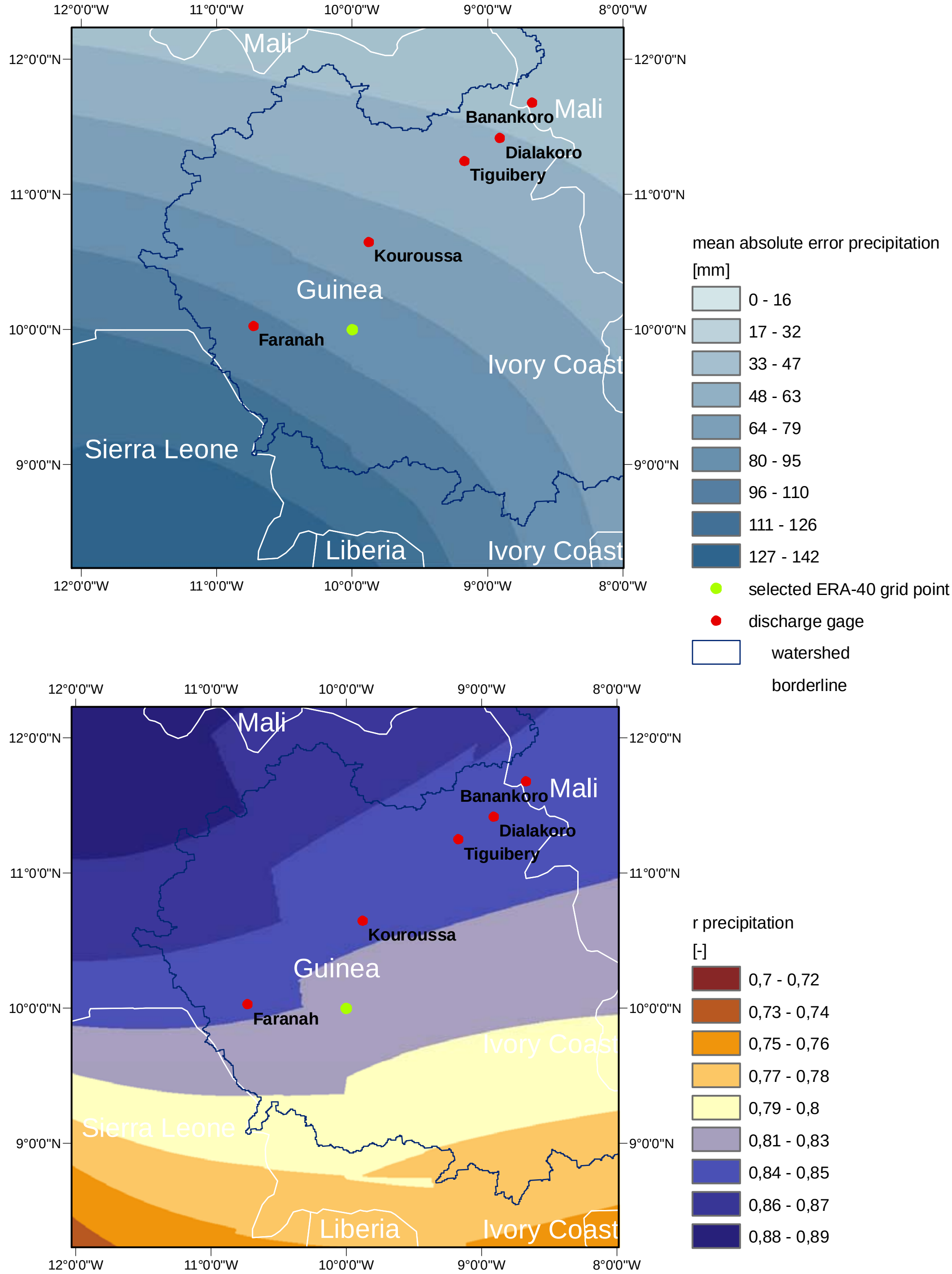

Figure A 16: Mean absolute error precipitation (top) and Pearson correlation coefficient r precipitation Upper Niger River Basin (bottom) (1958-2001).

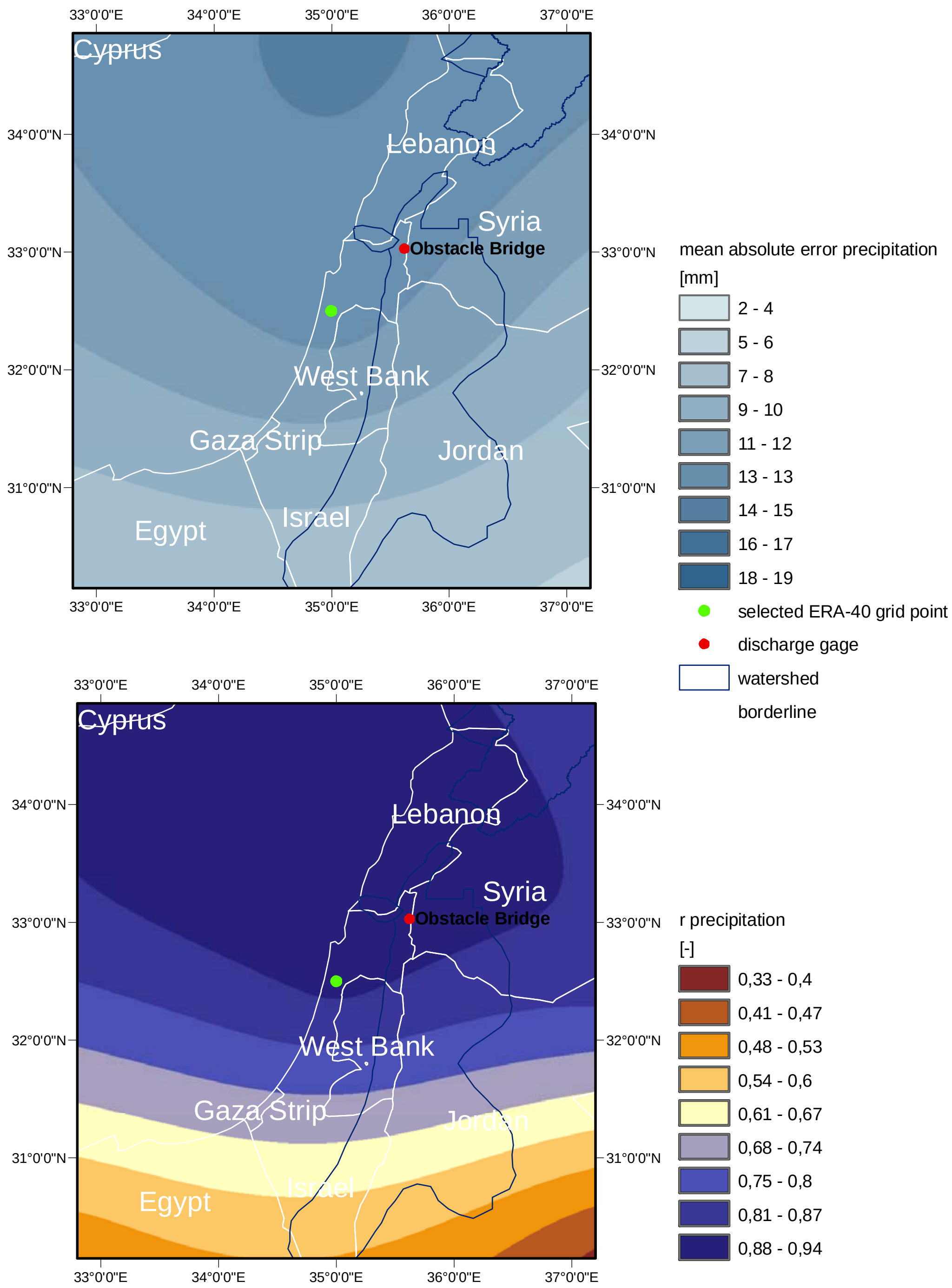

Figure A 17: Mean absolute error precipitation (top) and Pearson correlation coefficient r precipitation Jordan River Basin (bottom) (1958-2001).

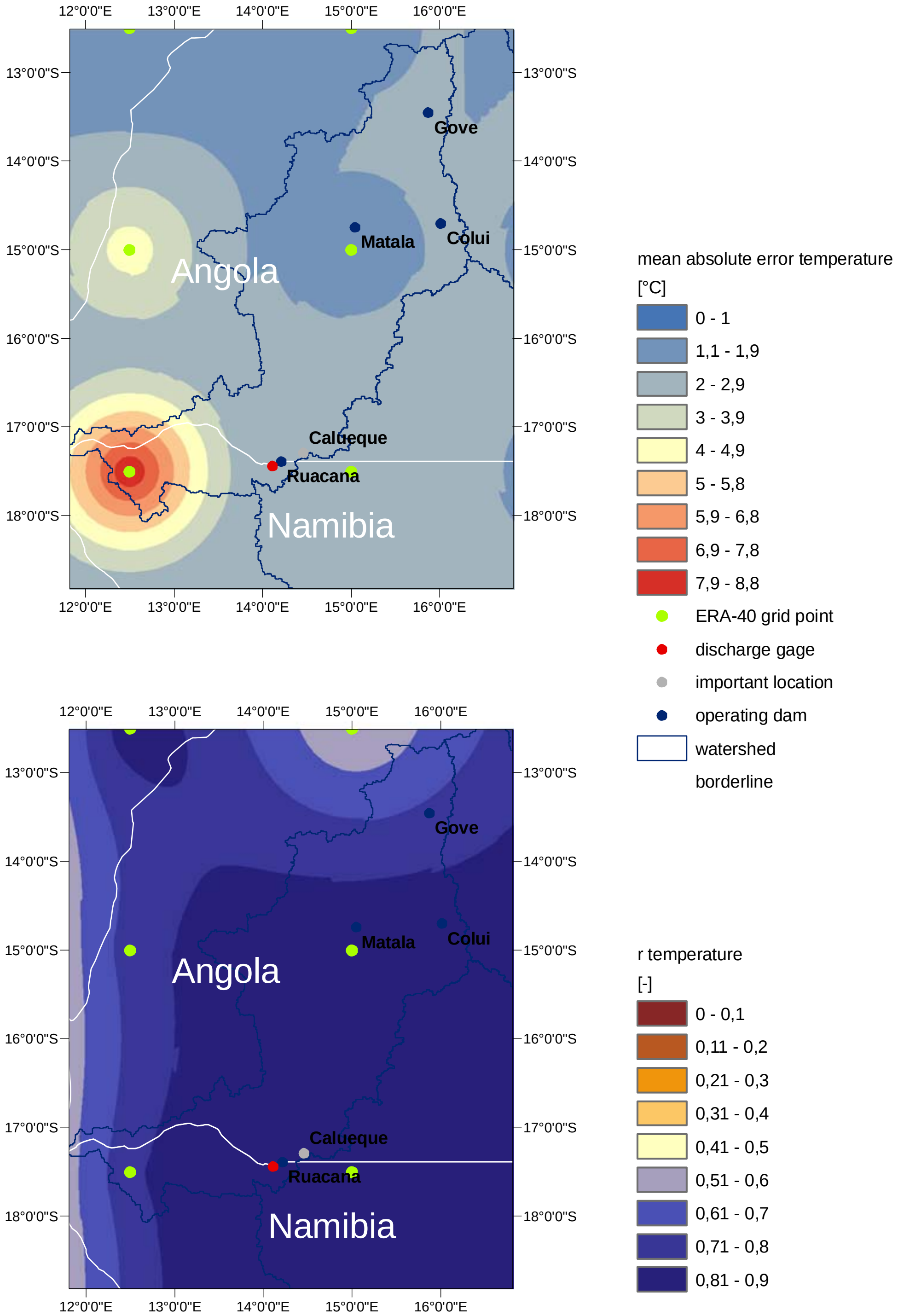

Figure A 18: Mean absolute error air temperature (top) and Pearson correlation coefficient r air temperature Kunene River Basin (bottom) (1958-2001).

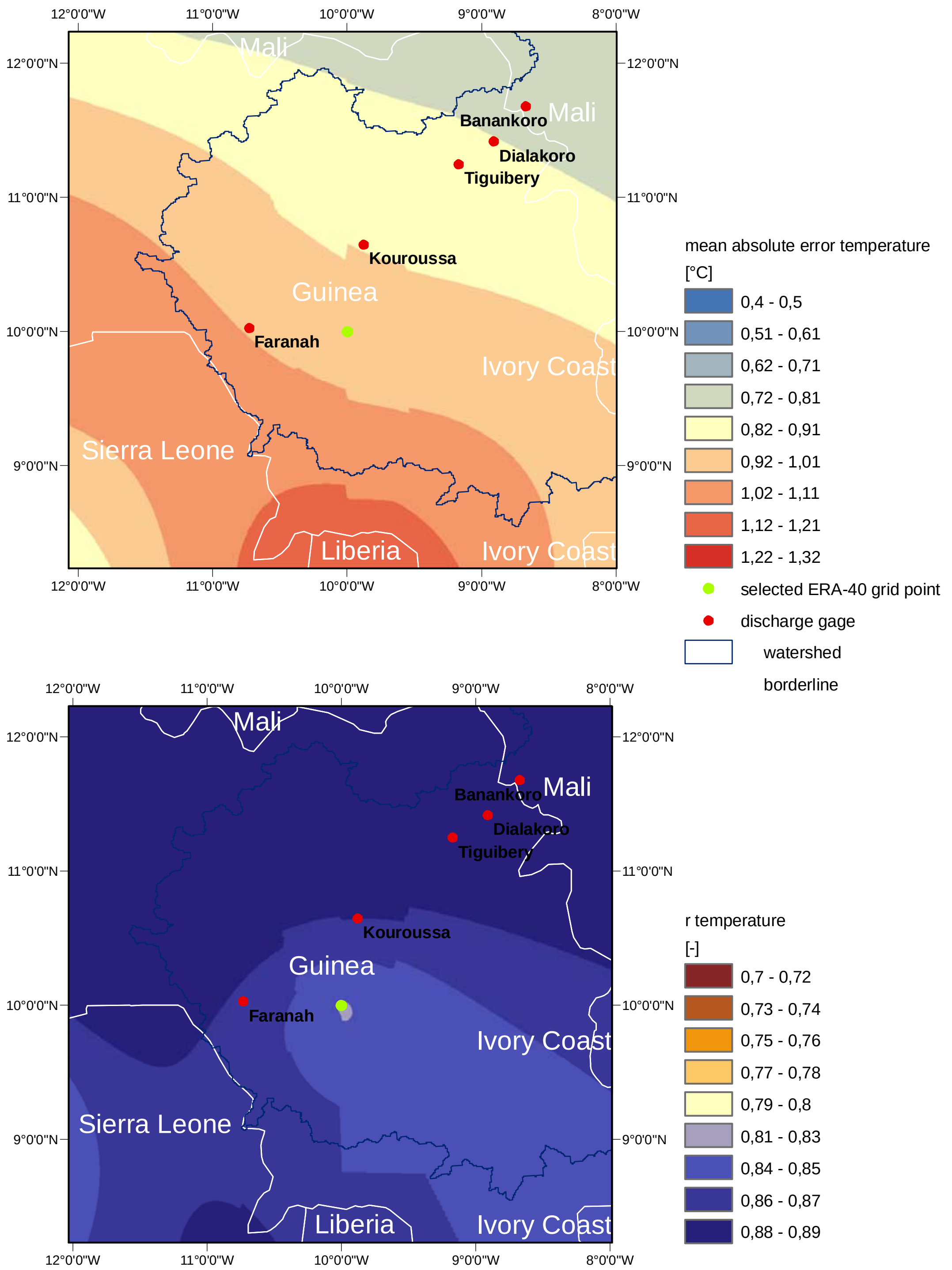

Figure A 19: Mean absolute error air temperature (top) and Pearson correlation coefficient r air temperature Upper Niger River Basin (bottom) (1958-2001).

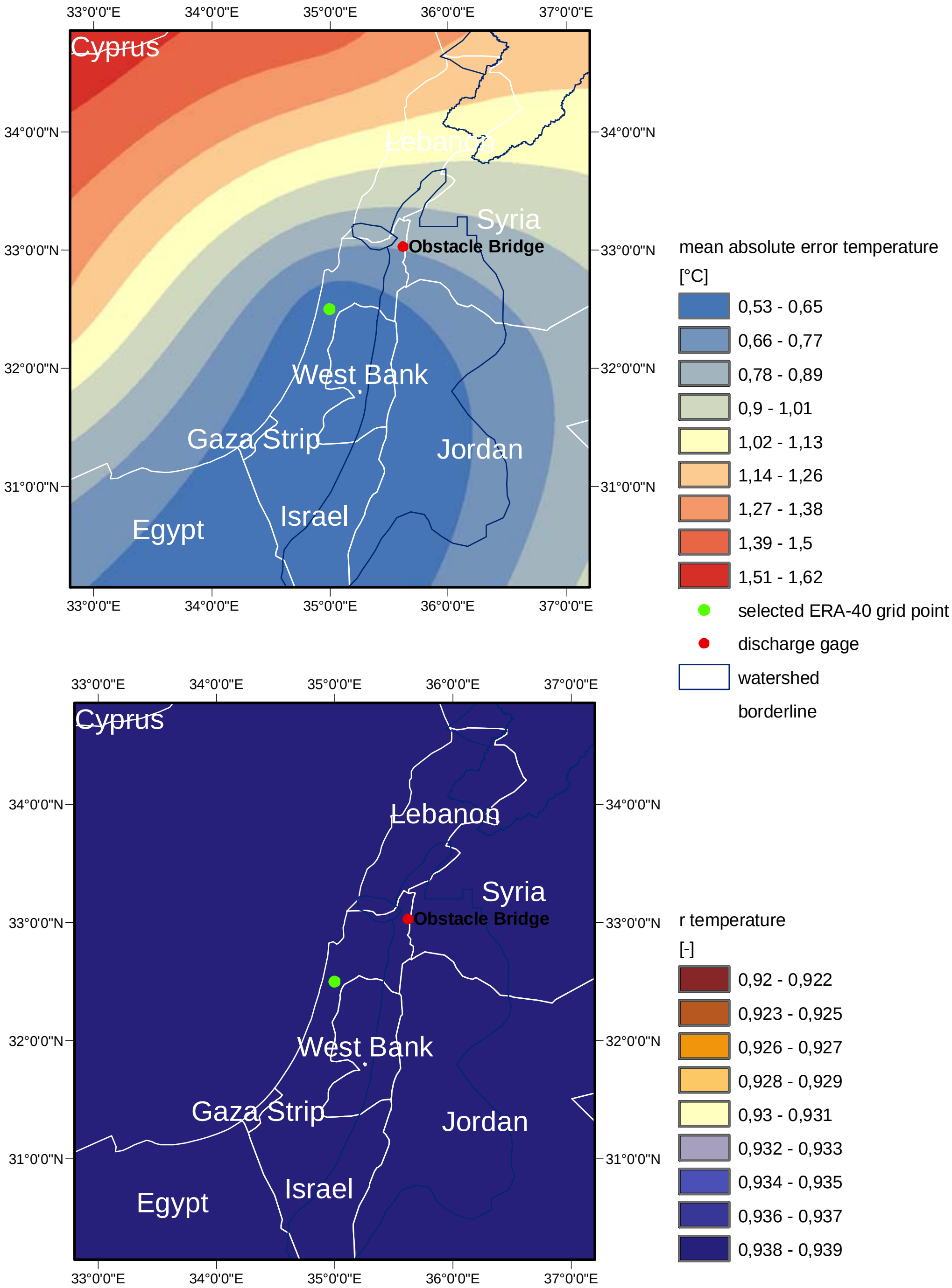

Figure A 20: Mean absolute error air temperature (top) and Pearson correlation coefficient r air temperature Jordan River Basin (bottom) (1958-2001).

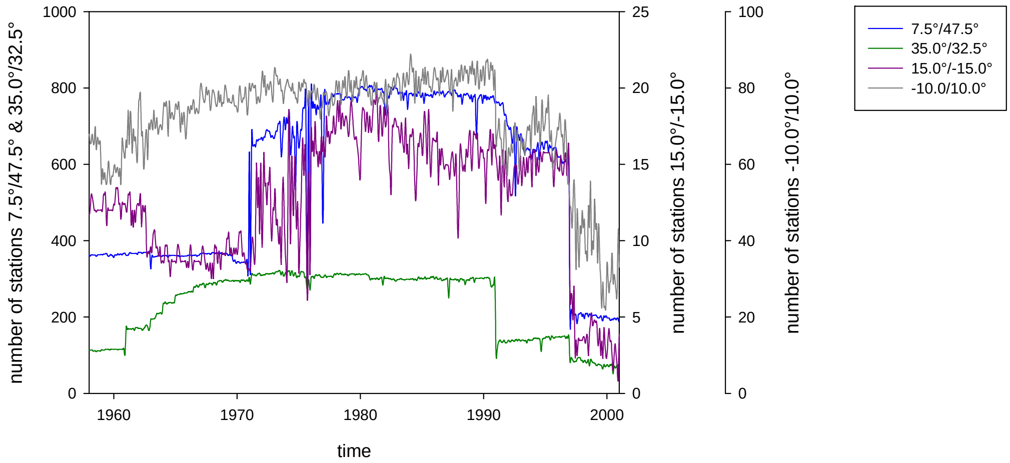

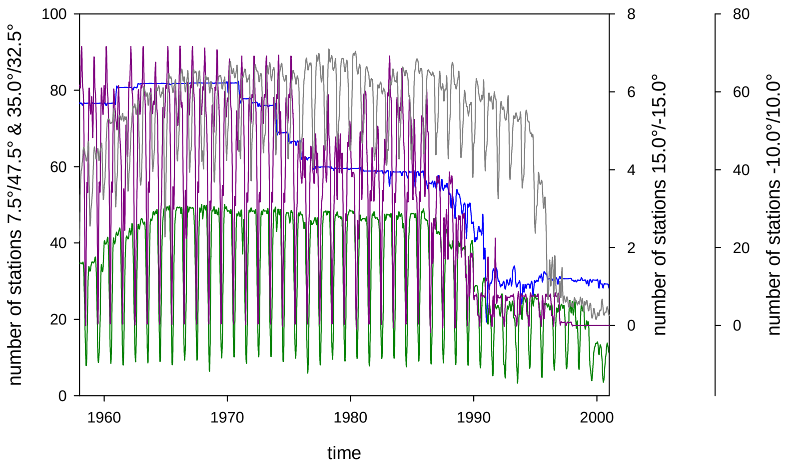

Figure A 21: Number of observation systems within the correlation distance of air temperature (top) and of precipitation (bottom) (1958-2002) of selected CRU grid points.

Analysis of Modelling Results

Table A 2: Parameter values & waterbalance obtained with Hamon's method - simple bucket model and ERA-40 data for the Niger and the Kunene River Basin.

river basin	Niger	Kunene	Kunene	Kunene	Kunene	Kunene	Kunene	Kunene	Kunene	Kunene
start_cal	1952	1962	1962	1962	1984	1984	1984	1962	1962	1962
end_cal	1965	1978	1978	1978	2002	2002	2002	2002	2002	2002
bias	0.4	0.2	0.2	0.2	0.2	0.2	0.2	0.2	0.2	0.2
AET	0.8	0.8	0.5	0.2	0.8	0.5	0.2	0.8	0.5	0.2
NS_cal	0.48	0.17	0.17	0.17	0.16	0.16	0.16	0.16	0.16	0.16
NS_val	-0.09	0.18	0.17	0.18	0.19	0.19	0.19	0.56	0.56	0.56
D	1400	400	600	1600	500	800	2100	500	800	2000
SP_{max}	280	80	120	320	100	160	420	100	160	400
elements_cal	83	192	192	192	216	216	216	428	428	428
elements_val	148	247	247	247	223	223	223	11	11	11
P [mm]	20624	3998	3998	3998	3998	3998	3998	3998	3998	3998
P_cal [mm]	4784	1786	1786	1786	1873	1873	1873	3852	3852	3852
P_val [mm]	15840	2212	2212	2212	2124	2124	2124	146	146	146
Q_o [mm]	9860	2326	2326	2326	2326	2326	2326	2326	2326	2326
Q_o_cal [mm]	4026	1048	1048	1048	1076	1076	1076	2241	2241	2241
Q_o_val [mm]	5835	1278	1278	1278	1250	1250	1250	85	85	85
Q_m [mm]	13881	1772	1708	1772	2001	2001	2049	2007	2007	2007
Q_m_cal [mm]	3197	791	763	791	911	911	934	1940	1940	1940
Q_m_val [mm]	10684	981	945	981	1090	1090	1116	67	67	67
at [mm]	5673	2149	2215	2149	1934	1934	1884	1939	1939	1939
at_cal [mm]	1308	932	960	932	915	915	892	1876	1876	1876
at_val [mm]	4365	1218	1254	1218	1019	1019	993	63	63	63
pt [mm]	22224	36086	36086	36086	36086	36086	36086	36086	36086	36086
pt_cal [mm]	7964	15433	15433	15433	18247	18247	18247	35211	35211	35211
pt_val [mm]	14261	20654	20654	20654	17839	17839	17839	876	876	876
waterbalance error cal [%]	1.45	1.19	1.19	1.19	1.78	1.78	1.78	0.55	0.55	0.55
waterbalance error val [%]	0.12	0.36	0.36	0.36	0.37	0.37	0.37	5.45	5.45	5.45

Table A 3: Parameter values & waterbalance obtained with Hamon's method - simple bucket model and ERA-40 data for the Jordan River Basin.

river basin	Jordan	Jordan	Jordan	Jordan	Jordan	Jordan	Jordan	Jordan	Jordan
start_cal	1969	1969	1969	1986	1986	1986	1969	1969	1969
end_cal	1985	1985	1985	2002	2002	2002	2002	2002	2002
bias	1.6	1.6	1.6	1.6	1.6	1.6	1.6	1.6	1.6
AET	0.8	0.5	0.2	0.8	0.5	0.2	0.8	0.5	0.2
NS_cal	0.47	0.47	0.47	0.75	0.75	0.75	0.52	0.52	0.52
NS_val	0.24	0.24	0.24	0.3	0.33	0.32	-2.62	-2.61	-2.63
D	2800	4400	11000	800	1400	3400	1200	2000	4600
SP_{max}	560	880	2200	160	280	680	240	400	920
elements_cal	182	182	182	192	192	192	386	386	386
elements_val	212	212	212	202	202	202	8	8	8
P [mm]	14937	14937	14937	14937	14937	14937	14937	14937	14937
P_cal [mm]	5897	5897	5897	8485	8485	8485	14702	14702	14702
P_val [mm]	9041	9041	9041	6452	6452	6452	236	236	236
Q_o [mm]	10668	10668	10668	10668	10668	10668	10668	10668	10668
Q_o_cal [mm]	5361	5361	5361	4804	4804	4804	10468	10468	10468
Q_o_val [mm]	5307	5307	5307	5865	5865	5865	200	200	200
Q_m [mm]	12600	12568	12568	9441	9716	9627	10583	10695	10464
Q_m_cal [mm]	4827	4914	4914	5362	5516	5467	10526	10638	10408
Q_m_val [mm]	7673	7654	7654	4079	4200	4161	57	57	56
at [mm]	2102	2134	2134	5265	4985	5075	4027	3913	4147
at_cal [mm]	824	837	837	29788	2799	2849	3995	3883	4114
at_val [mm]	1277	1297	1297	14669	2186	2226	31	30	32
pt [mm]	29788	29788	29788	29788	29788	29788	29788	29788	29788
pt_cal [mm]	13507	13507	13507	14669	14669	14669	29082	29082	29082
pt_val [mm]	16282	16282	16282	15120	15120	15120	706	706	706
waterbalance error cal [%]	0.59	0.59	0.59	0.36	0.36	0.36	0.24	0.24	0.24
waterbalance error val [%]	0.21	0.21	0.21	0.54	0.54	0.54	51.66	51.66	51.66

Table A 4: Parameter values & waterbalance obtained with Hamon's method - simple bucket model and CRU data for the Niger River Basin.

river basin	Niger	Niger	Niger	Niger	Niger	Niger	Niger	Niger	Niger
start_cal	1952	1952	1952	1966	1966	1966	1952	1952	1952
end_cal	1965	1965	1965	1979	1979	1979	1979	1979	1979
bias	0.6	0.6	0.6	0.6	0.6	0.6	0.6	0.6	0.6
AET	0.8	0.5	0.2	0.8	0.5	0.2	0.8	0.5	0.2
NS_cal	0.82	0.81	0.78	0.72	0.76	0.68	0.78	0.78	0.75
NS_val	0.75	0.71	0.46	0.61	0.69	0.64	0.66	0.4	0.65
D	300	300	600	200	200	200	300	200	600
SP_{max}	60	60	120	40	40	40	60	40	120
elements_cal	146	146	146	137	137	137	284	284	284
elements_val	148	148	148	157	157	157	10	10	10
P [mm]	29840	29840	29840	29840	29840	29840	29840	29840	29840
P_cal [mm]	15727	15727	15727	13070	13070	13070	28804	28804	28804
P_val [mm]	14113	14113	14113	16770	16770	16770	1036	1036	1036
Q_o [mm]	12952	12952	12952	12952	12952	12952	12952	12952	12952
Q_o_cal [mm]	7117	7117	7117	5404	5404	5404	12533	12533	12533
Q_o_val [mm]	5835	5835	5835	7549	7549	7549	419	419	419
Q_m [mm]	12679	10886	9394	12244	11083	10990	12695	11239	9402
Q_m_cal [mm]	6861	5975	5123	5098	4530	4510	12325	10900	9113
Q_m_val [mm]	5818	4911	4271	7145	6552	6480	370	339	288
at [mm]	17025	18813	20055	17343	18557	18673	17017	18649	20076
at_cal [mm]	8745	9665	10371	7789	8393	8426	16482	18037	19481
at_val [mm]	8280	9148	9684	9554	10164	10247	535	613	596
pt [mm]	29026	29026	29026	29026	29026	29026	29026	29026	29026
pt_cal [mm]	14378	14378	14378	13529	13529	13529	27992	27992	27992
pt_val [mm]	14648	14648	14648	15497	15497	15497	1034	1034	1034
waterbalance error cal [%]	0.19	0.14	0.86	1.14	1.10	1.00	-0.31	-0.47	0.47
waterbalance error val [%]	-0.94	-0.66	0.05	-0.13	-0.24	-0.30	-1.59	-0.84	0.06

Table A 5: Parameter values & waterbalance obtained with Hamon's method - simple bucket model and CRU data for the Kunene River Basin.

river basin	Kunene	Kunene	Kunene	Kunene	Kunene	Kunene	Kunene	Kunene	Kunene
start_cal	1962	1962	1962	1984	1984	1984	1962	1962	1962
end_cal	1978	1978	1978	2002	2002	2002	2002	2002	2002
bias	0.2	0.2	0.2	0.2	0.2	0.2	0.2	0.2	0.2
AET	0.8	0.5	0.2	0.8	0.5	0.2	0.8	0.5	0.2
NS_cal	0.37	0.37	0.38	0.31	0.32	0.32	0.36	0.36	0.36
NS_val	0.33	0.34	0.35	0.41	0.41	0.41	0.53	0.51	0.49
D	300	500	1300	300	500	1200	400	600	1400
SP_{max}	60	100	260	60	100	240	80	120	280
elements_cal	192	192	192	216	216	216	428	428	428
elements_val	251	251	251	227	227	227	15	15	15
P [mm]	5157	5157	5157	5157	5157	5157	5157	5157	5157
P_cal [mm]	2431	2431	2431	2299	2299	2299	4949	4949	4949
P_val [mm]	2727	2727	2727	2859	2859	2859	208	208	208
Q_o [mm]	2336	2336	2336	2336	2336	2336	2336	2336	2336
Q_o_cal [mm]	1048	1048	1048	1076	1076	1076	2241	2241	2241
Q_o_val [mm]	1289	1289	1289	1260	1260	1260	95	95	95
Q_m [mm]	1967	2018	2067	1972	2023	1972	2336	2253	2165
Q_m_cal [mm]	934	958	982	867	889	867	2265	2184	2099
Q_m_val [mm]	1033	1060	1086	1105	1134	1105	71	69	66
at [mm]	3083	3032	2982	3091	3039	3091	2718	2802	2892
at_cal [mm]	1438	1413	1390	1385	1362	1385	2632	2713	2800
at_val [mm]	1646	1618	1592	1705	1676	1705	86	89	92
pt [mm]	33932	33932	33932	33932	33932	33932	33932	33932	33932
pt_cal [mm]	14479	14479	14479	16810	16810	16810	32709	32709	32709
pt_val [mm]	19452	19452	19452	17122	17122	17122	1222	1222	1222
waterbalance error cal [%]	0.71	0.71	0.71	0.66	0.66	0.66	0.35	0.35	0.35
waterbalance error val [%]	0.62	0.62	0.62	0.59	0.59	0.59	8.07	8.07	8.07

Table A 6: Parameter values & waterbalance obtained with Hamon's method - simple bucket model and CRU data for the Jordan River Basin.

river basin	Jordan	Jordan	Jordan	Jordan	Jordan	Jordan	Jordan	Jordan	Jordan
start_cal	1969	1969	1969	1986	1986	1986	1969	1969	1969
end_cal	1985	1985	1985	2002	2002	2002	2002	2002	2002
bias	0.9	0.9	0.9	0.9	0.9	0.9	0.9	0.9	0.9
AET	0.8	0.5	0.2	0.8	0.5	0.2	0.8	0.5	0.2
NS_cal	0.64	0.64	0.64	0.73	0.73	0.73	0.7	0.7	0.7
NS_val	0.67	0.67	0.67	0.63	0.63	0.63	-0.9	-0.9	-0.9
D	3400	5200	13000	2000	3200	8000	2400	4000	9600
SP_{max}	680	1040	2600	400	640	1600	480	800	1920
elements_cal	182	182	182	192	192	192	386	386	386
elements_val	216	216	216	206	206	206	12	12	12
P [mm]	13130	13130	13130	13130	13130	13130	1310	1310	1310
P_cal [mm]	6122	6122	6122	6200	6200	6200	12669	12669	12669
P_val [mm]	7009	7009	7009	6930	6930	6930	461	461	461
Q_o [mm]	10718	10718	10718	10718	10718	10718	10718	10718	10718
Q_o_cal [mm]	5361	5361	5361	4804	4804	4804	10468	10468	10468
Q_o_val [mm]	5357	5357	5357	5914	5914	5914	250	250	250
Q_m [mm]	11085	11023	11023	10249	10249	10249	10505	10574	10505
Q_m_cal [mm]	5167	5138	5138	4836	4836	4836	10398	10466	10398
Q_m_val [mm]	5918	5885	5885	5413	5413	5413	107	108	107
at [mm]	1578	1641	1641	2452	2452	2452	2102	2033	2102
at_cal [mm]	732	762	762	1152	1152	1152	2076	2007	2076
at_val [mm]	846	879	879	1300	1300	1300	27	26	27
pt [mm]	30924	30924	30924	30924	30924	30924	30924	30924	30924
pt_cal [mm]	13832	13832	13832	15167	15167	15167	29937	29937	29937
pt_val [mm]	17092	17092	17092	15757	15757	15757	987	987	987
waterbalance error cal [%]	0.63	0.63	0.63	0.93	0.93	0.93	0.30	0.30	0.30
waterbalance error val [%]	0.80	0.80	0.80	0.56	0.56	0.56	33.96	33.96	33.96

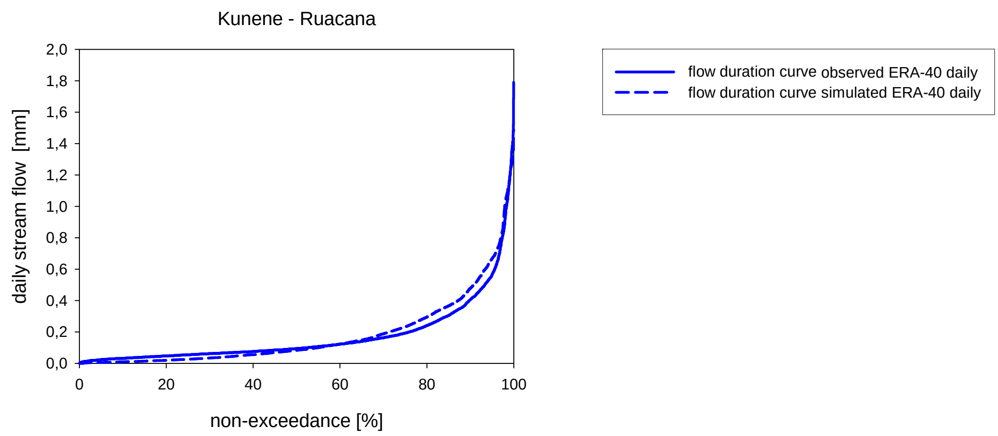

Figure A 22: Flow duration curves of observed and modelled daily stream flow of the Kunene River.

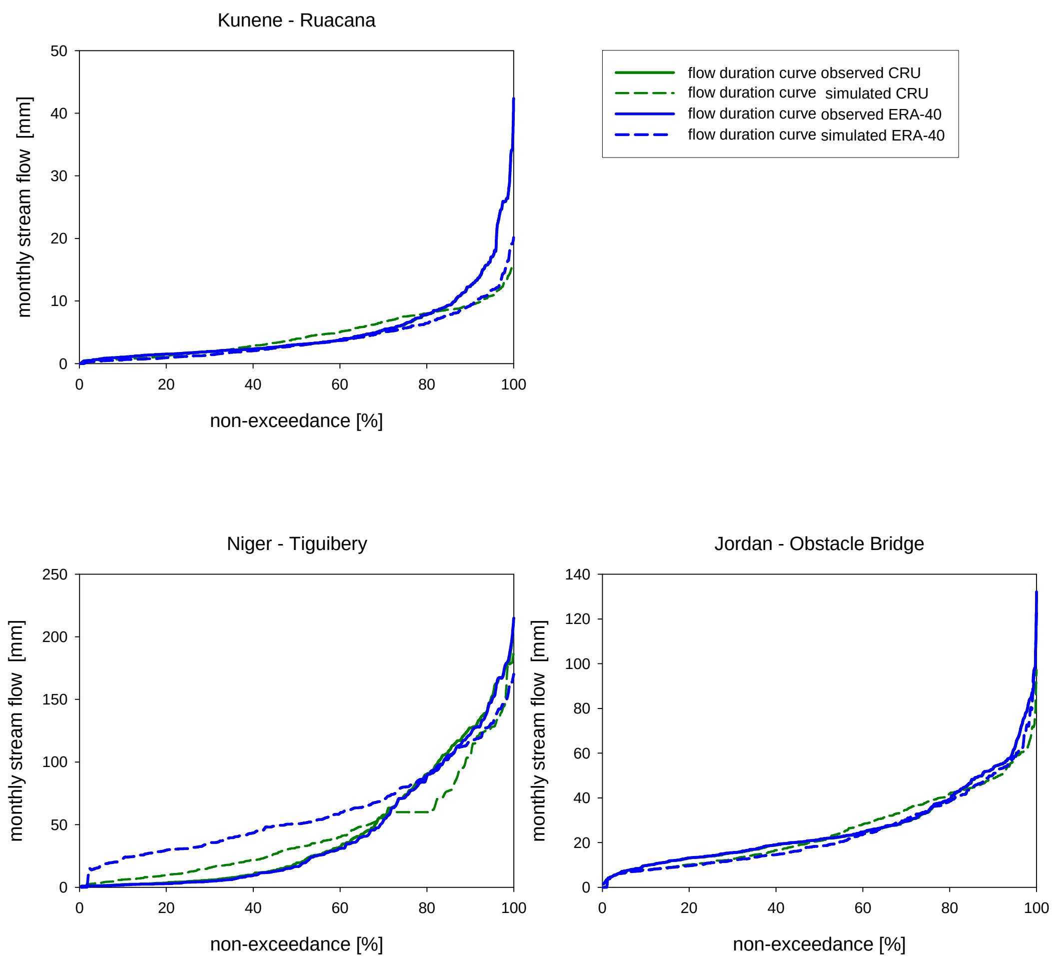

Figure A 23: Flow duration curves of observed and modelled monthly stream flow.

Ehrenwörtliche Erklärung

Hiermit erkläre ich, dass ich die Arbeit selbstständig und nur unter Verwendung der hier angegebenen Hilfsmittel angefertigt habe.

Freiburg, den 18. November 2009

Manuela Nied